Universitá di Pisa

Facoltá di Scienze Matematiche Fisiche e Naturali

Corso di Laurea Specialistica in Scienze Fisiche

Anno Accademico 2006-2007

Tesi di Laurea Specialistica

On Non-Gaussianity of the Cosmological Perturbation

Candidato: **Giovanni Petri**

Relatore: **Dr. Antonio Riotto**

Relatore: **Dr. Dario Grasso**

Contents

Chapter 1

Introduction

Since its accidental discovery by Penzias and Wilkinson in 1965, the Cosmological Microwave Background radiation (CMB) has been one of the fundamental observational pillars of the Big Bang cosmology, together with the Hubble diagram and the prediction of light element abundances. It has pitched the balance of opinion from the Steady State cosmology, proposed by Fred Hoyle, Thomas Gold, Hermann Bondi and others (see for example [1]) to the dynamical Big Bang view. The first measurements showed with good approximation a blackbody spectrum that well suited the idea of a hot, dense, opaque ball of expanding gas. During its first moments, the Universe was thought to be in full thermal equilibrium, with photons being continually emitted and absorbed, giving the radiation a blackbody spectrum. As the Universe expanded, it cooled to a temperature at which photons could no longer be created or destroyed. The temperature was still high enough for electrons and nuclei to remain unbound, however, and photons were efficiently scattered, keeping the early Universe opaque. The characteristic transparency of the present Universe came later, when the temperature fell to a few thousand Kelvin, so that electrons and nuclei began to recombine. Since photons scatter infrequently from neutral atoms, radiation decoupled from matter when nearly all the electrons had recombined, at the epoch of last scattering ($z \simeq 1100$), about 300,000 years after the Big Bang. These free streaming photons were subsequently redshifted by the expansion, which preserved the form of the spectrum but caused its temperature to fall, mean-

ing that the CMB photons now fall into the microwave region. The radiation is thought to be observable at every point in the Universe and comes from all directions with (almost) the same intensity. It was exactly the observed isotropy of the CMB to open the way to the inflationary paradigm. The Hubble horizon $H_{LS}{}^{-1}$ at the last scattering was much smaller than the horizon we would obtain tracing back the present one ($H_0{}^{-1}$). Looking at angular scales on the sky corresponding to $H_{LS}{}^{-1}$ we find that all those regions look like they were in thermal equilibrium at the last scattering. Yet, if we assume a radiation or matter dominated Universe and we trace back those regions we find that they were not even in causal contact. So the high isotropy of the CMB prompted the first reflections about how non causally connected regions could share the same properties. The Big Bang Universe needed a way to expand faster, much faster. Inflation, first proposed by Guth in 1981
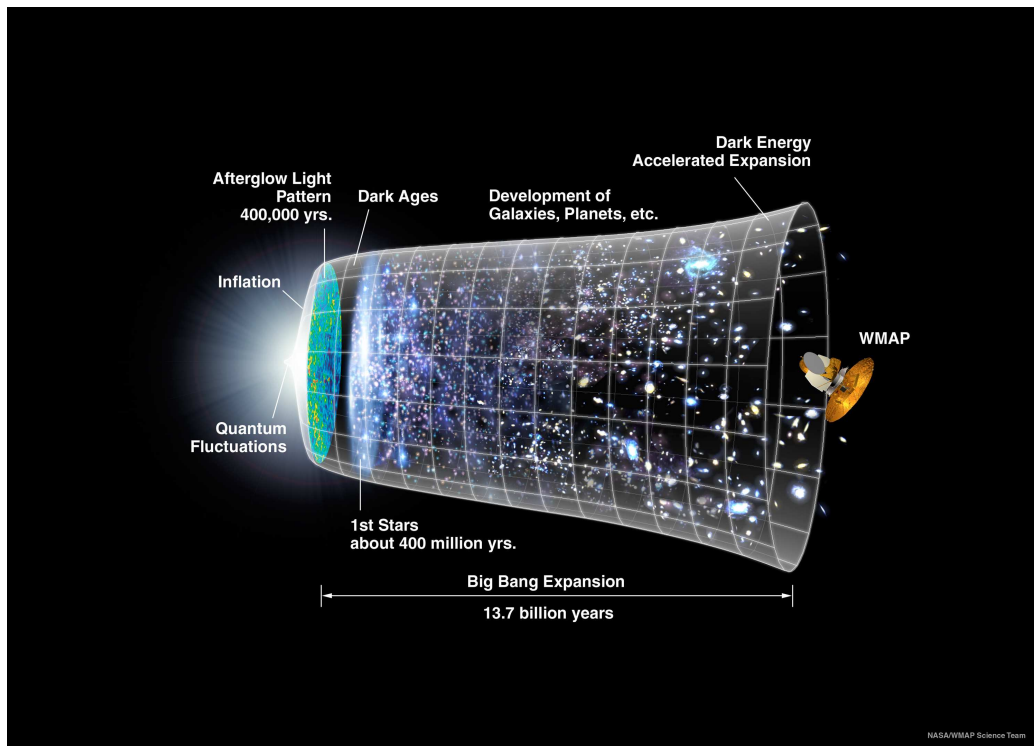

Figure 1.1: A graphical representation of the expansion of the Universe with the inflationary epoch represented as the dramatic expansion the left [WMAP press release, 2006]

[2], was born.

In the first formulation Inflation involved a brief period of rapid exponential expansion of the scale factor a, driven by the energy density of a scalar field, the inflaton, trapped in a false minimum of its potential. In this scenario, small localized regions would tunnel to the true vacuum and start growing. For the Universe to move as a whole to the true vacuum though these bubbles would need to coalesce. Careful calculations showed that they would not [3, 4]. To avoid the problem Linde, Albrecht and Steinard in 1982 [5, 6] made use of a scalar field slowly rolling to its minimum. The energy density of such a field is thought to be very close to constant and so it comes quickly to dominate the energy balance and thus drive Inflation.

In 1992 the Cosmological Background Explorer (*COBE*) detected for the first time CMB temperature anisotropies [7, 8] at a level of 1 part in 10^5. These anisotropies are the sign of perturbations at the last scattering surface. Inflation again provided an elegant explanation: microscopic quantum fluctuations of the inflaton field were magnified to cosmological scales during the inflationary era, generating cosmological curvature perturbations and thus creating matter perturbations, the primordial seeds for the structures that we observe today. As fluctuations wavelenghts were stretched by the exponential expansion, they eventually became larger than the horizon, which grew slower than a. This phenomenon is referred to as horizon exit: while *outside the horizon* the fluctuations *freeze* [5, 9], their amplitude remaining constant since they are larger than the scale over which causal physics can operate. After the end of Inflation, the frozen fluctuations gradually reentered the horizon becoming thus observable. Thus, the larger scale perturbations that we observe now were the ones who exited the horizon earlier during Inflation and therefore they are also the ones less likely to have been modified by causal under–horizon interactions.

The last confirmation of the inflationary paradigm has been recently provided by the data of the Wilkinson Microwave Anisotropy Probe (*WMAP*) mission [10]. The *WMAP* collaboration has produced a full–sky map of the angular variations of the CMB and a plot of the temperature anisotropies, with unprecedented accuracy (respectively fig. 1.3 and 1.2). *WMAP* data confirm the inflationary mechanism as responsible for the generation of cur-

vature (adiabatic) superhorizon fluctuations [11].
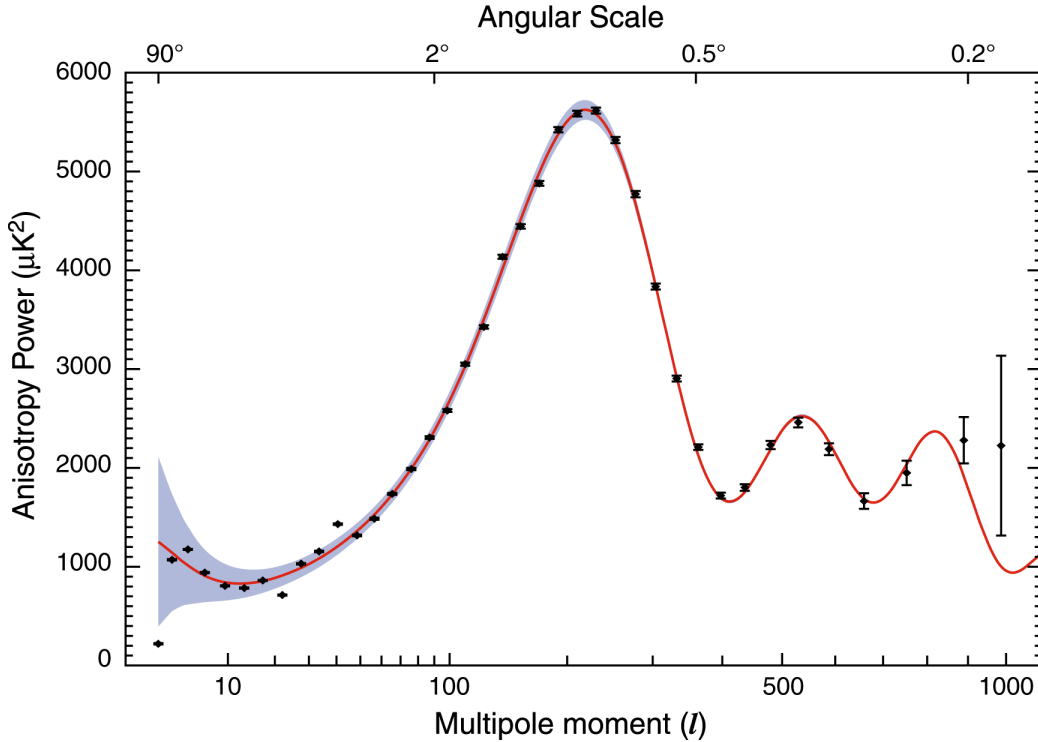
Figure 1.2: The power spectrum of the cosmic microwave background radiation temperature anisotropy in terms of the angular scale (or multipole moment).The correlations observed in the gray–shaded area on the left side of the first peak are the signature of the inflationary expansion. The data shown come from the WMAP (2006).

Since the primordial cosmological perturbations are tiny, the generation and evolution of fluctuations during Inflation havef been studied within linear perturbation theory. Within this approach, the primordial density perturbation is Gaussian; in other words, its Fourier components are uncorrelated and have random phases. Despite the simplicity of the inflationary paradigm, the mechanism by which cosmological adiabatic perturbations are generated is not yet established. In the standard slow–roll scenario associated to one–single field models of Inflation, the observed density perturbations are due to fluctuations of the inflaton field itself when it slowly rolls down along its potential. When Inflation ends, the inflaton ϕ oscillates about the minimum

Figure 1.3: The detailed, all-sky picture of the infant Universe from three years of WMAP data. The image reveals 13.7 billion year old temperature fluctuations (shown as color differences) that correspond to the seeds that grew to become the galaxies [WMAP press release].
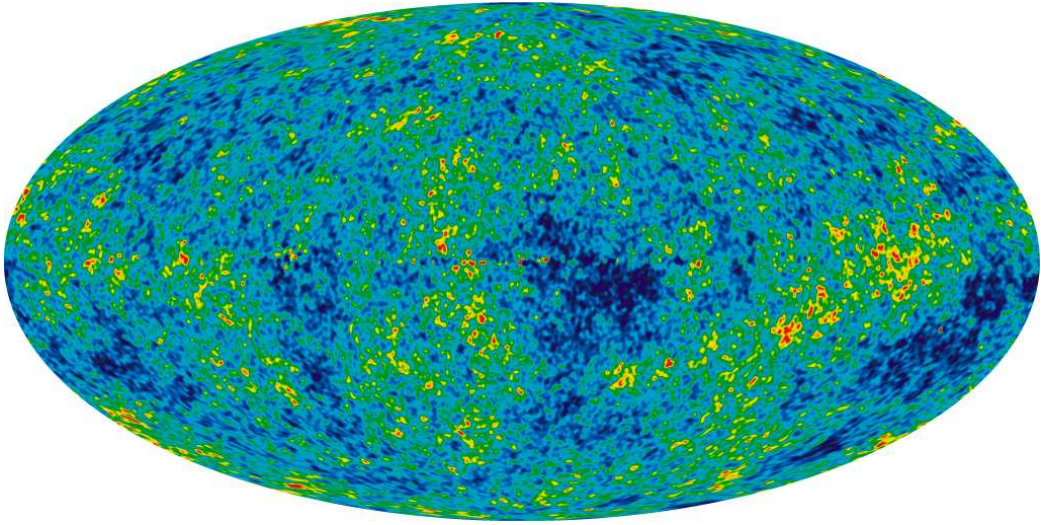
of its potential $V(\phi)$ and decays, thereby reheating the Universe. As a result of the fluctuations each region of the Universe goes through the same history but at slightly different times. The final temperature anisotropies are caused by Inflation lasting for different amounts of time in different regions of the Universe leading to adiabatic perturbations. Under this hypothesis, the *WMAP* dataset already allows to extract the parameters relevant for distinguishing among single–field Inflation models [11, 12].

However, *what if* the curvature perturbation is generated through the quantum fluctuations of a scalar field other than the inflaton? Consider, for instance, the curvaton scenario, where the final curvature perturbations are produced from an initial perturbation associated with the quantum fluctuations of the curvaton, a light scalar field, whose energy density is negligible during Inflation and curvaton isocurvature perturbations are transformed into adiabatic ones when the curvaton decays into radiation much after the end of Inflation. It liberates the inflaton from the duty of generating the cosmological curvature perturbation and therefore avoid slow–roll conditions. Their basic assumption is that the initial curvature perturbation due to the

inflaton field is negligible. Other mechanisms for the generation of cosmological perturbations have been proposed. A few examples are the inhomogeneous reheating scenario [13, 14, 15, 16], the ghost inflationary scenario [17] and the D–cceleration scenario [18].

So how can we discriminate among them? Different models provide different constraints on gravitational waves produced during Inflation, for example in the curvaton scenario the inflaton potential has to be small enough so that its contribution to the primordial curvature perturbation in the observed CMB anisotropy is negligible. Therefore the curvaton mechanisms would produce gravitational waves with an amplitude too small to be detectable [19]. A future detection would then favor slow-roll models while a failed detection would not give any information about the generating mechanisms of perturbations. Another powerful tool to constrain inflationary models is the spectral index n_ζ calculated from the spectrum of comoving curvature perturbations: slow–roll models for example predict $|n_\zeta - 1| \ll 1$ [20, 21]. Remarkably, the eventual accuracy $\Delta n_\zeta \sim 0.01$ offered by the future *Planck* satellite [22] is just what one might have specified in order to distinguish between various slow–roll models of Inflation. If cosmological perturbations are due to the inflaton field, then in ten or fifteen years there may be a consensus about the form of the inflationary potential, and at a deeper level we may have learned something valuable about the nature of the fundamental interactions beyond the Standard Model. However, we cannot exclude the possibility that there are other mechanisms for the creation of the cosmological perturbations, which generically predict a value of $n_\mathcal{R}$ very close to unity with a negligible scale dependence. Then, it implies that a precise measurement of the spectral index will not allow us to efficiently discriminate among different scenarios. We should then turn to a third observable which will prove fundamental in providing information about the mechanism chosen by Nature to produce the structures we see today. It is the deviation from a pure Gaussian statistics, *i.e.*, the presence of higher–order connected correlation functions of CMB anisotropies. The angular n–point correlation function for temperature anisotropies

$$\left\langle \frac{\delta T}{T}(\hat{\mathbf{n}}_1) \frac{\delta T}{T}(\hat{\mathbf{n}}_2) \dots \frac{\delta T}{T}(\hat{\mathbf{n}}_n) \right\rangle, \qquad (1.1)$$

is a simple statistic characterizing a clustering pattern of temperature fluctuations on the sky, $\frac{\delta T}{T}(\hat{\mathbf{n}})$, where the bracket denotes the ensemble average. If the fluctuation is Gaussian, then the two–point correlation function specifies all the statistical properties of $\frac{\delta T}{T}(\hat{\mathbf{n}})$, for the two–point correlation function is the only parameter in a Gaussian distribution. If it is not Gaussian, then we need higher–order correlation functions to determine the statistical properties: a non–vanishing *connected* three– or four–point correlation function of scalar perturbations, or their Fourier transform, the bispectrum and trispectrum, are indicators of a non–Gaussian feature in the cosmological perturbations. The importance of the bi– and trispectrum comes from the fact that they represent the lowest order statistics able to distinguish non–Gaussian from Gaussian perturbations. Thus an accurate calculation of the primordial spectra of cosmological perturbations has become an extremely important issue, as a number of present and future experiments, such as *WMAP* and *Planck*, will allow to constrain or detect non–Gaussianity of CMB anisotropy with high precision.

With the coming measurements and the possibility of non Gaussian fields, it becomes important to know how loop corrections to the scalar field influence the correlation functions and whether they must be accounted for in evaluating the non Gaussianity of the curvature perturbation. A number of papers addressed this problem using toy model potential of the form ϕ^n (usuallu $n = 3, 4$) and showed that in these theories the first order corrections in perturbation theory produce a logarithmic divergence in the correlation functions evaluated at late times during Inflation [23, 24, 25, 26, 27, 28, 29, 30], making the correlations useless for the prediction of non Gaussianity. Yet, none of those papers investigated whether that divergence and the ones arising at higher orders could be cured by means of resummations.

The goal of this thesis is then to investigate whether the resummation is possible. We will start with the free scalar field propagators in a Friedmann Robertson Walker Universe during a de Sitter stage and use them to build the higher order loop corrections for a $\lambda\phi^4$ theory. We will then try to resum a different diagram classes in order to see whether the divergences are reabsorbed and whether we find evidence that the full theory is not divergent in the late time limit. We will then present an argument to justify our choice

to neglect a large number of diagrams and to focus only on a small selection. Finally we will use the *resummed* 2–point correlation functions to calculate the 4–point correlation function and the observation of its behaviour for late times will give us an estimate of the non Gaussianity produced by the self–interacting scalar field.

In the next chapters we will slowly build up all the tools needed for this calculation. The thesis is structured as follows:

- Chapter 2 contains a more detailed review of the Big Bang cosmology and of the problems that led to the inflationary paradigm. We introduce also the theory of quantum fluctuations for a generic scalar field evolving in a fixed de Sitter background.

- Chapter 3 is about the curvature perturbation ζ that we already mentioned often. Section 3.21 utilizes the δN formalism to show how ζ is conserved superhorizon for adiabatic perturbations. Section 3.2 on the contrary briefly explains how can ζ evolve, also in case of adiabatic fluids.

- Chapter 4 is devoted to the non Gaussianity of perturbations. Building on the previous chapter, we show explicitly how the level of non Gaussianity can be parametrized in the two case of the inflaton and curvaton scenarios. Then in section 4.2 we put forth the formalism needed to calculate the 3– and 4–point ζ correlation functions and how it relates to the ϕ correlation functions.

- Chapter 5 introduces the Closed Path Time formalism. We will have to calculate expectation values of correlation functions on vacuum states, but during Inflation it is difficult to define past and future asymptotic states and thus the conventional in–out formalism fails. Therefore a different formalism is needed. In particular in section 5.3 we calculate the Feynman rules of the chosen self-interacting theory.

- Chapter 6 contains the actual calculations of higher order Feynman diagrams for the self–interacting scalar field. In section 6.1 we calculate the corrections to the two–point propagators and search for a resummation. Then, in section 6.2 we use the results to calculate the 4–point

correlation function and discuss its meaning, while in section 6.3 we justify the choice of neglecting certain diagrams.

- Chapter 7 summarizes the results and concludes the thesis.

Chapter 2

Big Bang and Inflation: an overview

2.1 Basics of the Big-Bang Model

The standard cosmology is based upon the maximally spatially symmetric Friedmann-Robertson-Walker (FRW) line element

$$ds^2 = -dt^2 + a(t)^2 \left[\frac{dr^2}{1 - kr^2} + r^2(d\theta^2 + \sin^2 \theta \, d\phi^2) \right]; \qquad (2.1)$$

where $a(t)$ is the cosmic-scale factor, $R_{\text{curv}} \equiv a(t)|k|^{-1/2}$ is the curvature radius, and $k = -1, 0, 1$ is the curvature signature. All three models are without boundary: the positively curved model is finite and "curves" back on itself; the negatively curved and flat models are infinite in extent. The Robertson-Walker metric embodies the observed isotropy and homogeneity of the Universe. It is interesting to note that this form of the line element was originally introduced for sake of mathematical simplicity; we now know that it is well justified at early times or today on large scales ($\gg 10\,\text{Mpc}$), at least within our visible patch.

The coordinates, r, θ, and ϕ, are referred to as *comoving* coordinates: A particle at rest in these coordinates remains at rest, *i.e.*, constant r, θ, and ϕ. A freely moving particle eventually comes to rest these coordinates, as its momentum is red shifted by the expansion, $p \propto a^{-1}$. Motion with respect to the comoving coordinates (or cosmic rest frame) is referred to as peculiar

velocity. Physical separations between freely moving particles are simply $a(t)$ times the coordinate separation. The momenta of freely propagating particles decrease, or "red shift," as $a(t)^{-1}$, and thus the wavelength of a photon stretches as $a(t)$, which is the origin of the cosmological red shift.

2.1.1   Friedmann Equations

The evolution of the scale factor $a(t)$ is governed by Einstein equations

$$R_{\mu\nu} - \frac{1}{2} R \, g_{\mu\nu} \equiv G_{\mu\nu} = 8\pi G \, T_{\mu\nu} \qquad (2.2)$$

where $R_{\mu\nu}$ $(\mu, \nu = 0, \cdots 3)$ is the Riemann tensor and R is the Ricci scalar constructed via the metric (2.1) [31] and $T_{\mu\nu}$ is the energy-momentum tensor. Under the hypothesis of homogeneity and isotropy, we can always write the energy-momentum tensor under the form $T_{\mu\nu} = \text{diag}\,(\rho, P, P, P)$ where ρ is the energy density of the system and P its pressure. They are functions of time. The evolution of the cosmic-scale factor is governed by the Friedmann equation

$$H^2 \equiv \left(\frac{\dot{a}}{a}\right)^2 = \frac{8\pi G \rho}{3} - \frac{k}{a^2}, \qquad (2.3)$$

where ρ is the total energy density of the Universe. Differentiating with respect to time both members of eq. (2.3) and using the the mass conservation equation

$$\dot{\rho} + 3H(\rho + P) = 0, \qquad (2.4)$$

we find the equation for the acceleration of the scale-factor

$$\frac{\ddot{a}}{a} = -\frac{4\pi G}{3}(\rho + 3P). \qquad (2.5)$$

Combining Eqs. (2.3) and (2.5) we find

$$\dot{H} = -4\pi G \,(\rho + P)\,. \qquad (2.6)$$

The evolution of the energy density of the Universe is governed by

$$d(\rho a^3) = -P d \left(a^3\right); \qquad (2.7)$$

which is the First Law of Thermodynamics for a fluid in the expanding Universe.

14

- For $P = \rho/3$, ultra-relativistic matter, $\rho \propto a^{-4}$ and $a \sim t^{\frac{1}{2}}$;

- for $P = 0$, very nonrelativistic matter, $\rho \propto a^{-3}$ and $a \sim t^{\frac{2}{3}}$;

- or $P = -\rho$, vacuum energy, $\rho = \text{const.}$

If the r.h.s. of the Friedmann equation is dominated by a fluid with equation of state $P = \gamma\rho$, it follows that $\rho \propto a^{-3(1+\gamma)}$ and $a \propto t^{2/3(1+\gamma)}$.

Through the Friedmann equation one can relate the curvature of the Universe to the energy density and expansion rate:

$$\Omega - 1 = \frac{k}{a^2 H^2}; \qquad \Omega = \frac{\rho}{\rho_{\text{crit}}}; \tag{2.8}$$

and the critical density today $\rho_{\text{crit}} = 3H^2/8\pi G = 1.88 h^2 \, \text{g cm}^{-3} \simeq 1.05 \times 10^4 \, \text{eV cm}^{-3}$. The correspondence between Ω and the spatial curvature of the Universe is direct:

- positively curved, $\Omega_0 > 1$;

- negatively curved, $\Omega_0 < 1$;

- flat ($\Omega_0 = 1$).

Model universes with $k \leq 0$ expand forever, while those with $k > 0$ necessarily recollapse. The curvature radius of the Universe is related to the Hubble radius and Ω by

$$R_{\text{curv}} = \frac{H^{-1}}{|\Omega - 1|^{1/2}}, \tag{2.9}$$

and physically this sets the scale over which effects of curvature become important.

The energy content of the Universe consists of matter and radiation (today, photons and neutrinos). Since the photon temperature is accurately known, $T_0 = 2.73 \pm 0.01 \, \text{K}$, the fraction of critical density contributed by radiation is also accurately known: $\Omega_R h^2 = 4.2 \times 10^{-5}$, where $h = 0.732^{+0.07}_{-0.03}$ is the present Hubble rate in units of $100 \, \text{km sec}^{-1} \, \text{Mpc}^{-1}$. The rest is some other

type of matter. Using WMAP data only, the best fit values for cosmological parameters for the power-law flat ΛCDM model are [32, 33]

$$
\begin{aligned}
\Omega_m h^2 &= 0.127^{+0.007}_{-0.013}, \\
\Omega_b h^2 &= 0.0223^{+0.0007}_{-0.0009}, \\
\Omega_c h^2 &= 0.1054^{+0.0078}_{-0.0077}, \\
\Omega_\Lambda &= 0.759 \pm 0.0034
\end{aligned}
$$

In a flat Universe, the combination of WMAP and the Supernova Legacy Survey (SNLS) data yields a significant constraint on the equation of state of the dark energy, $w = 0.97^{+0.07}_{-0.09}$. If we assume $w = 1$, then the deviations from the critical density, Ω_k , are small: the combination of WMAP and the SNLS data imply $\Omega_k = 0.015^{+0.020}_{-0.016}$. The combination of WMAP three year data plus the HST key project constraint on H_0 implies $\Omega_k = 0.010^{+0.016}_{-0.009}$ and $\Omega_\Lambda = 0.720.04$. So apparently, this Universe is born from a burst of rapid expansion, Inflation, during which quantum noise was stretched to astrophysical size seeding cosmic structure.

2.1.2   Early Universe Formalisms

We would like to introduce the concept of conformal time which will be useful in the next sections. The conformal time τ is defined through the following relation

$$
d\tau = \frac{dt}{a}. \tag{2.10}
$$

The metric (2.1) then becomes

$$
ds^2 = -a^2(\tau) \left[d\tau^2 - \frac{dr^2}{1 - kr^2} - r^2(d\theta^2 + \sin^2\theta \, d\phi^2) \right]. \tag{2.11}
$$

The reason why τ is called conformal is manifest from Eq. (2.11): the corresponding FRW line element is conformal to the Minkowski line element describing a static four dimensional hypersurface. Any function $f(t)$ satisfies the rule

$$
\dot{f}(t) = \frac{f'(\tau)}{a(\tau)}, \tag{2.12}
$$

$$
\ddot{f}(t) = \frac{f''(\tau)}{a^2(\tau)} - \mathcal{H}\frac{f'(\tau)}{a^2(\tau)}, \tag{2.13}
$$

where a prime now indicates differentation with respect to the conformal time τ and

$$\mathcal{H} = \frac{a'}{a}. \tag{2.14}$$

In particular we can set the following rules:

$$H = \frac{\dot{a}}{a} = \frac{a'}{a^2} = \frac{\mathcal{H}}{a}, \tag{2.15}$$

$$\ddot{a} = \frac{a''}{a^2} - \frac{\mathcal{H}^2}{a}, \tag{2.16}$$

$$\dot{H} = \frac{\mathcal{H}'}{a^2} - \frac{\mathcal{H}^2}{a^2}, \tag{2.17}$$

Finally, if the scale factor $a(t)$ scales like $a \sim t^n$, solving the relation (2.10) we find

$$a \sim t^n \implies a(\tau) \sim \tau^{\frac{n}{1-n}}. \tag{2.18}$$

We want to introduce now another important concept: the *particle horizon*. Photons travel on null paths characterized by $dr = dt/a(t)$; the physical distance that a photon could have traveled since the bang until time t, the distance to the particle horizon, is

$$\begin{aligned} R_H(t) &= a(t) \int_0^t \frac{dt'}{a(t')} \\ &= \frac{t}{(1-n)} = n\frac{H^{-1}}{(1-n)} \sim H^{-1} \qquad \text{for } a(t) \propto t^n, \quad n < 1. \end{aligned} \tag{2.19}$$

Using the conformal time, the particle horizon becomes

$$R_H(t) = a(\tau) \int_{\tau_0}^\tau d\tau, \tag{2.20}$$

where τ_0 indicates the conformal time corresponding to $t = 0$. Note, in the standard cosmology the distance to the horizon is finite, and up to numerical factors, equal to the age of the Universe or the Hubble radius, H^{-1}. For this reason, we will use horizon and Hubble radius interchangeably. Note also that a physical length scale λ is within the horizon if $\lambda < R_H \sim H^{-1}$. Since we can identify the length scale λ with its wavenumber k, $\lambda = 2\pi a/k$, we will have the following characterizations:

$$\frac{k}{aH} \ll 1 \Longrightarrow \text{SCALE } \lambda \text{ OUTSIDE THE HORIZON}$$

$$\frac{k}{aH} \gg 1 \Longrightarrow \text{SCALE } \lambda \text{ WITHIN THE HORIZON}$$

Another important quantity is the entropy within a horizon volume: $S_{\text{HOR}} \sim H^{-3}T^3$; during the radiation-dominated epoch $H \sim T^2/m_{\text{Pl}}$[34], so that

$$S_{\text{HOR}} \sim \left(\frac{m_{\text{Pl}}}{T}\right)^3 . \tag{2.21}$$

2.1.3 The Early Radiation-dominated Universe

In any case, at present, matter outweights radiation by a wide margin. However, since the energy density in matter decreases as a^{-3}, and that in radiation as a^{-4} (the extra factor due to the red shifting of the energy of relativistic particles), at early times the Universe was radiation dominated—indeed the calculations of primordial nucleosynthesis provide excellent evidence for this. Denoting the epoch of matter-radiation equality by subscript 'EQ,' and using $T_0 = 2.73\,\text{K}$, it follows that

$$a_{\text{EQ}} = 4.18 \times 10^{-5} \, (\Omega_0 h^2)^{-1}; \qquad T_{\text{EQ}} = 5.62(\Omega_0 h^2)\,\text{eV}; \tag{2.22}$$

$$t_{\text{EQ}} = 4.17 \times 10^{10}(\Omega_0 h^2)^{-2}\,\text{sec}. \tag{2.23}$$

At early times the expansion rate and age of the Universe were determined by the temperature of the Universe and the number of relativistic degrees of freedom:

$$\rho_{\text{rad}} = g_*(T)\frac{\pi^2 T^4}{30}; \qquad H \simeq 1.67 g_*^{1/2} T^2/m_{\text{Pl}}; \tag{2.24}$$

$$\Rightarrow a \propto t^{1/2}; \qquad t \simeq 2.42 \times 10^{-6} g_*^{-1/2}(T/\,\text{GeV})^{-2}\,\text{sec}; \tag{2.25}$$

where $g_*(T)$ counts the number of ultra-relativistic degrees of freedom ($\approx$ the sum of the internal degrees of freedom of particle species much less massive than the temperature) and $m_{\text{Pl}} \equiv G^{-1/2} = 1.22 \times 10^{19}\,\text{GeV}$ is the Planck mass. For example, at the epoch of nucleosynthesis, $g_* = 10.75$ assuming three, light ($\ll$ MeV) neutrino species; taking into account all the species in the standard model, $g_* = 106.75$ at temperatures much greater than $300\,\text{GeV}$.

A quantity of importance related to g_* is the entropy density in relativistic particles,

$$s = \frac{\rho + P}{T} = \frac{2\pi^2}{45} g_* T^3,$$

and the entropy per comoving volume,

$$S \quad \propto \quad a^3 s \quad \propto \quad g_* a^3 T^3.$$

By a wide margin most of the entropy in the Universe exists in the radiation bath. The entropy density is proportional to the number density of relativistic particles. At present, the relativistic particle species are the photons and neutrinos, and the entropy density is a factor of 7.04 times the photon-number density: $n_\gamma = 413\,\text{cm}^{-3}$ and $s = 2905\,\text{cm}^{-3}$.

In thermal equilibrium—which provides a good description of most of the history of the Universe—the entropy per comoving volume S remains constant. This fact is very useful. First, it implies that the temperature and scale factor are related by

$$T \propto g_*^{-1/3} a^{-1}, \tag{2.26}$$

which for $g_* = \text{const}$ leads to the familiar $T \propto a^{-1}$.

Second, it provides a way of quantifying the net baryon number (or any other particle number) per comoving volume:

$$N_B \equiv R^3 n_B = \frac{n_B}{s} \simeq (4-7) \times 10^{-11}. \tag{2.27}$$

The baryon number of the Universe tells us two things: (1) the entropy per particle in the Universe is extremely high, about 10^{10} or so compared to about 10^{-2} in the sun and a few in the core of a newly formed neutron star. (2) The asymmetry between matter and antimatter is very small, about 10^{-10}, since at early times quarks and antiquarks were roughly as abundant as photons. One of the great successes of particle cosmology is baryogenesis, the idea that B, C, and CP violating interactions occurring out-of-equilibrium early on allow the Universe to develop a net baryon number of this magnitude [35, 36].

Finally, the constancy of the entropy per comoving volume allows us to characterize the size of comoving volume corresponding to our present Hubble

volume in a very physical way: by the entropy it contains,

$$S_U = \frac{4\pi}{3} H_0^{-3} s \simeq 10^{90}. \tag{2.28}$$

The standard cosmology is tested back to times as early as about 0.01 sec; it is only natural to ask how far back one can sensibly extrapolate. Since the fundamental particles of Nature are point-like quarks and leptons whose interactions are perturbatively weak at energies much greater than $1\,\mathrm{GeV}$, one can imagine extrapolating as far back as the epoch where general relativity becomes suspect, i.e., where quantum gravitational effects are likely to be important: the Planck epoch, $t \sim 10^{-43}\,\mathrm{sec}$ and $T \sim 10^{19}\,\mathrm{GeV}$. Of course, at present, our firm understanding of the elementary particles and their interactions only extends to energies of the order of $100\,\mathrm{GeV}$, which corresponds to a time of the order of $10^{-11}\,\mathrm{sec}$ or so. We can be relatively certain that at a temperature of $100\,\mathrm{MeV} - 200\,\mathrm{MeV}$ ($t \sim 10^{-5}\,\mathrm{sec}$) there was a transition (likely a second-order phase transition) from quark/gluon plasma to very hot hadronic matter, and that some kind of phase transition associated with the symmetry breakdown of the electroweak theory took place at a temperature of the order of $300\,\mathrm{GeV}$ ($t \sim 10^{-11}\,\mathrm{sec}$).

2.2 The Problems of Big Bang Theory

The Big Bang cosmology presents three problems: the horizon or large-scale smoothness problem; the small-scale inhomogeneity problem (origin of density perturbations); and the flatness or oldness problem. They are not inconsistencies of the model, yet they seem to require very special initial data for the model to produce an Universe that is qualitatively similar to ours today.

2.2.1 The Flatness Problem

Let us assume that Einstein equations are valid until the Planck era ($T_{\mathrm{Pl}} \sim m_{\mathrm{Pl}} \sim 10^{19}\,\mathrm{GeV}$). From eq. (2.8), we read that if the Universe is perfectly flat, then ($\Omega = 1$) at all times. On the other hand, if there is even a small curvature term, the time dependence of ($\Omega - 1$) is quite different.

During a radiation-dominated period, we have that $H^2 \propto \rho_R \propto a^{-4}$ and

$$\Omega - 1 \propto \frac{1}{a^2 a^{-4}} \propto a^2. \tag{2.29}$$

During Matter Domination, $\rho_M \propto a^{-3}$ and

$$\Omega - 1 \propto \frac{1}{a^2 a^{-3}} \propto a. \tag{2.30}$$

In both cases $(\Omega - 1)$ decreases going backwards with time. Since we know that today $(\Omega_0 - 1)$ is of order unity at present, we can deduce its value at t_{Pl} (the time at which the temperature of the Universe is $T_{\mathrm{Pl}} \sim 10^{19}$ GeV)

$$\frac{\mid \Omega - 1 \mid_{T=T_{\mathrm{Pl}}}}{\mid \Omega - 1 \mid_{T=T_0}} \approx \left(\frac{a_{\mathrm{Pl}}^2}{a_0^2}\right) \approx \left(\frac{T_0^2}{T_{\mathrm{Pl}}^2}\right) \approx \mathcal{O}(10^{-64}). \tag{2.31}$$

where 0 stands for the present epoch, and $T_0 \sim 10^{-13}$ GeV is the present-day temperature of the CMB radiation. In order to get the correct value of $(\Omega_0 - 1) \sim 1$ at present, the value of $(\Omega - 1)$ at early times have to be fine-tuned to values amazingly close to zero, but without being exactly zero. This is the reason why the flatness problem is also dubbed the 'fine-tuning problem'.

2.2.2   The Entropy Problem

Let us now see how the hypothesis of adiabatic expansion of the Universe is connected with the flatness problem. From the Friedman equation (2.3) we know that during a radiation-dominated period

$$H^2 \simeq \rho_R \simeq \frac{T^4}{m_{\mathrm{Pl}}^2}, \tag{2.32}$$

from which we deduce

$$\Omega - 1 = \frac{k m_{\mathrm{Pl}}^2}{a^4 T^4} = \frac{k m_{\mathrm{Pl}}^2}{S^{\frac{2}{3}} T^2}. \tag{2.33}$$

Adiabatic expansions means that S is constant over the evolution of the Universe. Hence:

$$|\Omega - 1|_{t=t_{\mathrm{Pl}}} = \frac{m_{\mathrm{Pl}}^2}{T_{\mathrm{Pl}}^2} \frac{1}{S_U^{2/3}} = \frac{1}{S_U^{2/3}} \approx 10^{-60}. \tag{2.34}$$

We see that $(\Omega - 1)$ is so close to zero at early epochs because the total entropy of our Universe is so incredibly large. The problem of understanding why the (classical) initial conditions corresponded to a Universe that was so "fine-tuned" to spatial flatness is the flatness problem. Such a balance is possible in principle but it feels weird to demand a precision of one over 10^{60} for the initial data. On the other hand, the flatness problem arises because the entropy in a comoving volume is conserved. Therefore, if the expansion was not adiabatic for some finite time intervals the flatness problem could be solved.

2.2.3   The Horizon Problem

According to the standard cosmology, photons decoupled from the rest of the components (electrons and baryons) at a temperature of the order of 0.3 eV. This corresponds to the so-called surface of 'last-scattering' at a red shift of about 1100 and an age of about $180,000 \, (\Omega_0 h^2)^{-1/2} \, \mathrm{yrs}$. From the epoch of last-scattering onwards, photons free-stream and reach us basically untouched. Detecting primordial photons is therefore equivalent to take a picture of the Universe when the latter was about 300,000 yrs old. The spectrum of the cosmic background radiation (CBR) is consistent that of a black body at temperature $2.726 \pm 0.01 \, \mathrm{K}$ over more than three decades in wavelength (FIRAS instrument on the COBE[37]). The length corresponding to our present Hubble radius (which is approximately the radius of our observable Universe) at the time of last-scattering was

$$\lambda_H(t_{\mathrm{LS}}) = R_H(t_0) \left(\frac{a_{\mathrm{LS}}}{a_0} \right) = R_H(t_0) \left(\frac{T_0}{T_{\mathrm{LS}}} \right).$$

During the matter-dominated period instead the Hubble length has decreased with a different law

$$H^2 \propto \rho_M \propto a^{-3} \propto T^3.$$

So at last-scattering we get

$$H_{LS}^{-1} = R_H(t_0) \left(\frac{T_{LS}}{T_0} \right)^{-3/2} \ll R_H(t_0).$$

The length corresponding to our present Hubble radius was much larger that the horizon at that time. This can be shown comparing the volumes built with these two scales

$$\frac{\lambda_H^3(T_{LS})}{H_{LS}^{-3}} = \left(\frac{T_0}{T_{LS}}\right)^{-\frac{3}{2}} \approx 10^6. \qquad (2.35)$$

From the last equation we see that there were about 10^6 causally disconnected regions within the volume that now corresponds to our horizon. Such an huge number is difficult to explain with a process other than an early hot and dense phase in the history of the Universe that would lead to a precise black body [38] for a bath of photons which were causally disconnected the last time they interacted with the surrounding plasma.

Suppose, that λ indicates the distance between two photons we detect today. From Eq. (2.35) we discover that at the time of emission (last-scattering) the two photons could not talk to each other. This highlights another feature of the horizon problem which is related to the problem of initial conditions for the cosmological perturbations. In fact we see that photons which were causally disconnected at the last-scattering surface have the same small anisotropies! The existence of particle horizons in the standard cosmology (non inflationary cosmology) precludes explaining the smoothness as a result of microphysical events: the horizon at decoupling, the last time one could imagine temperature fluctuations being smoothed by particle interactions, corresponds to an angular scale on the sky of about 1°, which precludes temperature variations on larger scales from being erased [34].

To account for the small-scale lumpiness of the Universe today, density perturbations with horizon-crossing amplitudes of 10^{-5} on scales of $1\,\mathrm{Mpc}$ to $10^4\,\mathrm{Mpc}$ or so are required. However, in the standard cosmology the physical size of a perturbation, which grows as the scale factor, begins larger than the horizon and relatively late in the history of the Universe crosses inside the horizon. This precludes a causal microphysical explanation for the origin of the required density perturbations.

Therefore to solve these problems of the Big Bang theory we need to modify it assuming a non-adiabatic period (entropy and flatness problems) and a primordial expansion period during which physical scales evolved faster

than the horizon H^{-1}.

In fact, if there is such a period, length scales λ which are within the horizon today, $\lambda < H^{-1}$ (such as the distance between two detected photons) and were outside the horizon for some period, $\lambda > H^{-1}$ (for istance at the time of last-scattering when the two photons were emitted), had a chance to be within the horizon at some earlier epoch, $\lambda < H^{-1}$ again. If we find a mechanism that produces these conditions, the homogeneity and the isotropy of the CMB can be explained by saying that photons that we receive today and were emitted from the last-scattering surface from causally disconnected regions have the same temperature because they were in causal contact at some primordial stage of the evolution of the Universe.

Then, the inflationary condition can be written in terms of the scale factor: a given scale λ scales like $\lambda \sim a$ and $H^{-1} = a/\dot{a}$; we impose during some period:

$$\left(\frac{\lambda}{H^{-1}}\right)^{\cdot} = \ddot{a} > 0.$$

Hence, *an inflationary stage is a period of the Universe during which the latter accelerates* $(\ddot{a} > 0)$ [2].

2.3   The Inflationary Paradigm

Now that the problems of the standard Big Bang cosmology are clear, we present the basics of the mechanism that solves them elegantly, Inflation [1].

As far as the dynamics of Inflation is concerned one can consider again a homogeneous and isotropic Universe described by the Friedmann–Robertson–Walker (FRW) metric (2.1). If -as we will always assume- the Universe is filled with matter described by the energy–momentum tensor $T_{\mu\nu}$ of a perfect fluid with energy density ρ and pressure P, the Einstein equations

$$G_{\mu\nu} = 8\pi G_{\mathrm{N}}\, T_{\mu\nu}\,, \tag{2.36}$$

with $G_{\mu\nu}$ the Einstein tensor and G_{N} the Newtonian gravitational constant give the Friedmann equations [31]

$$H^2 = \frac{8\pi G_{\mathrm{N}}}{3}\, \rho - \frac{K}{a^2}\,, \tag{2.37}$$

---

[1]For more details we refer to some reviews on the subject [39, 40, 41].

$$\frac{\ddot{a}}{a} = -\frac{4\pi G_{\mathrm{N}}}{3}(\rho + 3P)\,, \tag{2.38}$$

where $H = \dot{a}/a$ is the Hubble expansion parameter and dots denote differentiation with respect to cosmic time t. Eq. (2.38) shows that a period of Inflation is possible if the pressure P is negative with

$$P < -\frac{\rho}{3}\,. \tag{2.39}$$

In particular a period of the history of Universe during which $P = -\rho$ is called a *de Sitter stage*. From the energy continuity equation $\dot{\rho} + 3H(\rho + P) = 0$ and eq. (2.37) (neglecting the curvature K which is redshifted away as a^{-2}) we see that in a de Sitter phase $\rho = \mathrm{constant}$ and

$$H = H_I = \mathrm{constant}\,. \tag{2.40}$$

Solving Eq. (2.38) we also see the scale–factor grows exponentially

$$a(t) = a_i\, e^{H_I(t-t_i)}\,, \tag{2.41}$$

where t_i is the time Inflation starts. The condition (2.39) can be satisfied by a scalar field, the inflaton ϕ. So we consider the action for a minimally–coupled scalar field ϕ, which is given by [23, 25]

$$S = \int d^4x \sqrt{-g}\,\mathcal{L} = \int d^4x \sqrt{-g}\left[-\frac{1}{2}g^{\mu\nu}\partial_\mu\phi\partial_\nu\phi - V(\phi)\right]\,, \tag{2.42}$$

where g is the determinant of the metric tensor $g_{\mu\nu}$, $g_{\mu\nu}$ is the contravariant metric tensor, such that $g_{\mu\nu}g^{\nu\lambda} = \delta_\mu^\lambda$; $V(\phi)$ specifies the scalar field potential. One can vary the action with respect to ϕ and obtains the Klein–Gordon equation

$$\Box\phi = \frac{\partial V}{\partial \phi}\,, \tag{2.43}$$

where $\Box$ is the covariant D'Alembert operator

$$\Box\phi = \frac{1}{\sqrt{-g}}\,\partial_\nu\left(\sqrt{-g}\,g^{\mu\nu}\,\partial_\mu\phi\right)\,. \tag{2.44}$$

In a FRW Universe (2.1), the evolution equation for the scalar field ϕ becomes

$$\ddot{\phi} + 3H\dot{\phi} - \frac{\nabla^2\phi}{a^2} + V'(\phi) = 0\,, \tag{2.45}$$

where $V'(\phi) = (dV(\phi)/d\phi)$.

The friction term $3H\dot{\phi}$ is important since it means that a scalar field rolling down its potential suffers a friction due to the expansion of the Universe. The energy–momentum tensor for a minimally–coupled scalar field ϕ is given by [42]

$$T_{\mu\nu} = -2\frac{\partial\mathcal{L}}{\partial g^{\mu\nu}} + g_{\mu\nu}\mathcal{L} = \partial_\mu\phi\partial_\nu\phi + g_{\mu\nu}\left[-\frac{1}{2}g^{\alpha\beta}\partial_\alpha\phi\partial_\beta\phi - V(\phi)\right] . \quad (2.46)$$

We want now to study the perturbations of the scalar field. So we now split the inflaton field as

$$\phi(t,\mathbf{x}) = \phi_0(t) + \delta\phi(t,\mathbf{x}),$$

where ϕ_0 is the expectation value of the inflaton field on the initial isotropic and homogeneous state, while $\delta\phi(t,\mathbf{x})$ represents the quantum fluctuations around ϕ_0, which are the feature we are interested in.

First we follow the evolution of the "classical" part ϕ_0. The evolution of the quantum fluctuations will be treated later. The separation is possible because quantum fluctuations are much smaller than the classical value and therefore negligible when looking at the classical evolution. A homogeneous scalar field $\phi(t)$ behaves like a perfect fluid with background energy density and pressure given by

$$\rho_\phi = \frac{\dot{\phi}^2}{2} + V(\phi) \qquad (2.47)$$

$$P_\phi = \frac{\dot{\phi}^2}{2} - V(\phi). \qquad (2.48)$$

Therefore assuming $V(\phi) \gg \dot{\phi}^2$, we obtain the following condition $P_\phi \simeq -\rho_\phi$. We find then that a scalar field whose energy is dominant in the Universe and whose potential energy dominates over the kinetic term gives Inflation. Hence, Inflation is driven by the vacuum energy of the inflaton field. Ordinary matter fields, in the form of a radiation fluid, and the spatial curvature K are usually neglected during Inflation because their contribution to the energy density is redshifted away during the accelerated expansion.

Let us specify a little better now which are the conditions under which a

scalar field can induce an inflationary period. The equation of motion of an homogeneous scalar field is

$$\ddot{\phi} + 3H\dot{\phi} + V'(\phi) = 0 \,. \qquad (2.49)$$

We want to have a finite inflationary period, so we want the field to roll down its potential to a minimum. To have this we require again $\dot{\phi}^2 \ll V(\phi)$, so that one can neglect the kinetic contributions to the scalar field behaviour. Such a *slow-roll* period can be achieved if the inflaton field ϕ is in a region where the potential is sufficiently flat. Since the potential is very flat also the second time derivative of the field will be small. We will assume that this is true and we will quantify this condition soon. Assuming that the inflaton field dominates the energy density of the Universe, the Friedmann equation (2.37) becomes

$$H^2 \simeq \frac{8\pi G_{\mathrm{N}}}{3} V(\phi), \qquad (2.50)$$

and the new equation of motion becomes

$$3H\dot{\phi} = -V'(\phi) \,, \qquad (2.51)$$

which gives $\dot{\phi}$ as a function of $V'(\phi)$. Using Eq. (2.51) the slow–roll conditions then require

$$\dot{\phi}^2 \ll V(\phi) \Longrightarrow \frac{(V')^2}{V} \ll H^2 \qquad (2.52)$$

and

$$\ddot{\phi} \ll 3H\dot{\phi} \Longrightarrow V'' \ll H^2. \qquad (2.53)$$

Equations. (2.52) and (2.53) represent the flatness conditions on the potential which are conveniently parametrized in terms of the the *slow–roll parameters*, built from V and its derivatives with respect to ϕ [21, 43, 44]. In particular, we define the two usual slow–roll parameters [21]:

$$\epsilon = \frac{m_{\mathrm{P}}^2}{2} \left(\frac{V'}{V} \right)^2 \,, \eta = m_{\mathrm{P}}^2 \left(\frac{V''}{V} \right) \qquad (2.54)$$

Achieving a successful period of Inflation requires the slow–roll parameters to be $\epsilon, |\eta| \ll 1$. For example, if we write the parameter ϵ as $\epsilon = -\dot{H}/H^2$, thus

quantifying how much the Hubble rate H changes with time during Inflation, we notice that

$$\frac{\ddot{a}}{a} = \dot{H} + H^2 = (1 - \epsilon) H^2,$$

forces $\epsilon < 1$ to obtain an inflationary period. As soon as this condition fails, Inflation ends. At first–order in the slow–roll parameters ϵ and η can be considered constant, since the potential is very flat. In fact it is easy to see that that $\dot{\epsilon}, \dot{\eta} = \mathcal{O}(\epsilon^2, \eta^2)$, where by that we indicate general combinations of the slow–roll parameters of lowest order and next order respectively.

The number of inflationary models that have been proposed so far is enormous, differing for the kind of potential and for the underlying particle physics theory [21]. We just want to mention here that a useful classification in connection with the observations may be the one in which the single–field inflationary models are divided into three broad groups as "small field", "large field" (or chaotic) and "hybrid" type, according to the region occupied in the $(\epsilon - \eta)$ space by a given inflationary potential [45]. Typical examples of the large–field models $(0 < \eta < 2\epsilon)$ are polynomial potentials $V(\phi) = \Lambda^4 (\phi/\mu)^p$, and exponential potentials, $V(\phi) = \Lambda^4 \exp(\phi/\mu)$. The small–field potentials ($\eta < -\epsilon$) are typically of the form $V(\phi) = \Lambda^4 [1 - (\phi/\mu)^p]$, while generic hybrid potentials $(0 < 2\epsilon < \eta)$ are of the form $V(\phi) = \Lambda^4 [1 + (\phi/\mu)^p]$. In fact according to such a scheme, the *WMAP* dataset already allows to extract the parameters relevant for distinguishing among single–field Inflation models [11, 46, 12, 47].

The crucial quantity for the inflationary dynamics and for understanding the generation of the primordial perturbations during Inflation is the Hubble radius (also called the Hubble horizon size) $R_H = H^{-1}$, since it represents the characteristic length scale beyond which causal processes cannot operate. During Inflation the comoving Hubble horizon, $(aH)^{-1}$, decreases in time as the scale–factor, a, grows quasi–exponentially, and the Hubble radius remains almost constant. Therefore, a given comoving length scale, L, will become larger than the Hubble radius and *leave the Hubble horizon*. On the other hand, the comoving Hubble radius increases as $(aH)^{-1} \propto a^{1/2}$ and a during radiation and matter dominated era, respectively.

Inflation was born to solve the horizon and flatness problems. Therefore

we do not need simply a period of accelerated expansion of the Universe, but a period *long enough* to solve those problems. Long enough means that during that period a small, smooth patch smaller the Hubble radius manages to grow to encompass at least the observable Universe. A useful way to measure the amount of Inflation is in terms of the number of e–foldings, defined as

$$N_{\text{TOT}} = \int_{t_i}^{t_f} H dt \,, \tag{2.55}$$

where t_i and t_f are the time Inflation starts and ends respectively. The smoothness of the observable Universe requires then that the largest scale we observe today, the present horizon H_0^{-1} (~ 4200 Mpc), was reduced during Inflation to a value λ_{H_0} at t_i, which is smaller than H_I^{-1} during Inflation. Hence, we must have $N_{\text{TOT}} > N_{\text{min}}$, where $N_{\text{min}} \approx 60$ is the number of e–foldings before the end of Inflation when the present Hubble radius leaves the horizon. Another useful quantity is the number of e–foldings from the time when a given wavelength λ leaves the horizon during Inflation to the end of Inflation,

$$N_\lambda = \int_{t(\lambda)}^{t_f} H dt = \ln\left(\frac{a_f}{a_\lambda}\right) \,, \tag{2.56}$$

where $t(\lambda)$ is the time when λ leaves the horizon during Inflation and $a_\lambda = a(t(\lambda))$. The cosmologically interesting scales probed by the CMB anisotropies correspond to $N_\lambda \simeq 40 - 60$.

2.3.1   Inflation and Cosmological Perturbations

Let us proceed now to the important point, $\delta\phi(t, \mathbf{x})$. In the inflationary paradigm associated with these vacuum fluctuations there are primordial energy density perturbations, which survive after Inflation and are the origin of all the structures in the Universe. Our current understanding of the origin of structure in the Universe is that once the Universe became matter dominated ($z \sim 3200$) primeval density inhomogeneities ($\delta\rho/\rho \sim 10^{-5}$) were amplified by gravity and grew into the structure we see today [48, 49]. *COBE* confirmed the existence of these CMB anisotropies. In this section we just want to summarize in a qualitative way the process by which such "seed"

perturbations are generated during Inflation, since the aim of this thesis is exactly the study of those perturbations at nonlinear level.

First of all, in order for structure formation to occur via gravitational instability, there must have been small preexisting fluctuations on relevant physical length scales (say, a galaxy scale ~ 1 Mpc) which left the Hubble radius in the radiation–dominated and matter–dominated eras. Unfortunately in the standard Big–Bang model these small perturbations have to be put in by hand, being impossible to produce fluctuations on any length scales larger than the horizon size. Inflation elegantly solves this issue since it generates both density perturbations and gravitational waves. As we mentioned in the previous section, a key ingredient of this mechanism is the fact that during Inflation the comoving Hubble horizon $(aH)^{-1}$ decreases with time. Consequently, the wavelength of a quantum fluctuation in the scalar field whose potential energy drives Inflation soon exceeds the Hubble radius. The quantum fluctuations arise on scales which are much smaller than the comoving Hubble radius $(aH)^{-1}$, which is the scale beyond which causal processes cannot operate. On such small scales one can use the usual flat space–time quantum field theory to describe the scalar field vacuum fluctuations. The inflationary expansion then stretches the wavelength of quantum fluctuations to outside the horizon; thus, gravitational effects become more and more important and amplify the quantum fluctuations, the result being that a net number of scalar field particles are created by the changing cosmological background [4, 3]. On large scales the perturbations just follow a classical evolution. Since microscopic physics does not affect the evolution of fluctuations when its wavelength is outside the horizon, the amplitude of fluctuations is "frozen-in" and fixed at some nonzero value $\delta\phi$ at the horizon crossing, because of a large friction term $3H\dot{\phi}$ in the equation of motion of the field ϕ. The amplitude of the fluctuations on super-horizon scales then remains almost unchanged for a very long time, whereas its wavelength grows exponentially. Therefore, the appearance of such frozen fluctuations is equivalent to the appearance of a classical field $\delta\phi$ that does not vanish after having averaged over some macroscopic interval of time.

The fluctuations of the scalar field produce primordial perturbations in the energy density, ρ_ϕ, which are then inherited by the radiation and matter

to which the inflaton field decays during reheating after Inflation. Once Inflation has ended, however, the Hubble radius increases faster than the scale–factor, so the fluctuations eventually reenter the Hubble radius during the radiation or matter–dominated eras. The fluctuations that exit around 60 e-foldings or so before reheating reenter with physical wavelengths in the range accessible to cosmological observations. These spectra are therefore signatures of Inflation and give us a direct observational connection to physics of Inflation. These inflationary fluctuations can be measured by a variety different ways, including the analysis of CMB anisotropies. The *WMAP* collaboration has produced a full–sky map of the angular variations of the CMB, with unprecedented accuracy. The *WMAP* data confirm the detection of adiabatic *super-horizon fluctuations* which are a distinctive signature of an early epoch of acceleration [11].

Let us understand now how fluctuations are born and behave. Since gravity acts on any component of the Universe, small fluctuations of the inflaton field are intimately related to fluctuations of the space–time metric, giving rise to perturbations of the curvature ζ, which may loosely considered as a gravitational potential. The physical wavelengths λ of these perturbations grow exponentially and leave the horizon when $\lambda > H^{-1}$. On superhorizon scales, curvature fluctuations are frozen in and considered as classical. Finally, when the wavelength of these fluctuations reenters the horizon, at some radiation or matter–dominated epoch, the curvature (gravitational potential) perturbations of the space–time give rise to matter (and temperature) perturbations $\delta\rho$ via the Poisson equation. These fluctuations will then start growing, thus giving rise to the structures we observe today.

The mechanism by which the quantum fluctuations of the inflaton field are produced during an inflationary epoch is not peculiar to the inflaton field itself, rather it is generic to any scalar field evolving in an accelerated background. As we shall see, the inflaton field is peculiar in that it dominates the energy density of the Universe, thus possibly producing also metric perturbations.

In the following, we shall describe in a quantitative way how the quantum fluctuations of a generic scalar field evolve during an inflationary stage [39, 43, 41].

2.3.2 Quantum Fluctuations of a Generic Scalar Field during a de Sitter Stage

Let us first consider the case of a scalar field χ with an effective potential $V(\chi)$ in a pure de Sitter stage, during which H is constant. Notice that χ is a scalar field different from the inflaton – or the inflatons – that are driving the accelerated expansion.

As above we split the scalar field $\chi(\tau, \mathbf{x})$ as

$$\chi(\tau, \mathbf{x}) = \chi(\tau) + \delta\chi(\tau, \mathbf{x}) , \tag{2.57}$$

where $\chi(\tau)$ is the homogeneous classical value of the scalar field and $\delta\chi$ are its fluctuations and τ is the conformal time, related to the cosmic time t through $d\tau = dt/a(t)$. The scalar field χ is quantized by implementing the standard technique of second quantization. To proceed we first make the following field redefinition

$$\widetilde{\delta\chi} = a\delta\chi . \tag{2.58}$$

Introducing the creation and annihilation operators $a_\mathbf{k}$ and $a_\mathbf{k}^\dagger$ we promote $\widetilde{\delta\chi}$ to an operator which can be decomposed as [25]

$$\widetilde{\delta\chi}(\tau, \mathbf{x}) = \int \frac{d^3\mathbf{k}}{(2\pi)^{3/2}} \left[u_k(\tau)a_\mathbf{k}e^{i\mathbf{k}\cdot\mathbf{x}} + u_k^*(\tau)a_\mathbf{k}^\dagger e^{-i\mathbf{k}\cdot\mathbf{x}} \right] . \tag{2.59}$$

The creation and annihilation operators for $\widetilde{\delta\chi}$ (not for $\delta\chi$) satisfy the usual commutation relations

$$[a_\mathbf{k}, a_{\mathbf{k}'}] = 0, \quad [a_\mathbf{k}, a_{\mathbf{k}'}^\dagger] = \delta^{(3)}(\mathbf{k} - \mathbf{k}') , \tag{2.60}$$

and the modes $u_k(\tau)$ are normalized so that they satisfy the condition

$$u_k^* u_k' - u_k u_k^{*\prime} = -i, \tag{2.61}$$

deriving from the usual canonical commutation relations between the operators $\widetilde{\delta\chi}$ and its conjugate momentum $\Pi = \widetilde{\delta\chi}'$. Here primes denote derivatives with respect to the conformal time τ (not t).

The evolution equation for the scalar field $\chi(\tau, \mathbf{x})$ is given by the Klein–Gordon equation

$$\Box\chi = \frac{\partial V}{\partial\chi} , \tag{2.62}$$

where $\square$ is the D'Alembert operator defined in Eq. (2.44). The Klein–Gordon equation gives in an unperturbed FRW Universe

$$\chi'' + 2\,\mathcal{H}\chi' = -a^2\frac{\partial V}{\partial \chi}\,,\tag{2.63}$$

where $\mathcal{H} \equiv a'/a$ is the Hubble expansion rate in conformal time. Now, we perturb the scalar field but neglect the metric perturbations in the Klein–Gordon equation (2.62), the eigenfunctions $u_k(\tau)$ obey the equation of motion

$$u_k'' + \left(k^2 - \frac{a''}{a} + m_\chi^2 a^2 \right) u_k = 0\,,\tag{2.64}$$

where $m_\chi^2 = \partial^2 V/\partial\chi^2$ is the effective mass of the scalar field. The modes $u_k(\tau)$ at very short distances are not aware of the expansion, in that their oscillations are much faster than the expansion, and thus they must reproduce the form for the ordinary flat space–time quantum field theory. Thus, well within the horizon, in the limit $k/aH \rightarrow \infty$, the modes should approach plane waves of the form

$$u_k(\tau) \rightarrow \frac{1}{\sqrt{2k}}e^{-ik\tau}.\tag{2.65}$$

Before recovering the exact solution of eq. (2.64), let us study the limiting behaviour of Eq. (2.64) on sub-horizon and superhorizon scales. On sub-horizon scales $k^2 \gg a''/a$, the mass term is negligible so that Eq (2.64) reduces to

$$u_k'' + k^2 u_k = 0\,,\tag{2.66}$$

whose solution as expected is a plane wave

$$u_k \propto e^{-ik\tau}\,.\tag{2.67}$$

Thus fluctuations with wavelength within the cosmological horizon oscillate as in eq. (2.65). As mentioned above this is what we expect in the ultraviolet limit, *i.e.* wavelengths much smaller than the horizon scales see the space–time as flat. On the other hand, on superhorizon scales $k^2 \ll a''/a$, eq. (2.64) reduces to

$$u_k'' - \left(\frac{a''}{a} - m_\chi^2 a^2 \right) u_k = 0\tag{2.68}$$

We are interested in what happens in the case of a massless scalar field $(m_\chi^2 = 0)$. There are two solutions of eq. (2.68), a growing and a decaying mode:

$$u_k = B_+(k)a + B_-(k)a^{-2} \,. \tag{2.69}$$

We can fix the amplitude of the growing mode, B_+, by matching the (absolute value of the) solution (2.69) to the plane wave solution (2.65) when the fluctuation with wavenumber k leaves the horizon $(k = aH)$

$$|B_+(k)| = \frac{1}{a\sqrt{2k}} = \frac{H}{\sqrt{2k^3}} \,, \tag{2.70}$$

so that the quantum fluctuations of the original scalar field χ on superhorizon scales are constant,

$$|\delta\chi_k| = \frac{|u_k|}{a} = \frac{H}{\sqrt{2k^3}} \,. \tag{2.71}$$

Exact Solution

We can now derive the exact solution without any matching tricks [25, 20]. The exact solution to eq. (2.64) introduces some corrections due to a non–vanishing mass of the scalar field. In a de Sitter stage, as $a = -(H\tau)^{-1}$

$$\frac{a''}{a} - m_\chi^2 a^2 = \frac{2}{\tau^2}\left(1 - \frac{1}{2}\frac{m_\chi^2}{H^2}\right) \,, \tag{2.72}$$

so that eq. (2.64) can be rewritten as

$$u_k'' + \left(k^2 - \frac{\nu_\chi^2 - \frac{1}{4}}{\tau^2}\right)u_k = 0 \,, \tag{2.73}$$

where

$$\nu_\chi^2 = \left(\frac{9}{4} - \frac{m_\chi^2}{H^2}\right) \,. \tag{2.74}$$

When the mass m_χ^2 is constant in time, eq. (2.73) is a Bessel equation whose general solution for *real* ν_χ reads

$$u_k(\tau) = \sqrt{-\tau}\left[c_1(k)\,H_{\nu_\chi}^{(1)}(-k\tau) + c_2(k)\,H_{\nu_\chi}^{(2)}(-k\tau)\right] \,, \tag{2.75}$$

where $H^{(1)}_{\nu_\chi}$ and $H^{(2)}_{\nu_\chi}$ are the Hankel functions of first and second kind, respectively. Imposing now that in the ultraviolet regime $k \gg aH$ ($-k\tau \gg 1$) the solution matches the plane–wave solution $e^{-ik\tau}/\sqrt{2k}$ and knowing that

$$H^{(1)}_{\nu_\chi}(x \gg 1) \sim \sqrt{\frac{2}{\pi x}}\, e^{i\left(x - \frac{\pi}{2}\nu_\chi - \frac{\pi}{4}\right)} \quad , H^{(2)}_{\nu_\chi}(x \gg 1) \sim \sqrt{\frac{2}{\pi x}}\, e^{-i\left(x - \frac{\pi}{2}\nu_\chi - \frac{\pi}{4}\right)},$$

we set $c_2(k) = 0$ and $c_1(k) = \frac{\sqrt{\pi}}{2}\, e^{i\left(\nu_\chi + \frac{1}{2}\right)\frac{\pi}{2}}$, which also satisfy the normalization condition (2.61). The exact solution becomes

$$u_k(\tau) = \frac{\sqrt{\pi}}{2}\, e^{i\left(\nu_\chi + \frac{1}{2}\right)\frac{\pi}{2}}\, \sqrt{-\tau}\, H^{(1)}_{\nu_\chi}(-k\tau). \tag{2.76}$$

We are particularly interested in the asymptotic behaviour of the solution when the mode is well outside the horizon. On superhorizon scales, since $H^{(1)}_{\nu_\chi}(x \ll 1) \sim \sqrt{2/\pi}\, e^{-i\frac{\pi}{2}}\, 2^{\nu_\chi - \frac{3}{2}}\, (\Gamma(\nu_\chi)/\Gamma(3/2))\, x^{-\nu_\chi}$, the fluctuation (2.76) becomes

$$u_k(\tau) = e^{i\left(\nu_\chi - \frac{1}{2}\right)\frac{\pi}{2}} 2^{\left(\nu_\chi - \frac{3}{2}\right)} \frac{\Gamma(\nu_\chi)}{\Gamma(3/2)} \frac{1}{\sqrt{2k}} (-k\tau)^{\frac{1}{2} - \nu_\chi}. \tag{2.77}$$

Thus we find that on superhorizon scales, the fluctuation of the scalar field $\delta\chi_k \equiv u_k/a$ with a non–vanishing mass is not exactly constant, but it acquires a dependence upon time

$$|\delta\chi_k| = 2^{(\nu_\chi - 3/2)} \frac{\Gamma(\nu_\chi)}{\Gamma(3/2)} \frac{H}{\sqrt{2k^3}} \left(\frac{k}{aH}\right)^{\frac{3}{2} - \nu_\chi} \quad \text{(on superhorizon scales)} \tag{2.78}$$

Notice that the solution (2.78) is valid for values of the scalar field mass $m_\chi \leqslant 3/2H$. If the scalar field is very light, $m_\chi \ll 3/2H$, we can introduce the parameter $\eta_\chi = (m_\chi^2/3H^2)$ in analogy with the slow–roll parameters ϵ and η for the inflaton field, and make an expansion of the solution in eq. (2.78) to lowest order in $\eta_\chi = (m_\chi^2/3H^2) \ll 1$ to find

$$|\delta\chi_k| = \frac{H}{\sqrt{2k^3}} \left(\frac{k}{aH}\right)^{\frac{3}{2} - \nu_\chi}, \tag{2.79}$$

with

$$\frac{3}{2} - \nu_\chi \simeq \eta_\chi. \tag{2.80}$$

Eq. (2.79) is the fundamental result for the evolution of perturbations. In fact when the scalar field χ is light($m_\chi \ll 3/2H$), its quantum fluctuations, first generated on subhorizon scales, get gravitationally amplified and stretched to superhorizon scales due to the accelerated expansion of the inflationary Universe.

Power Spectrum

We want to introduce here another useful method to characterize the perturbations, the power spectrum. It measures the amplitude of quantum fluctuations at a given scale k. Since we are in flat space, we can expand in Fourier space the random field $f(t, \mathbf{x})$ by

$$f(t, \mathbf{x}) = \int \frac{d^3 \mathbf{k}}{(2\pi)^{3/2}} \, e^{i\mathbf{k} \cdot \mathbf{x}} \, f_{\mathbf{k}}(t) \,, \tag{2.81}$$

We define then the power spectrum $\mathcal{P}_f(k)$ as

$$\langle f_{\mathbf{k}_1} f_{\mathbf{k}_2}^* \rangle \equiv \frac{2\pi^2}{k^3} \, \mathcal{P}_f(k) \, \delta^{(3)}(\mathbf{k}_1 - \mathbf{k}_2) \,, \tag{2.82}$$

indeed from the definition (2.82) the mean square value of $f(t, \mathbf{x})$ in real space is

$$\langle f^2(t, \mathbf{x}) \rangle = \int \frac{dk}{k} \, \mathcal{P}_f(k) \,. \tag{2.83}$$

One may note then that the power–spectrum, $\mathcal{P}_f(k)$ is the contribution to the variance per unit logarithmic interval in the wavenumber k.

In the case of a scalar field χ the power–spectrum $\mathcal{P}_{\delta\chi}(k)$ can be evaluated by combining equations. (2.58), (2.59) and (2.60) [25, 29]

$$\langle \delta\chi_{\mathbf{k}_1} \delta\chi_{\mathbf{k}_2}^* \rangle = \frac{|u_k|^2}{a^2} \delta^{(3)}(\mathbf{k}_1 - \mathbf{k}_2) \,, \tag{2.84}$$

yielding

$$\mathcal{P}_{\delta\chi}(k) = \frac{k^3}{2\pi^2} |\delta\chi_k|^2 \,, \tag{2.85}$$

where, as usual, $\delta\chi_k \equiv u_k/a$.

The expression in eq. (2.85) is completely general. In the case of a de Sitter phase and a very light scalar field χ, with $m_\chi \ll 3/2H$ we find from eq. (2.79) that the power–spectrum on superhorizon scales is given by

$$\mathcal{P}_{\delta\chi}(k) = \left(\frac{H}{2\pi} \right)^2 \left(\frac{k}{aH} \right)^{3 - 2\nu_\chi} \,, \tag{2.86}$$

where ν_χ is given by eq. (2.80). A useful expression to keep in mind is that of a massless free scalar field in de Sitter space. In this case from eq. (2.76) with $\nu_\chi = 3/2$ one obtains

$$\delta\chi_k = (-H\tau) \left(1 - \frac{i}{k\tau} \right) \frac{e^{-ik\tau}}{\sqrt{2k}} \,. \tag{2.87}$$

The corresponding two–point correlation function for the Fourier modes is

$$
\begin{aligned}
\langle \delta\chi(\mathbf{k_1})\delta^*\chi(\mathbf{k_2})\rangle &= \delta^{(3)}(\mathbf{k_1} - \mathbf{k_2})\frac{H^2\tau^2}{2k_1}\left(1 + \frac{1}{k^2\tau^2}\right) && (2.88) \\
&\approx \delta^{(3)}(\mathbf{k_1} - \mathbf{k_2})\frac{H^2}{2k_1^3} \quad (\text{for } k_1\tau \ll 1)\,, && (2.89)
\end{aligned}
$$

with a power–spectrum which, on superhorizon scales, is given by

$$
\mathcal{P}_{\delta\chi}(k) = \left(\frac{H}{2\pi}\right)^2\,, \tag{2.90}
$$

which is exactly scale invariant. We stress that fluctuations of the scalar field can be generated on superhorizon scales as in eq. (2.78) only if the scalar field is light. If it is very massive in fact ($m_\chi \gg 3/2H$) the fluctuations of the scalar field remain in the vacuum state and do not produce perturbations on cosmologically relevant scales. We introduced here the correlation function since in the following two-point and four-point correlation functions will be the language that we will use in the calculations of the contributions of loop graphs to the perturbations. In fact result (2.90) is the fundamental result over which we will build the corrections in chapters 5 and 6 where we will analyze the importance of higher order diagrams in the perturbations and their contribution to the non Gaussianity.

Chapter 3

The Curvature Perturbation ζ

This chapter is dedicated to the study of the cosmological curvature perturbation (usually indicated by ζ) and its conservation under suitable hypothesis at all perturbation orders and during any era. This is of the greatest importance in the contest of this thesis, since the curvature perturbation is observable as opposed to scalar field perturbation, which cannot be directly measured. In particular, it is possible to obtain the conservation without invoking any field equation for gravity [50, 51]. Section 3.21 shows how a suitable geometry can be chosen and which are the requirements for conservation of ζ, while Section 3.2 goes a little forward, looking into how the curvature perturbation can evolve.

3.1 ΔN Formalism

3.1.1 Separate Universes and Geometry

Assuming a smooth spacetime it is possible to decompose the metric in the usual (3+1) ADM form. Defining $\mathcal{N}$ the lapse function , β^i the shift vector and γ_{ij} the usual spatial metric, the line element becomes:[1]

$$ds^2 = -\mathcal{N}^2 dt^2 + \gamma_{ij}(dx^i + \beta^i dt)(dx^j + \beta^j dt)\,. \qquad (3.1)$$

---

[1] As usual, Greek indices will take the values $\mu, \nu = 0, 1, 2, 3$, Latin indices $i, j = 1, 2, 3$. The spatial indices are raised or lowered by γ^{ij} or γ_{ij}.

The time-like vector n^μ normal to the hypersurface $x^0 = t = \text{constant}$ is $n_\mu = [-\mathcal{N}, 0]$ and $n^\mu = \left[\frac{1}{\mathcal{N}}, -\frac{\beta^i}{\mathcal{N}}\right]$. Since we are interested in perturbations, we will write the spatial metric as a product of two terms:

$$\gamma_{ij} \equiv e^{2\alpha}\tilde{\gamma}_{ij}\,, \tag{3.2}$$

where α and $\tilde{\gamma}_{ij}$ depend on spacetime coordinates and $det[\tilde{\gamma}_{ij}] = 1$. The condition on the determinant makes the exponential factor a locally-defined scale factor. We factor an $a(t)$ to show explicitly the dependence on inhomogeneities:

$$e^\alpha \equiv a(t)e^{\psi(t,x^i)}\,, \tag{3.3}$$

where $\psi(x_i, t)$ is the perturbation, that we assume to be small and with a vanishing value when averaged over a region of scale H^{-1}. Again, the spatial metric can be factored as $\tilde{\gamma} \equiv Ie^H$, where I is the identity matrix and H a traceless matrix[2]. Now that the metric is set, we need a theoretical frame to calculate the perturbations. We use here the gradient expansion approach, which is a spatial gradient expansion of the inhomogeneities. To be able to do this, there are two requirements:

- a smoothing scale, over which each observable quantity can be considered as smooth;

- a parameter χ to be used in the expansion of the power series;

The smoothing scale is not meant to smooth the field equations of any gravity theory in use, but more simply as a smoothing that gives a good approximation of the actual Universe on coordinate scales greater than k^{-1}, which immediately translates to $a(t)/k$ in our observable Universe. In a linear perturbation theory this would mean dropping the wavenumber greater than k in the Fourier expansion, but this is not our case since we want to obtain a non-linear general result. So we define the formal parameter χ to be used for the expansion. One can already assume:

$$\chi \equiv \frac{k}{aH}\,, \tag{3.4}$$

[2]This comes from the conditions on determinat of γ_{ij} through $det(e^H) = e^{Tr(H)}$

where H is the unperturbed Hubble parameter. This identification is interesting because the limit $\chi \to 0$ corresponds to the late time limit during Inflation, which is the era we are interested in. The central physical assumption is then: *in the limit of small χ the Universe is locally homogeneous and isotropic on a sufficiently large coordinate scale[3].*

What does it mean exactly local isotropy on large scale?
To explain it [52, 53, 54, 55] we consider that each different super-horizon sized region ($\gtrsim H^{-1}$) of the Universe is evolving as an indipendent Robertson-Walker Universe. Let us denote λ_s the typical coordinate size of the regions and assume that they are locally homogeneous over such scale, even if different regions may have different densities and pressures. We patch them together over a length scale $\simeq \lambda$, which is the perturbation coordinate length we are interested in. We then introduce also another length, λ_{BG}, to be considered as the background against which perturbations are defined. One may observe that it is not evident that each super-horizon region should behave as an unperturbed Universe. Still, there must be a scale λ_s over which it becomes a viable approximation, since, if there were not such a scale, then it would be impossible to define an unperturbed Robertson-Walker background and thus perturbations. This is usually called the *separate universes hypotesis*. Since we are considering a perturbed Universe we have the Hubble scale, the k^{-1} scale and eventually other scales coming from the stress-energy tensor, but as long as these are not larger than k^{-1} local isotropy and homogeneity are a good approximation in the late time limit (i.e. super-horizon era). Locally measurable parts of the metric are then those of a FLRW metric. Thus it is possible to find a set of coordinates where the metric in any local region becomes:

$$ds^2 = -dt^2 + a^2(t)\delta_{ij}dx^i dx^j \, . \tag{3.5}$$

In the limit $\chi \to 0$ the metric (3.5) is supposed to become globally valid. So we can obtain informations about the metric components by comparison with (3.1). The shift vector must disappear and so we have $\beta_i = O(\chi)$. The case of the spatial metric $\tilde{\gamma}_{ij}$ is a little different since it is time-dependent. It

---

[3]i.e. a FLRW Universe.

is not possible to locally transform it by a coordinate transformation, since there will be also a contribution from its time derivative. So to maintain the FLRW Universe we need also $\dot{\gamma}_{ij} = O(\chi)$. However, if $\dot{\gamma}_{ij}$ is linear in χ, it decays as $\tilde{a}^{-3}$ in Einstein gravity [50]. Since we are interested in conserved perturbations, it can be ignored. Therefore the condition on $\dot{\gamma}_{ij}$ is $O(\chi^2)$ and the line element (3.1) becomes:

$$ds^2 = -\mathcal{N}^2 dt^2 + 2\beta_i dx^i dt + \gamma_{ij} dx^i dx^j . \tag{3.6}$$

At this point we need to connect the metric with the energy density in space-time or in other words we need to choose a form for the stress-energy tensor. Being the involved cosmological scales so large, the hypothesis of "separate universes" let us assume the scale-free perfect fluid form for the stress-energy tensor.

$$T_{\mu\nu} \equiv [\rho(x^\mu) + P(x^\mu)] u_\mu u_\nu + g_{\mu\nu} P(x^\mu) . \tag{3.7}$$

What we will do now is choosing an appropriate set of coordinates (namely spatial coordinates comoving with the fluid) to calculate the 4-velocity divergence in the comoving frame and substitute it in the energy conservation equation. This should provide us with a direct relation between the yet ill-defined "perturbed Hubble parameter", ψ and $\mathcal{N}$.

The calculation proceeds as follows. We choose spatial coordinates comoving with the fluid, which are the ones whose threads $x^i = $ constant coincide with the comoving worldlines (integral curves of the 4-velocity field u^μ). The spatial velocity consistently vanishes ($v_i = \frac{u^i}{u^0} = 0$) and in components the 4-velocity is:

$$u^\mu = \left[\frac{1}{\sqrt{\mathcal{N}^2 - \beta^k \beta_k}}, 0\right] = \left[\frac{1}{\mathcal{N}}, 0\right] + O(\chi^2), \tag{3.8}$$

$$u_\mu = \left[-\sqrt{\mathcal{N}^2 - \beta^k \beta_k}, \frac{\beta_i}{\sqrt{\mathcal{N}^2 - \beta^k \beta_k}}\right] = \left[-\mathcal{N}, \frac{\beta_i}{\mathcal{N}}\right] + O(\chi^2). \tag{3.9}$$

The expansion of u^μ in the comoving coordinates is given by:

$$\theta \equiv \nabla_\mu u^\mu = \frac{1}{\sqrt{-g}} \partial_\mu \left(\sqrt{-g} u^\mu\right) = \frac{1}{e^{3\alpha}} \partial_0 \left(e^{3\alpha} u^0\right) \tag{3.10}$$

$$= \frac{1}{e^{3\alpha}} \partial_t \left(\frac{e^{3\alpha}}{\sqrt{\mathcal{N}^2 - \beta^i \beta_i}} \right) = \frac{3\dot{\alpha}}{\mathcal{N}} + O(\chi^2)$$

where $\tilde{\gamma}_{ij}$ does not appear because $\det \tilde{\gamma}_{ij} = 1$. The relation between the coordinate time $x^0 = t$ and the proper time τ along u^μ can be read directly from (3.8),

$$\frac{dt}{d\tau} = u^0 = \frac{1}{\sqrt{\mathcal{N}^2 - \beta^i \beta_i}} . \tag{3.11}$$

At this point we can insert into the energy conservation equation (calculated along worldlines),

$$0 = -u_\mu \nabla_\nu T^{\mu\nu} = \left[\frac{d}{d\tau} \rho + (\rho + P) \nabla_\mu u^\mu \right] = \left[\frac{d}{d\tau} \rho + (\rho + P) \theta \right] , \tag{3.12}$$

and multiply on each side by $\sqrt{\mathcal{N}^2 - \beta^k \beta_k}$,

$$\sqrt{\mathcal{N}^2 - \beta^k \beta_k} \left[\frac{d}{d\tau} \rho + (\rho + P) \theta \right] = \dot{\rho} + 3 (\rho + P) \dot{\alpha} + O(\chi^2) = 0 . \tag{3.13}$$

Equation (3.13) is the starting point for the curvature perturbation conservation, which we will treat in detail in section 3.1.2. However, before going ahead, it is useful to write down the expansion of the unit timelike vector normal to the constant t hypersurface, because this is closely related to θ and to the "perturbed Hubble parameter" we mentioned above. So, θ_n is:

$$\theta_n \equiv \nabla_\mu n^\mu = \frac{3\dot{\alpha}}{\mathcal{N}} - \frac{1}{\mathcal{N} e^{3\alpha}} \partial_i \left(e^{3\alpha} \beta^i \right) . \tag{3.14}$$

Comparing (3.14) and (3.8) we see that θ and θ_n coincide at order χ. On the base of this equivalence the "perturbed Hubble parameter" we mentioned can be defined more precisely. In particular we define the *local perturbed Hubble parameter* as:

$$\tilde{H} \equiv \frac{1}{3} \theta_n . \tag{3.15}$$

Derivating equation (3.3)

$$\frac{d}{dt} e^\alpha = \dot{\alpha} e^\alpha = \dot{a}(t) e^\psi + a(t) \dot{\psi} e^\psi , \tag{3.16}$$

and dividing by e^α,

$$\dot{\alpha} = \frac{\dot{a}}{a} + \dot{\psi} , \tag{3.17}$$

42

we obtain the expression for $\dot{\alpha}$ in terms of a and ψ. Finally substituting in (3.15), the result is:

$$\tilde{H} = \frac{1}{\mathcal{N}} \left(\frac{\dot{a}}{a} + \dot{\psi} \right) + O(\chi^2) , \qquad (3.18)$$

The coincidence of θ and θ_n at the linear order implies the same coincidence for any choice of threading that maintains $\beta^i = O(\chi)$. In fact, at any point (t, x^i), the threading change affects θ_n only at the order $O(\chi^2)$ hence it cannot break the equivalence. Secondly, we applied this machinery to the whole fluid, but it can be applied without modifications to any smaller volume of the fluid, as long as:

a) the subvolume does not exchange energy (i.e. behaves adiabatically), and

b) the comoving threading in respect to the subvolume maintains the condition $\beta^i = O(\chi)$.

3.1.2   Slicings

The ingredients of this section are spatial slices and slicings. As observed above the choice of threading of spacetime is effectively unique, because all the threadings are equivalent up to order χ^2, while we stop at χ. To completely characterize the spacetime foliation we need to specify a slicing or better we need to know how a change of slicing affects ψ. So we define the number of e-foldings of expansion along a comoving worldline [55, 51]:

$$N(t_2, t_1; x^i) \equiv \frac{1}{3} \int_{t_1}^{t_2} \theta \, \mathcal{N} dt = -\frac{1}{3} \int_{t_1}^{t_2} dt \, \frac{\dot{\rho}}{\rho + P} \bigg|_{x^i} , \qquad (3.19)$$

N is also called *integrated expansion*. Substituting equation (3.18) and performing the integration it follows:

$$\psi(t_2, x^i) - \psi(t_1, x^i) = N(t_2, t_1; x^i) - \ln \left[\frac{a(t_2)}{a(t_1)} \right] \qquad (3.20)$$

If we define the unperturbed background number of e-foldings as $N_0(t_2, t_1) \equiv \ln[a(t_2)/a(t_1)]$, the latter equation takes the form:

$$\psi(t_2, x^i) - \psi(t_1, x^i) = N(t_2, t_1; x^i) - N_0(t_2, t_1) \qquad (3.21)$$

The interpretation is straight-forward. Let us first assume to go from a flat slice at t_1 to another flat slice at t_2. By definition on flat slices ψ vanishes and so the left-hand side of equation (3.21) too, giving $N(t_2, t_1; x^i) = N_0(t_2, t_1)$. Note that N_0, being the unperturbed value, has no dependence on position and that the number of e-foldings between any two flat slices coincides with the unperturbed background value [51]. Let us now assume to move along two different slicings. Let them coincide at a given time, say t_1 in our notation, for a given point x^i. Let us specify now the slicings: the one denoted by the underscript "ρ" starts on a flat slice at t_1 and ends on an uniform-density slice at t_2, while the one denoted by "f" moves on flat slices for all times between t_1 and t_2. Applying eq. (3.21) we have:

$$\psi_\rho(t_2, x^i) - \psi_\rho(t_1, x^i) = N_\rho(t_2, t_1; x^i) - N_0(t_2, t_1)$$
$$\psi_f(t_2, x^i) - \psi_f(t_1, x^i) = N_f(t_2, t_1; x^i) - N_0(t_2, t_1)$$

but, since at $t = t_1$ the two slicings coincide and are on a flat slice, $\psi_\rho(t_1, x^i) = \psi_f(t_1, x^i) = 0$. Subtracting the second line from the first, we obtain:

$$\psi_\rho(t_2, x^i) = N_\rho(t_2, t_1; x^i) - N_0(t_2, t_1) \equiv \ \Delta N_\rho(t_2, t_1, x^i) \quad (3.22)$$

Note that eq. (3.22) is a completely non-linear version of the δN [51, 55] formalism and it follows directly from the geometry without specifying any field equation for gravity.

If we now assume P to be a function only of ρ, it possible to simplify the integrand function in eq. (3.19):

$$\int_{t_1}^{t_2} dt \frac{\dot\rho}{\rho + P} \rightarrow \int_{\rho(t_1, x^i)}^{\rho(t_2, x^i)} \frac{d\rho}{\rho + P}$$

obtaining so:

$$\psi(t_2, x^i) - \psi(t_1, x^i) = -\ln\left[\frac{a(t_2)}{a(t_1)}\right] - \frac{1}{3} \int_{\rho(t_1, x^i)}^{\rho(t_2, x^i)} \frac{d\rho}{\rho + P} \qquad (3.23)$$

44

Hence have constructed a time-slicing indipendent conserved quantity:

$$-\zeta(x^i) \equiv \psi(t, x^i) + \frac{1}{3} \int_{\rho(t)}^{\rho(t, x^i)} \frac{d\rho}{\rho + P} \qquad (3.24)$$

which on uniform-density slices ($\delta\rho = 0$) takes the comfortable form:

$$-\zeta(t) \equiv \psi_\rho(t) \qquad (3.25)$$

It must be stressed that this result holds only for adiabatic perturbations ($P = P(\rho)$). This result can be explained also as follow: if we set the integrated expansion $N = 0$ on an initial spacetime slice and integrate the local continuity equation [51]:

$$\frac{d\rho}{dN} = -3(\rho + P) \qquad (3.26)$$

we obtain $\rho = \rho(N + \Delta N)$, where ΔN is the integration constant for each worldline determined by the density on the initial slice ($N = 0$). Starting from a flat slice and considering an uniform-N sequence of slices, we see that ΔN does not depend on time by construction. So if we move along an uniform-N slicing, which we just showed on super-horizon scales is also an uniform-density slicing, ΔN is conserved and so ζ. In others words, *under the assumption of adiabatic perturbations uniform-density slices are separated by uniform expansion, therefore along uniform-density slicings ζ is conserved*. We want to stress again the importance of this result since it is:

- completely non-linear and thus valid for all orders in the perturbations, provided the adiabatic condition is satisfied;

- obtained without assuming a form for gravity and thus valid for any gravity field equations.

The non-linear result can be used to calculate the curvature perturbation in perturbation theory to any order. Using the nonlinear result (3.22), one can write at perturbation order n $\delta N_n = -\zeta_n$, where δN_n is obtained expanding N in power series of $\delta\rho$ centered on a flat slicing up

to order n and using the energy conservation eq. (3.13). For example, the result at second order is [51]:

$$\delta N_2 = \frac{H}{\dot{\rho}_0}\delta\rho_2 - 2\frac{H}{\dot{\rho}_0^2}\dot{\delta}\rho_1\delta\rho_1 + \left(H\frac{\ddot{\rho}_0}{\dot{\rho}_0} - \dot{H}\right)\left(\frac{\delta\rho_1}{\dot{\rho}_0}\right)^2 \qquad (3.27)$$

where the right-hand side is evaluated on flat slices.

3.2   Non-adiabatic Perturbations and Evolution of ζ

We showed at the non-linear level how ζ is conserved in adiabatic perturbations. Now the natural question is: how does ζ *change* when we consider non-adibatic perturbations? We address the problem using perturbation theory this time, namely we start at first order in density perturbations. We invoke the local conservation of the energy $n^\nu \mathrm{T}^\mu_{\nu;\mu} = 0$ and obtain the gauge-indipendent expression [55]:

$$\dot{\delta\rho} = -3H(\delta\rho + \delta P) + 3(\rho + P)[\dot{\psi} - \nabla^2(\sigma + v)] + \frac{\beta_k \beta^k}{\mathcal{N}^2} \qquad (3.28)$$

where σ is a scalar describing the shear and $\nabla^i v$ is the 3-velocity of the fluid. We assume the gradients are small and we neglect the shear terms [56], keeping the first two terms on the right side of eq. (3.28). On uniform-density slices $\psi = -\zeta$ and $\delta\rho = 0$ and therefore the adiabatic part of the pressure perturbation, δP_{ad}, vanishes. Hence the only contribute comes from non-adiabatic perturbations, $\delta P = \delta P_{nad}$. Equation (3.28) becomes then:

$$\dot{\zeta} = -\frac{H}{\rho + P}\delta P_{\mathrm{nad}} \qquad (3.29)$$

At first order, this reproduce the conservation of curvature perturbations ζ in the uniform-density gauge on large scales for adiabatic perturbations.
A scalar field cannot be in general described by an equation of state

$P(\rho)$ due to the total energy being split in kinetic and potential energy. However, the existence of an attractor solution for a strongly-damped inflaton field allows one to drop the decaying mode as Inflation progresses and ensures a unique relation between the field value and its first derivative.

The relation between the scalar field and the curvature depends on the chosen gauge. We calculate then the scalar field value in the comfortable flat gauge ($\psi = 0$, also called *uniform-curvature*) and then trasform to the uniform-density gauge in order to recover ζ.

The field perturbations have the gauge-invariant definition [57]

$$\delta\phi + \frac{\dot{\phi}}{H}\psi \,. \tag{3.30}$$

where by gauge invariant we mean that (3.30) does not change under

$$
\begin{aligned}
t &\rightarrow t + \delta t \\
\delta\phi &\rightarrow \delta\phi - \dot{\phi}\delta\phi \\
\psi &\rightarrow \psi + H\delta t
\end{aligned}
\tag{3.31}
$$

On flat slices then field perturbations take the form $\delta\phi_\psi = \delta\phi$. On comoving slices the scalar field is uniform and so $\delta\phi_c = 0$. Inserting the latter in eq.(3.30),

$$\delta\phi_\psi = \delta\phi_c + \frac{\dot{\phi}_c}{H}\psi_c = \frac{\dot{\phi}_c}{H}\psi_c \,, \tag{3.32}$$

and finally:

$$\psi_c = \frac{H}{\dot{\phi}}\delta\phi_\psi \,, \tag{3.33}$$

where the time derivative is taken over coordinate time. The curvature perturbation on comoving hypersurfaces ψ_c is usually denoted $-\zeta$. Moreover in an arbitrary gauge, for a scalar field, density and pressure perturbations have the form:

$$
\begin{aligned}
\delta\rho &= \dot{\phi}\,\dot{\delta\phi} - A\dot{\phi}^2 + V'\delta\phi \,, \tag{3.34} \\
\delta P &= \dot{\phi}\,\dot{\delta\phi} - A\dot{\phi}^2 - V'\delta\phi \,, \tag{3.35}
\end{aligned}
$$

where $V' \equiv dV/d\phi$ and $A = 1 - 1/\mathcal{N}$ [41]. Subtracting the second from the first we have:

$$\delta\rho - \delta P = 2V'\delta\phi \tag{3.36}$$

Assuming again adiabatic perturbation on a uniform-density slice and $V' \neq 0$, $\delta\rho$ and δP vanish giving $\delta\phi_\rho = 0$. Using eq. (3.33) to first order in $\delta\rho$:

$$-\zeta = \frac{H}{\dot{\phi}^{(0)}}\delta\phi_\psi \tag{3.37}$$

We can use this simple result to study the case of multiple adiabatic fluids.

3.2.1 Multiple Adiabatic Fluids

Let us suppose to have a a certain number of fluids. Each fluid behaves adiabatically. So, from eq. (3.29), we see that:

$$\dot{\zeta}_i = H\frac{\delta\rho_i}{\dot{\rho}_i} = 0\,, \tag{3.38}$$

where ζ_i is the curvature perturbation of the $i-$th fluid and the first equality comes from the continuity equation. We can then define the total curvature perturbation ζ:

$$\zeta = H\frac{\delta\rho}{\dot{\rho}} = H\frac{\sum_i \delta\rho_i}{\sum_i \dot{\rho}_i}\,, \tag{3.39}$$

which can be rewritten as:

$$\zeta = \sum_i \frac{\dot{\rho}_i}{\dot{\rho}}\zeta_i\,. \tag{3.40}$$

If we take the time derivative of ζ we see that in general it is different from zero. In fact:

$$\dot{\zeta} = \sum_i \left(\frac{d}{dt}\left[\frac{\dot{\rho}_i}{\dot{\rho}}\right]\zeta_i + \frac{\dot{\rho}_i}{\dot{\rho}}\dot{\zeta}_i\right) = \sum_i \frac{d}{dt}\left[\frac{\dot{\rho}_i}{\dot{\rho}}\right]\zeta_i\,. \tag{3.41}$$

This result is not surprising, since it is another way to express the fact that an ensemble of adiabatic fluids is not globally adiabatic. Say we

have two fluids. For them we can write the adiabatic relation $P_1 = w_1 \rho_1$ and $P_2 = w_2 \rho_2$. The total density and pressure are $\rho = \rho_1 + \rho_2$ and $P = P_1 + P_2$. However it is not possible to write P as $w\rho$, meaning that the sum of the two fluids is not adiabatic. This example is not a simple exercise because the resultant non-adiabacity and thus non conservation of ζ has to be taken into account in models where more than one field is present, e.g. in the curvaton scenario where radiation and the curvaton field do not interact but are present together.

Chapter 4

Non-Gaussianity

Why Non-Gaussianity of ζ? In short, because it is a powerful tool to discriminate among different inflationary mechanisms. The primordial cosmological perturbations are very small and so their generation and evolution has been usually studied with linear perturbation theory. Within the limits of this approach primordial perturbations are obviously consistent with Gaussianity. Still, being the mechanism by which perturbations are actually produced during Inflation not yet clear, we need to go deeper. In the next years it will become possible to measure with accuracy the amount of non-Gaussianity in CMB anisotropies and so it will be important to go beyond the linear treatment. There are in fact many different models which are consistent with Inflation and the creation of perturbations but predict -sometimes widely- different values for the non linear contributions to ζ. Therefore, Non Gaussianity is the tool that will help in pinpointing which mechanism is the actual one by putting constraints on the amplitude of higher order correlation functions in different inflationary scenarios.

4.1 Scenarios

In chapter 2 we described Inflation. Now we want to present the two major mechanisms for generating perturbations during or at the end

of Inflation in order to outline how the effects of non linearities may be important in discriminating which is actually responsible for the inflationary era. They are the standard scenario, where the inflaton is responsible for both the expansion and the generation of perturbations, and the curvaton scenario, –the simplest multi–field scenario– where the inflaton produces only the expansion and a second scalar field –the curvaton– generates the primordial perturbations. We show how they produce radically different predictions for the amount of non gaussianity of the perturbations.

4.1.1   The Standard Scenario

We assume there is only one scalar field responsible for the expansion and the perturbations, the inflaton ϕ. Using the δN formalism for a single field, the curvature perturbation ζ can be expanded as:

$$\zeta = \delta N = \sum_n \frac{1}{n!} \frac{\partial^n N}{\partial \phi^n} (\delta \phi)^n \qquad (4.1)$$

For our current purposes an expansion to the second order it sufficient and so we write

$$\zeta = \frac{\partial N}{\partial \phi} \delta \phi + \frac{1}{2} \frac{\partial^2 N}{\partial \phi^2} (\delta \phi)^2 \,, \qquad (4.2)$$

where using eq. (3.19) one has

$$N' \equiv \frac{\partial N}{\partial \phi} = \frac{\partial N}{\partial t} \frac{\partial t}{\partial \phi} = \frac{H}{\dot{\phi}} \,, \qquad (4.3)$$

and for the second derivative

$$\begin{aligned} N'' \equiv \frac{\partial^2 N}{\partial \phi^2} &= \frac{\partial}{\partial \phi} \left(\frac{H}{\dot{\phi}} \right) \\ &= \frac{1}{\dot{\phi}} \left[\frac{\dot{H}}{\dot{\phi}} - \frac{H}{\dot{\phi}^2} \ddot{\phi} \right] \end{aligned} \qquad (4.4)$$

Moreover we have $\dot{H} = -4\pi G(P + \rho)$, but for a scalar field $P = \frac{\dot{\phi}^2}{2} - V$ and $\rho = \frac{\dot{\phi}^2}{2} + V$. Substituting we have

$$\dot{H} = -4\pi G \dot{\phi}^2 \equiv -\epsilon H^2 \,, \qquad (4.5)$$

with $\epsilon = 4\pi G \dot\phi^2/H^2$. The second derivative of N in respect to ϕ is then

$$\frac{\partial^2 N}{\partial \phi^2} = -\frac{\epsilon H^2}{\dot\phi^2} - \frac{1}{\dot\phi^2}\left(\frac{H\ddot\phi}{\phi}\right) \qquad (4.6)$$

Usually $-\ddot\phi/(H\dot\phi)$ is defined as $\delta = \eta - \epsilon$ [42]. The curvature perturbation is then

$$\begin{aligned}
\zeta &= \left(H\frac{\delta\phi}{\dot\phi}\right) + \frac{1}{2}(\eta - 2\epsilon)\left(H\frac{\delta\phi}{\dot\phi}\right)^2 \\
&= \zeta^{(1)} + \frac{1}{2}(\eta - \epsilon)(\zeta^{(1)})^2 \qquad (4.7)
\end{aligned}$$

where clearly $\zeta^{(1)} = H\frac{\delta\phi}{\dot\phi}$ and it represents the linear-order curvature perturbation. We note that in the standard scenario, due to the constraints on the slow–roll parameters, $|\eta - 2\epsilon| \ll 1$. So, where does the non Gaussianity come from here? Gaussianity means that the two-point correlation function $\langle\zeta\zeta\rangle$ is the only one containing information, while the connected part of higher order correlation functions is reducible to products of the former. Non Gaussianity then means having a connected 3-point correlation which contains terms indipendent of $\langle\zeta\zeta\rangle$. Let us write it, using eq. (4.2)

$$\langle\zeta\zeta\zeta\rangle_c = \frac{1}{2}(\eta - \epsilon)\langle\zeta^{(1)}\zeta^{(1)}(\zeta^{(1)})^2\rangle_c + \langle\zeta^{(1)}\zeta^{(1)}\zeta^{(1)}\rangle_c, \qquad (4.8)$$

and, if we now write explicitly the dependence on $\delta\phi$, equation (4.32) becomes

$$\langle\zeta\zeta\zeta\rangle_c = (N')^2\frac{N''}{2}\langle\delta\phi\delta\phi(\delta\phi)^2\rangle_c + (N')^3\langle\delta\phi\delta\phi\delta\phi\rangle_c, \qquad (4.9)$$

plus other terms of higher order in the perturbations that we can neglect at this stage. We can see here clearly the two sources of non Gaussianity: gravity and the scalar field ϕ itself. The effect of gravity is twofold. On one side, it acts at the level of the derivatives of N. On the other side, as shown in [58, 59], it produces a non vanishing 3-point correlator even if we assume the field to be perfectly Gaussian distributed, once the gravitational coupling as been accounted for. Thus even a Gaussian inflaton produces non linearities in the perturbations.

We note though that the coefficients before the two terms in eq. (4.9) are $O(\epsilon, \eta)$ and so the contribution of non Gaussianity is expected to be small. If we now drop the requirement of Gaussianity on ϕ, e. g. we consider a self-interacting scalar field, then the term $\langle \delta\phi\delta\phi\delta\phi\delta\phi \rangle_c$ in general acquires a contribution from the intrinsic non linearity of ϕ. If this term develops divergences at some order, it may overcome the damping of slow–roll parameters and produce a large observable non Gaussianity. For a detailed analysis of 3- and 4- point correlation functions in single field Inflation we refer to [60, 61, 63]. A comfortable formalism for the n-point correlation functions will be presented in section 4.2.

4.1.2   The Curvaton Scenario

One alternative to the standard scenario is the curvaton one: here the cosmological perturbations are not produced by the inflaton but by a second scalar field σ during Inflation. The second field, the curvaton, is subdominant during Inflation and so it produces isocurvature fluctuations. It becomes important near the end of the inflationary era when its energy becomes a relevant part of the total energy and it begins to oscillate around the minimum of its potential. This may happen when the Hubble rate drops under the curvaton mass. We split σ as already done in the zero order value and the perturbation:

$$\sigma = \bar{\sigma}(t) + \delta\sigma(t, \mathbf{x}) \,, \tag{4.10}$$

The curvaton is supposed to generate the perturbations through its oscillations so we choose a simple quadratic potential $V(\sigma) = 1/2m^2\sigma^2$.

$$\ddot{\bar{\sigma}} + 2H\dot{\bar{\sigma}} + V' \;=\; 0 \tag{4.11}$$

$$\delta\ddot{\sigma}_k + 2H\delta\dot{\sigma}_k + k^2\delta\sigma + m^2\delta\sigma_k \;=\; 0 \,, \tag{4.12}$$

which are respectively the equation of motion for the zero-order (infinite wavelength) mode and for the perturbations modes expanded to first order. If we assume a massive curvaton we can neglect the kinetic term and we have the two case:

- $H \gg m \rightarrow \delta\sigma \simeq$ constant ,

- $H \ll m \rightarrow \delta\sigma_k(t) \simeq \delta\sigma_k(t_i) \cos[m(t - t_i)]$.

In the second case also $\bar{\sigma}(t) = \bar{\sigma}(t_i) \cos[m(t - t_i)]$ and so one obtains

$$\frac{\delta\sigma}{\bar{\sigma}} = const. \, , \tag{4.13}$$

which is not a surprise since eq. (4.13) is of the form of a conserved curvature perturbation. We consider now the density $\bar{\rho}_\sigma = 1/2(\dot{\bar{\sigma}}^2 + m^2\bar{\sigma}^2)$ and its time derivative

$$\dot{\bar{\rho}}_\sigma = \ddot{\bar{\sigma}}\dot{\bar{\sigma}} + m^2\bar{\sigma}\dot{\bar{\sigma}} = \dot{\bar{\sigma}}[-3H\dot{\bar{\sigma}}] = -3H(\dot{\bar{\sigma}})^2 \, . \tag{4.14}$$

For definiteness we consider the average of $\dot{\bar{\rho}}$ over many oscillations (H),

$$\langle\dot{\bar{\rho}}_\sigma\rangle = \frac{1}{T}\int_0^T \dot{\bar{\rho}}_\sigma dt = -2H\langle\bar{\rho}_\sigma\rangle \, , \tag{4.15}$$

and then we obtain this way:

$$\frac{\delta\rho}{\bar{\rho}_\sigma} = 2\frac{\delta\sigma}{\bar{\sigma}} \, . \tag{4.16}$$

The density of the oscillating field can be written as $\bar{\rho}_\sigma \simeq m^2\bar{\sigma}^2$ and thus $\delta\rho_\sigma = 2m^2\bar{\sigma}\delta\sigma + m^2(\delta\sigma)^2$. We can substitute that in the expression

$$\zeta_\sigma = H\frac{\delta\rho_\sigma}{\dot{\bar{\rho}}_\sigma} \, , \tag{4.17}$$

obtaining the curvature perturbation to second order in the perturbations

$$\zeta_\sigma = \frac{1}{3}\left(2\frac{\delta\sigma}{\bar{\sigma}} + \frac{(\delta\sigma)^2}{\bar{\sigma}^2}\right) \tag{4.18}$$

$$= \zeta_\sigma^{(1)} + \frac{3}{4}\left(\zeta_\sigma^{(1)}\right)^2 \, . \tag{4.19}$$

To reproduce a result similar to eq. (4.7), we want to link ζ_σ to the radiation curvature perturbation, ζ_γ. The curvaton is supposed to oscillate

generating the perturbations and then to decay with a $\Gamma \simeq H$ (sudden-decay approximation) to relativistic matter. So its curvature is transferred to the radiation. At first order we can then write $\zeta_\gamma^{(1)} = r\frac{2}{3}\frac{\delta\sigma}{\sigma}$, where r is defined by [20]

$$r = \frac{-3H\rho_\sigma}{-3H\rho_\sigma - 4H\rho_\gamma}\bigg|_{decay} = \frac{3\rho_\sigma}{3\rho_\sigma + 4\rho_\gamma}\bigg|_{decay} \qquad (4.20)$$

One can invert the latter equation and use it to obtain a relation at second order in ζ_γ,

$$\begin{aligned}
\zeta &= \zeta_\gamma = r\zeta_\sigma = r\zeta_\sigma^{(1)} + r\frac{3}{4}(\zeta_\sigma^{(1)})^2 \\
&= \zeta_\gamma^{(1)} + \frac{1}{r}\frac{27}{16}\left(\zeta_\gamma^{(1)}\right)^2 .
\end{aligned} \qquad (4.21)$$

We can already note a difference in respect to the inflaton scenario: in front of the quadratic term of eq. (4.21) there is a coefficient that goes as r^{-1}. If we suppose that the curvaton energy density was subdominant at the moment of decay, r^{-1} can become very large thus amplifying non Gaussian effects, where in eq. (4.7) the slow–roll parameters suppressed them. We see already that a measure of the non linearity is a powerful tool to discriminate between different inflationary mechanisms.

4.1.3 Experimental Limits on Non-Gaussianity Parameters

There are two approaches to testing non-Gaussianity of the CMB. The first is blind tests, which make no assumptions about the form of non-Gaussianity and has the merit of being model-indipendent, while losing some statistical power in comparison to the second approach, which tests specific types of non-Gaussianity providing a better precision of quantitative constraints at the cost of model-dependence. Here we just want to report quickly the current observational results on the non linearity parameters to give a general idea of what is the state of the art. The most recent data come from the 3-year WMAP survey

published in 2006 [32, 33] which have been analyzed in [62] for example. The results are

$$-36 < \quad f_{\text{NL}} \quad < 100 \quad \text{at } 95\% \text{ C.L.} , \tag{4.22}$$

We note that the limits on the non linearity parameter are still quite wide allowing the possibility of high non Gaussianity models, like for example multiple fields Inflation. However at present there is not yet compelling evidence for primordial non-Gaussianity. Detection can be made possible by the future WMAP and *Plank* data combining temperature and polarization anisotropies, which could bring the precision to $f_{NL} \simeq 1$.

4.2 N-point Functions and Spectra

In the last two sections we showed simply how non Gaussianity can originate in the single-field case of the inflaton and in the simpler multifield scenario, the curvaton one. Let us proceed now to the tools of the trade: we introduce a general formalism for any number of scalar fields which will let us comfortably handle higher order correlation functions of ζ, so that we will be able to link them to the calculations performed on the *scalar field* correlators in chapter 6.

Following [63, 64] we write ϕ^A, where the superscript labels the fields in field space[1]. The connected 2-, 3- and 4-point functions of the fields are defined by:

$$\langle \delta\phi^A_{\mathbf{k_1}} \, \delta\phi^B_{\mathbf{k_2}} \rangle = C^{AB}(k)(2\pi)^3 \delta^3(\mathbf{k_1} + \mathbf{k_2}) , \tag{4.23}$$

$$\langle \delta\phi^A_{\mathbf{k_1}} \, \delta\phi^B_{\mathbf{k_2}} \, \delta\phi^C_{\mathbf{k_3}} \rangle = B^{ABC}(k_1, k_2, k_3)(2\pi)^3 \delta^3(\mathbf{k_1} + \mathbf{k_2} + \mathbf{k_3}) ,$$

$$\langle \delta\phi^A_{\mathbf{k_1}} \, \delta\phi^B_{\mathbf{k_2}} \, \delta\phi^C_{\mathbf{k_3}} \, \delta\phi^D_{\mathbf{k_4}} \rangle_c = T^{ABCD}(\mathbf{k_1}, \mathbf{k_2}, \mathbf{k_3}, \mathbf{k_4})(2\pi)^3 \delta^3(\mathbf{k_1} + \mathbf{k_2} + \mathbf{k_3} + \mathbf{k_4}) .$$

At linear order, the primordial power spectra depends purely on $\zeta^{(1)}$, in fact, defining $N_A \equiv \partial N/\partial\phi^A$,

$$\zeta^{(1)} = N_A \phi^{(1)A} , \tag{4.24}$$

---

[1]For example if we have n fields, $\phi^A \phi^B$ is a $n \times n$ matrix in field space

where the superscript denotes the perturbation order. The power spectrum is thus

$$\langle \zeta_{\mathbf{k}}^{(1)} \zeta_{\mathbf{k'}}^{(1)} \rangle = P_\zeta(k)(2\pi)^3 \delta^3(\mathbf{k} + \mathbf{k'}) \,, \tag{4.25}$$

where

$$P_\zeta(k) = N_A N_B C^{AB}(k) \quad , \quad C^{AB}(k) = \delta^{AB} P(k) = \frac{(2\pi)^3}{4\pi k^3} \mathcal{P}(k) \tag{4.26}$$

with $\mathcal{P}(k)$ defined by eq. (2.90).

The 3-point function of the curvature perturbations (again to leading order) depends on $\zeta^{(1)}$, (4.24) and

$$\zeta^{(2)} = N_A \phi^{(2)A} + N_{AB} \phi^{(1)A} \phi^{(1)B} \,. \tag{4.27}$$

The primordial bispectrum is thus

$$\begin{aligned} \langle \zeta_{\mathbf{k}_1} \zeta_{\mathbf{k}_2} \zeta_{\mathbf{k}_3} \rangle &= N_A N_B N_C \langle \phi_{\mathbf{k}_1}^A \phi_{\mathbf{k}_2}^B \phi_{\mathbf{k}_3}^C \rangle + \frac{1}{2} N_{A_1 A_2} N_B N_C \\ & \left[\langle \left(\phi^{A_1} * \phi^{A_2} \right)_{\mathbf{k}_1} \phi_{\mathbf{k}_2}^B \phi_{\mathbf{k}_3}^C \rangle + (2 \text{ perms}) \right] \,, \end{aligned} \tag{4.28}$$

where $'*'$ denotes the convolution, defined by

$$\left(\phi^A * \phi^B \right)_{\mathbf{k}} = \frac{1}{(2\pi)^3} \int d^3 k' \phi_{\mathbf{k}-\mathbf{k'}}^A \phi_{\mathbf{k'}}^B \,. \tag{4.29}$$

Hence the bispectrum of the curvature perturbation is

$$\langle \zeta_{\mathbf{k}_1} \zeta_{\mathbf{k}_2} \zeta_{\mathbf{k}_3} \rangle \equiv B_\zeta(k_1, k_2, k_3)(2\pi)^3 \delta^3 \mathbf{k}_1 + \mathbf{k}_2 + \mathbf{k}_3 \,, \tag{4.30}$$

where to leading order [65]

$$\begin{aligned} B_\zeta(k_1, k_2, k_3) &= N_A N_B N_C B^{ABC}(k_1, k_2, k_3) \\ & + N_A N_{BC} N_D \left[C^{AC}(k_1) C^{BD}(k_2) \right. \\ & \left. + C^{AC}(k_2) C^{BD}(k_3) + C^{AC}(k_3) C^{BD}(k_1) \right] \,. \end{aligned} \tag{4.31}$$

Finally, we define the trispectrum. The four-point function of the curvature perturbation at leading order will depend on $\zeta^{(1)}$, (4.24), $\zeta^{(2)}$, (4.27), and

$$\zeta^{(3)} = N_A \phi^{(3)A} + N_{AB} \left(\phi^{(1)A} \phi^{(2)B} + \phi^{(2)A} \phi^{(1)B} \right) + N_{ABC} \phi^{(1)A} \phi^{(1)B} \phi^{(1)C} \tag{4.32}$$

The four-point function at leading order is [63] $\langle \zeta_{\mathbf{k}_1} \zeta_{\mathbf{k}_2} \zeta_{\mathbf{k}_3} \zeta_{\mathbf{k}_4} \rangle_c =$

$$
\begin{aligned}
= \quad & N_A N_B N_C N_D \langle \phi^A_{\mathbf{k}_1} \phi^B_{\mathbf{k}_2} \phi^C_{\mathbf{k}_3} \phi^D_{\mathbf{k}_4} \rangle_c \qquad\qquad\qquad\qquad\qquad (4.33) \\
& + \frac{1}{2} N_{A_1 A_2} N_B N_C N_D \left[\langle \left(\phi^{A_1} * \phi^{A_2} \right)_{\mathbf{k}_1} \phi^B_{\mathbf{k}_2} \phi^C_{\mathbf{k}_3} \phi^D_{\mathbf{k}_4} \rangle + (3 \text{ perms}) \right] \\
& + \frac{1}{4} N_{A_1 A_2} N_{B_1 B_2} N_C N_D \left[\langle \left(\phi^{A_1} * \phi^{A_2} \right)_{\mathbf{k}_1} \left(\phi^{B_1} * \phi^{B_2} \right)_{\mathbf{k}_2} \phi^C_{\mathbf{k}_3} \phi^D_{\mathbf{k}_4} \rangle + (5 \text{ perms}) \right] \\
& + \frac{1}{3!} N_{A_1 A_2 A_3} N_B N_C N_D \left[\langle \left(\phi^{A_1} * \phi^{A_2} * \phi^{A_3} \right)_{\mathbf{k}_1} \phi^B_{\mathbf{k}_2} \phi^C_{\mathbf{k}_3} \phi^D_{\mathbf{k}_4} \rangle + (3 \text{ perms}) \right] .
\end{aligned}
$$

The first term of the expansion above is the intrinsic 4-point function of the fields [30]. The disconnected part of this term would only give a contribution if the sum of any two k vectors is zero, e.g. if $\mathbf{k}_1 + \mathbf{k}_2 = 0$. We will exclude this case, which is equivalent to neglecting parallelograms of the wavevectors.

The second term of (4.33) consists of permutations of terms of the form

$$
\frac{1}{2} N_{A_1 A_2} N_B N_C N_D \frac{1}{(2\pi)^3} \int d^3 q \langle \phi^{A_1}_{\mathbf{q}} \phi^{A_2}_{\mathbf{k}_1 - \mathbf{q}} \phi^B_{\mathbf{k}_2} \phi^C_{\mathbf{k}_3} \phi^D_{\mathbf{k}_4} \rangle . \qquad (4.34)
$$

This five-point function is zero for the first-order, Gaussian, perturbations, hence the leading order contribution is sixth-order, due to the second order contribution of one of the fields. Hence we use Wick's theorem to split the 5-point function in to lower point functions. There is no contribution to (4.34) from the split into a four-point and a one-point function. Only the split into a two-point and three-point function gives a contribution. However the first possible contraction in (4.34), $\langle \phi^{A_1}_{\mathbf{k}_1 - q} \phi^{A_2}_q \rangle$, does not contribute since it is only non-zero when $k_1 = 0$. Therefore we can reduce the above term into a power spectra and a trispectrum in 6 different ways, which gives three distinct pairs of terms. In total the second term of (4.33) is

$$
N_{A_1 A_2} N_B N_C N_D (2\pi)^3 \delta^3(\mathbf{k_t}) \left[C^{A_1 B}(k_1) B^{A_2 B C}(k_{12}, k_3, k_4) + \right.
$$
$$
\left. (11 \text{ perms}) \right] , \qquad (4.35)
$$

where we use the shortened notation $k_{ij} = |\mathbf{k}_i + \mathbf{k}_j|$ and $\mathbf{k}_t = \mathbf{k}_1 + \mathbf{k}_2 + \mathbf{k}_3 + \mathbf{k}_4$. The 12 permutations come from having 3 distinct choices for the indices of the wavenumber k_{ij} (only three distinct choices because

$k_{ij} = k_{ji}$ and $k_{12} = k_{34}$ etc). We then choose which two wavenumbers form the remaining arguments of B^{ABC}, either k_i, k_j or the other pair of wavenumbers, and finally we choose which of the two indices i or j is attached to the wavenumber k_i that is the argument of C.

Continuing this argument for the second and third terms of (4.33), we find the connected part of the trispectrum of the curvature perturbation is

$$\langle \zeta_{\mathbf{k_1}} \zeta_{\mathbf{k_2}} \zeta_{\mathbf{k_3}} \zeta_{\mathbf{k_4}} \rangle_c \equiv T_\zeta(\mathbf{k_1}, \mathbf{k_2}, \mathbf{k_3}, \mathbf{k_4})(2\pi)^3 \delta^3(\mathbf{k_1} + \mathbf{k_2} + \mathbf{k_3} + \mathbf{k_4}),$$
(4.36)

where $T_\zeta(\mathbf{k_1}, \mathbf{k_2}, \mathbf{k_3}, \mathbf{k_4}) =$

$$N_A N_B N_C N_D T^{ABCD}(\mathbf{k_1}, \mathbf{k_2}, \mathbf{k_3}, \mathbf{k_4}) \qquad (4.37)$$
$$+ N_{A_1 A_2} N_B N_C N_D \left[C^{A_1 B}(k_1) B^{A_2 BC}(k_{12}, k_3, k_4) + (11 \text{ perms}) \right]$$
$$+ N_{A_1 A_2} N_{B_1 B_2} N_C N_D \left[C^{A_2 B_2}(k_{13}) C^{A_1 C}(k_3) C^{B_1 D}(k_4) + (11 \text{ perms}) \right]$$
$$+ N_{A_1 A_2 A_3} N_B N_C N_D \left[C^{A_1 B}(k_2) C^{A_2 C}(k_3) C^{A_3 D}(k_4) + (3 \text{ perms}) \right].$$

If now we assume the scalar field perturbations to be independent, Gaussian random fields, as we expect shortly after Hubble-exit during Inflation in the slow-roll limit [66, 67] then the bispectrum for the fields, B^{ABC}, and connected part of the trispectrum, T^{ABCD}, both vanish. In this case the bispectrum of the primordial curvature perturbation (4.31) at leading (fourth) order, can be written as a simple sum of products of 2 two-point correlators,

$$B_\zeta(\mathbf{k_1}, \mathbf{k_2}, \mathbf{k_3}) = \frac{6}{5} f_{NL} \left[P_\zeta(k_1) P_\zeta(k_2) + P_\zeta(k_2) P_\zeta(k_3) \right. \quad (4.38)$$
$$\left. + P_\zeta(k_3) P_\zeta(k_1) \right], \quad (4.39)$$

where the dimensionless non-linearity parameter is given by [68]

$$f_{NL} = \frac{5}{6} \frac{N_A N_B N^{AB}}{(N_C N^C)^2}. \qquad (4.40)$$

The trispectrum (4.37) in this case reduces to

$$T_\zeta(\mathbf{k_1}, \mathbf{k_2}, \mathbf{k_3}, \mathbf{k_4}) = N_{AB} N^{AC} N^B N_C \left[P(k_{13}) P(k_3) P(k_4) + (11 \text{ perms}) \right]$$
$$+ N_{ABC} N^A N^B N^C \left[P(k_2) P(k_3) P(k_4) + (3 \text{ perms}) \right],$$

Hence we can write the trispectrum as

$$T_\zeta(\mathbf{k}_1, \mathbf{k}_2, \mathbf{k}_3, \mathbf{k}_4) = \tau_{NL} \left[P_\zeta(k_{13}) P_\zeta(k_3) P_\zeta(k_4) + (11 \text{ perms}) \right] \quad (4.41)$$
$$+ \frac{54}{25} g_{NL} \left[P_\zeta(k_2) P_\zeta(k_3) P_\zeta(k_4) + (3 \text{ perms}) \right] .$$

where comparing the above two expressions we see

$$\tau_{NL} = \frac{N_{AB} N^{AC} N^B N_C}{(N_D N^D)^3}, \quad (4.42)$$

$$g_{NL} = \frac{25}{54} \frac{N_{ABC} N^A N^B N^C}{(N_D N^D)^3}. \quad (4.43)$$

The expression for τ_{NL} from multiple fields is given in [69].

In the preceding sections we introduced the inflaton and curvaton scenarios. These are single field scenarios or, differently said, there is a single direction in the field space, since there only one field who dominates. In this case, the curvature perturbation is again given by

$$\zeta = N'\delta\phi + \frac{1}{2} N'' \delta\phi^2 + \frac{1}{6} N''' \delta\phi^3 + \cdots, \quad (4.44)$$

where again $N' = dN/d\phi$ and analogously higher derivatives. If in addition we assume that the field perturbation is purely Gaussian, $\phi = \phi^{(1)}$, then the non-Gaussianity of the primordial perturbation has a simple "local form" where the full non-linear perturbation at any point in real space, $\zeta(\mathbf{x})$, is a local function of a single Gaussian random field, $\phi^{(1)}$. Thus we can write [70]

$$\zeta = \zeta^{(1)} + \frac{3}{5} f_{NL} \zeta^{(1)2} + \frac{9}{25} g_{NL} \zeta^{(1)3} + \cdots, \quad (4.45)$$

where $\zeta^{(1)}$ is Gaussian because it is directly proportional to the initial Gaussian field perturbation, $\phi^{(1)}$, and the dimensionless non-linearity parameters, f_{NL} and g_{NL}, are given by

$$f_{NL} = \frac{5}{6} \frac{N''}{(N')^2}, \quad (4.46)$$

$$g_{NL} = \frac{25}{54} \frac{N'''}{(N')^3}, \quad (4.47)$$

The numerical factors in Eq. (4.45) arise because the original definition is given in terms of the Bardeen potential on large scales (in the matter dominated era, md), $\Phi_{H\text{md}} = (3/5)\zeta_1$, so we have [71, 89],

$$\frac{3}{5}\zeta = \Phi_{H\text{md}} + f_{NL}\Phi_{H\text{md}}^2 + g_{NL}\Phi_{H\text{md}}^3 + \cdots . \qquad (4.48)$$

The primordial bispectrum and trispectrum are then given by equations. (4.38) and (4.41), where the non-linearity parameters f_{NL} and g_{NL}, given in eqs. (4.40) and (4.43), reduce to eqs. (4.46) and (4.47) respectively, and τ_{NL} given in eq. (4.42) reduces to

$$\tau_{NL} \;\; = \;\; \frac{(N'')^2}{(N')^4} = \frac{36}{25}f_{NL}^2 \,. \qquad (4.49)$$

For completeness we report here the results obtained for the two described scenarios [50, 51, 64, 70, 63, 20, 68].

Single Field Scenario In standard single field Inflation, one can calculate the non-linearity parameters f_{NL} and g_{NL} in terms of the slow-roll parameters (2.54) at Hubble-exit plus a third one

$$\xi^2 \equiv m_p{}^4\frac{V'V'''}{V^2} \,. \qquad (4.50)$$

Hence the non-linearity parameters for single field Inflation (4.46–4.47) are given by

$$f_{NL} \;\; = \;\; \frac{5}{6}(\eta - 2\epsilon) \,, \qquad (4.51)$$
$$\tau_{NL} \;\; = \;\; (\eta - 2\epsilon)^2 \,, \qquad (4.52)$$
$$g_{NL} \;\; = \;\; \frac{25}{54}\left(2\epsilon\eta - 2\eta^2 + \xi^2\right) \,. \qquad (4.53)$$

Note however that we have not calculated the full bispectrum and trispectrum at leading order in slow roll, because we assumed that the initial field fluctuations were Gaussian. If we included the contribution from the non-Gaussianity of the fields at Hubble exit, the bispectrum would have one extra term (4.31) and the trispectrum would have two

extra terms, (4.37). The extra term for the trispectrum is at the same order in slow roll, because [67] $B^{ABC}(\mathbf{k}_1, \mathbf{k}_2, \mathbf{k}_3) \sim \mathcal{O}(\epsilon^{\frac{1}{2}})$ and the second term of (4.37) is also of the same order. However Seery, Lidsey and Sloth find [30], $T^{ABCD}(\mathbf{k}_1, \mathbf{k}_2, \mathbf{k}_3, \mathbf{k}_4) \sim \mathcal{O}(1)$ which means the first term of (4.37) is suppressed by one less order in slow roll then the other three terms. However they find the contribution of this term is still too small to be observable, even in the multiple field case [30]. All of these extra terms from the non-Gaussian field fluctuations are momentum dependent, while all of the non-linearity parameters are independent of momentum.

Curvaton Scenario In the curvaton scenario the energy density of the curvaton is some function of the field value at Hubble-exit, $\rho_\sigma \propto g^2(\sigma_*)$, and hence the primordial curvature perturbation when the curvaton decays is of local form (4.45). In the sudden-decay approximation the non-linearity parameters are [68, 72]

$$f_{NL} = \frac{5}{4r}\left(1 + \frac{gg''}{g'^2}\right) - \frac{5}{3} - \frac{5r}{6}, \qquad (4.54)$$

and [70]

$$g_{NL} = \frac{25}{54}\left[\frac{9}{4r^2}\left(\frac{g^2 g'''}{g'^3} + 3\frac{gg''}{g'^2}\right) - \frac{9}{r}\left(1 + \frac{gg''}{g'^2}\right)\right.$$
$$\left. + \frac{1}{2}\left(1 - 9\frac{gg''}{g'^2}\right) + 10r + 3r^2\right], \qquad (4.55)$$

and τ_{NL} satisfies (4.49) and r satisfies $0 < r \leq 1$, . As we argued in previous section there is a significant non-Gaussianity if the curvaton does not dominate the total energy density of the Universe when it decays, $r \ll 1$. In that case equations (4.54) and (4.55) reduce to

$$f_{NL} \simeq \frac{5}{4r}\left(1 + \frac{gg''}{g'^2}\right), \qquad (4.56)$$

$$g_{NL} \simeq \frac{25}{24r^2}\left(\frac{g^2 g'''}{g'^3} + 3\frac{gg''}{g'^2}\right). \qquad (4.57)$$

In this chapter we presented how non Gaussianity can be present in the curvature pertubation ζ and how it can be calculated in the context of correlation functions. We are interested in evaluating the contribution of non linearities intrinsic to the scalar field, so we need to calculate the correlation functions at the various orders between states at equal times. In the next chapter we will then introduce a powerful formalism to treat this problem.

Chapter 5

CTP Formalism

The Closed Time Path (CTP) formalism or *in-in* formalism has been first proposed by Schwinger and developed by Keldysh, Koreman and others [73, 74, 75]. It is different from the conventional *in-out* formalism in that it does not involve asymptotic free states but rather focuses on same time states in order to obtain the expectation values of observables rather than transition amplitudes. Thus it is very useful in our case because it allows us to evaluate the correlation functions between vacuum states at some very early time, where we could not easily specify the asymptotic future and past states needed in the conventional approach.

In the convential approach indeed the effective field equation is derivable form the effecive action Γ, which is the Legendre trasform of the generating functional W related to the vacuum persistance amplitude $\langle 0_+|0_-\rangle$ by

$$\langle 0_+|0_-\rangle_J = e^{iW[J]} = \int D\phi \, e^{i(S[g,\phi]+J\phi)} \,, \qquad (5.1)$$

where $|0_\pm\rangle$ denote the asymptotic vacuum states. Here J is an external source, S is the action, g is the spacetime metric and $D\phi$ is the measure of the functional integral over the scalar field ϕ. As spacetime evolves, the out vacuum can in general be different from the in vacuum due to particle production. Thus one can calculate *matrix elements* $\langle 0_+|T|0_-\rangle$ of a certain operator T rather than its *expectations value*

$\langle T \rangle = \langle 0_- | T | 0_- \rangle$ calculated at the same time. Transforming in-out elements to in-in values is possible, but one needs to sum over a set of intermediate complete states, which involves knowing the Bogolubov coefficients. One can also use functional tranforms but these are more likely to be of formal than practical value. We note that the CTP formalism is an initial-value problem, a functional integral method formulated with respect to the same initial state, while the conventional formulation is a boundary-value problem, since it needs asymptotic regions.

How is the CTP formalism built? We let the vacuum evolve indipendently under two different external sources $J^+(x)$ and $J^-(x)$ and compare the result with a common state $|\psi\rangle$ in the future [76]. The generating functional $W[J^+, J^-]$ is defined as

$$e^{iW[J^+,J^-]} = \sum_\phi \langle 0_- | \phi \rangle_{J^-} \langle \phi | 0_+ \rangle_{J^+} . \qquad (5.2)$$

where $|\phi\rangle$ is a common eigenvector of the field operator Φ_H at some large time t^*, $\Phi_H(\mathbf{x}, t)|\phi\rangle = \phi(\mathbf{x})|\phi\rangle$. The set $|\phi\rangle$ is complete and orthonormal. In the path integral representation, this can be thought of as a sum over paths which go forward in time in the presence of J^+ from $|0_-\rangle$ to $|\phi\rangle$ on a hypersurface Σ of costant time t^* and backwards in time along the same hypersurface in the presence of J^-. This is the reason why the formalism is called *Closed Time Path*. The effective in-in action is defined by [76]

$$\Gamma[\hat{\phi}^+, \hat{\phi}^-] = W[J^+, J^-] - J^+\hat{\phi}^+ + J^-\hat{\phi}^- , \qquad (5.3)$$

where $\hat{\phi}^\pm \equiv \pm\delta W[J^+, J^-]/\delta J^\pm$. When $J^+ = J^- = 0$ they are the expectations values of ϕ_H with respect to $|0_-\rangle$, i.e.

$$\hat{\phi}^+(x) = \hat{\phi}^-(x) = \langle 0_- | \phi_H(x) | 0_- \rangle . \qquad (5.4)$$

It can be easily seen that this formalism doubles the sources and fields therefore increasing the number of Feynmann diagrams which need to be accounted for. Yet, it is worth it, because the advantage that one gets is great. The effective action and field equations are real and

causal and hence their results are more easily physically interpretable. More, the formalism has multiple Green's functions which are treated in the same way, obeying the same set of matrix equations. The CTP formalism then is particularly powerful in tackling statistical problems, where causal and correlational properties of a time-dependent system are important.

5.1 Basic Formalism

Following Schwinger [73], we introduce the two external sources $J^+(x)$ and $J^-(x)$ and consider the quantity

$$Z[J^+, J^-] = {}_{J^-}\langle 0_- | 0_+ \rangle_{J^+} . \tag{5.5}$$

In contrast with the in-out formalism, where one lets the in vacuum evolve under the influence of an external source and compares the result with the out vacuum, in the in-in formalism, one lets the in vacuum evolve indipendently under two sources J^+ and J^-, and compare the results in the future. We may rewrite the latter as

$$
\begin{aligned}
Z[J^+, J^-] = & \int D\phi \left\langle 0_- \left| \tilde{T} exp \left[-i \int_{-\infty}^{t*} dt \int d^3x J^-(x) \phi_H(x) \right] \right| \phi \right\rangle \\
& \left\langle \phi \left| T exp \left[i \int_{-\infty}^{t*} dt \int d^3x J^+(x) \phi_H(x) \right] \right| 0_- \right\rangle ,
\end{aligned} \tag{5.6}
$$

where $\tilde{T}$ denotes antitemporal order. Here $|\phi\rangle$ is an element of a complete, orthonormal set of common eigenvectors of the field operators at some late time t^*,

$$\phi_H(\mathbf{x}, t) |\psi\rangle = \Phi(\mathbf{x}) |\phi\rangle \tag{5.7}$$

From the definitions (5.5) and (5.6), one can obtain the following relations [76]:

$$Z[J, J] = 1, \quad Z[J^+, J^-] = (Z[J^-, J^+])^*, \tag{5.8}$$

and

$$(-i)^{n-m} \left. \frac{\partial^{n+m} Z[J^+, J^-]}{\partial J^-(x_1)\dots\partial J^-(x_m)\partial J^+(y_1)\dots\partial J^+(y_n)}\right|_{J^+,J^-=0} =$$
$$\langle 0_-|\tilde{T}[\phi_H(x_1)\dots\phi_H(x_m)]T[\phi_H(y_1)\dots\phi_H(y_n)]|0_-\rangle. \quad (5.9)$$

We see that expectations value can be be obtained by variation of the sources J^+ and J^- as in eq. (5.13). In particular for a time-dependent Hamiltonian system $H(t)$ that starts in a state $|in\rangle$ at time t_{in}, we can write the expectation value as:

$$\langle Q(t)\rangle = \left\langle \text{in} \left| \left[\bar{\text{T}} \exp\left(i\int_{t_{\text{in}}}^{t} dt' \, H(t')\right)\right] Q \left[\text{T} \exp\left(-i\int_{t_{\text{in}}}^{t} dt' \, H(t')\right)\right]\right| \text{in}\right\rangle.$$
$$(5.10)$$

5.2   Green's Functions

Now we move to a curved space, namely to a de Sitter background. We write the Lagrangian density for a scalar field with potential $V(\phi)$ as

$$\mathscr{L}[\phi] = \sqrt{-g}\left(g^{\mu\nu}\frac{1}{2}\partial_\mu\phi\partial_\nu\phi - \frac{1}{2}m^2\phi^2 - \frac{1}{2}\xi R\phi^2 - V(\phi)\right) + \delta\mathscr{L}, \quad (5.11)$$

where the metric has signature $-+++$ and ξ is the conformal parameter. Choosing $m = 0$ and $\xi = 0$ we select a massless minimally coupled scalar field. The generating functional becomes [25]

$$Z[J_+, J_-, \rho(t_{\text{in}})] = \int \mathcal{D}\phi_{\text{in}}^+ \mathcal{D}\phi_{\text{in}}^- \langle\phi_{\text{in}}^+|\rho(t_{\text{in}})|\phi_{\text{in}}^-\rangle \qquad (5.12)$$
$$\int_{\phi_{\text{in}}^+}^{\phi_{\text{in}}^-} \mathcal{D}\phi^+\mathcal{D}\phi^- e^{i\int_{t_{\text{in}}}^{t} dt' \int d^3x\left(\mathcal{L}[\phi^+]-\mathcal{L}[\phi^-]+J_+\phi^++J_-\phi^-\right)}.$$

Note that the generating functional depends explicitly on the initial density matrix $\rho(t_{in})$. The path integral on the second line can be written in short-hand notation as

$$\int \mathcal{D}\phi \, \exp\left[i\int_{\mathcal{C}} dt' \int d^3x \, (\mathcal{L}[\phi] + J\phi)\right], \qquad (5.13)$$

Figure 5.1: An example of Keldysh Contour $\mathcal{C}$

where $\mathcal{C}$ is the so-called Schwinger-Keldysh contour which runs from t_{in} to t and back. The field ϕ and source J are split up in ϕ^+, J_+ on the first part of this contour, and ϕ^-, J_- on the second part, with the condition $\phi^+(t) = \phi^-(t)$.

To calculate perturbatively correlation functions we need to have the free two-point functions. There are 4 possible time orderings and, using eq. (5.13) one obtains:

$$
\begin{aligned}
G^{-+}(x,y) &= i\langle\phi(x)\phi(y)\rangle^{(0)}, & (5.14)\\
G^{+-}(x,y) &= i\langle\phi(y)\phi(x)\rangle^{(0)}, & (5.15)
\end{aligned}
$$

and

$$
\begin{aligned}
G^{++}(x,y) &= i\langle\mathrm{T}\phi(x)\phi(y)\rangle^{(0)} & (5.16)\\
&= \theta(x_0 - y_0)G^{-+}(x,y) + \theta(y_0 - x_0)G^{+-}(x,y),\\
G^{--}(x,y) &= i\langle\bar{\mathrm{T}}\phi(x)\phi(y)\rangle^{(0)} & (5.17)\\
&= \theta(x_0 - y_0)G^{+-}(x,y) + \theta(y_0 - x_0)G^{-+}(x,y),
\end{aligned}
$$

where by the superscript (0) we denote the free field correlation functions. They obey the important identity

$$
G^{++}(x,y) + G^{--}(x,y) = G^{-+}(x,y) + G^{+-}(x,y), \qquad (5.18)
$$

and they can be put together in a matrix:

$$
\mathbf{G}(x,y) = \begin{pmatrix} G^{++}(x,y) & G^{+-}(x,y) \\ G^{-+}(x,y) & G^{--}(x,y) \end{pmatrix}. \qquad (5.19)
$$

Note that the two point functions depend on the initial conditions via the dependence on $\rho(t_i)$ of the generating functional eq. (5.13).

68

It is useful to transform the ϕ^+ and ϕ^- fields to a different basis, which is a variation of the Keldysh basis (see also [77]):

$$\begin{pmatrix} \phi_C \\ \phi_\Delta \end{pmatrix} = \begin{pmatrix} (\phi^+ + \phi^-)/2 \\ \phi^+ - \phi^- \end{pmatrix} = \mathbf{R} \begin{pmatrix} \phi^+ \\ \phi^- \end{pmatrix}, \qquad (5.20)$$

with

$$\mathbf{R} = \begin{pmatrix} 1/2 & 1/2 \\ 1 & -1 \end{pmatrix}. \qquad (5.21)$$

The free two point functions in this basis can easily be obtained by the transformation

$$\mathbf{G}_K(x, y) = \mathbf{R} \mathbf{G}(x, y) \mathbf{R}^T = \begin{pmatrix} iG_C(x, y) & G_R(x, y) \\ G_A(x, y) & 0 \end{pmatrix}, \qquad (5.22)$$

with

$$\begin{aligned} G_C(x, y) &= -\frac{i}{2} \left(G^{-+}(x, y) + G^{+-}(x, y) \right), & (5.23) \\ G_R(x, y) &= G^{++}(x, y) - G^{+-}(x, y) \\ &= \theta(x_0 - y_0) \left(G^{-+}(x, y) - G^{+-}(x, y) \right), & (5.24) \\ G_A(x, y) &= G^{++}(x, y) - G^{-+}(x, y) \\ &= \theta(y_0 - x_0) \left(G^{+-}(x, y) - G^{-+}(x, y) \right), & (5.25) \end{aligned}$$

where we have used identity eq. (5.18). Also the "$G_{\Delta\Delta}$" propagator in the matrix (5.22) (the element (2,2) of $\mathbf{G}_K(x, y)$) is identically zero due to eq. (5.18), as can be seen by performing directly the product. Finally the G_R and G_A two point functions are often called the retarded and advanced propagators and $G_A(x, y) = G_R(y, x)$.

The correlation functions in the Keldish base obey the equations

$$\left(\Box_x + m^2 + \xi R(x) \right) G(x, y) = 0, \qquad (5.26)$$

$$\left(\Box_x + m^2 + \xi R(x) \right) G_{R,A}(x, y) = \frac{\delta^4(x - y)}{\sqrt{-g(x)}}, \qquad (5.27)$$

where

$$\Box_x = \frac{1}{\sqrt{-g(x)}} \partial_\mu \left(\sqrt{-g(x)} \, g^{\mu\nu}(x) \partial_\nu \right). \qquad (5.28)$$

5.3 Feynman Rules

We want to calculate the non Gaussianity due to the intrinsic non linearity of the scalar field, this translates into calculating higher order graphs. We will do that in the next chapter, but before we need a method to draw those graphs. So what we need is a set of Feynman rules for our theory. We choose a self–interacting field and in particular we choose the potential to be $V(\phi) = \frac{\lambda}{4!}\phi^4$. The Lagrangian density becomes:

$$\mathscr{L}[\phi] = \sqrt{-g} \left(g^{\mu\nu}\frac{1}{2}\partial_\mu\phi\partial_\nu\phi + \frac{\lambda}{4!}\phi^4 \right)$$

Taking into account the minus produced by the orientation of the line of integration [1], the Lagrangian density becomes:

$$\mathscr{L}[\phi^+, \phi^-] = \sqrt{-g} \left(g^{\mu\nu}\frac{1}{2}\partial_\mu\phi^+\partial_\nu\phi^+ - \frac{\lambda}{4!}(\phi^+)^4 - g^{\mu\nu}\frac{1}{2}\partial_\mu\phi^-\partial_\nu\phi^- - \frac{\lambda}{4!}(\phi^-)^4 \right)$$

We perform now the field transformation as in eq.(5.20). The terms of the Lagrangian density containing derivatives become:

$$g^{\mu\nu}\partial_\mu(\frac{\phi^+ + \phi^-}{2})\partial_\nu(\phi^+ - \phi^-) = g^{\mu\nu}(\partial_\mu\phi_C\partial_\nu\phi_\Delta)$$

while the terms of potential become:

$$-\frac{\lambda}{4!}[(\phi^+)^4 - (\phi^-)^4] = -\frac{\lambda}{4!}2\phi_C\phi_\Delta\left(2\phi_C{}^2 + \frac{\phi_\Delta{}^2}{2}\right)$$

Putting all the terms together $\mathscr{L}[\phi_C, \phi_\Delta]$ is:

$$\mathscr{L}[\phi_C, \phi_\Delta] = \sqrt{-g}\left[g^{\mu\nu}\partial_\mu\phi_C\partial_\nu\phi_\Delta - \frac{\lambda}{4!}\left(4\phi_C{}^3\phi_\Delta + \phi_C\phi_\Delta{}^3\right)\right] \quad (5.29)$$

As expected there are two different interaction terms, thus two vertices. From now on we will utilize the conformal time τ, defined as $\tau = -\int_t^\infty dt'/a(t')$. Note that, as a function of τ, the scale factor is $a(\tau) =$

---

[1]ϕ_+ lives in the space $Im\tau > 0$, while ϕ_- lives in$Im\tau < 0$ and we are going from τ to ∞ in the positive plane and then back to τ in the negative plane

$-(H\tau)^{-1}$. Using eq. (2.87) one can derive the free two-point functions:

$$
\begin{aligned}
G_C(k, \tau_1, \tau_2) &= \frac{H^2}{2k^3} \left[(1 + k^2 \tau_1 \tau_2) \cos k(\tau_1 - \tau_2) \right. & (5.30) \\
&\quad \left. + k(\tau_1 - \tau_2) \sin k(\tau_1 - \tau_2) \right], \\
G_R(k, \tau_1, \tau_2) &= \theta(\tau_1 - \tau_2) \frac{H^2}{k^3} \left[(1 + k^2 \tau_1 \tau_2) \sin k(\tau_1 - \tau_2) \right. & (5.31) \\
&\quad \left. - k(\tau_1 - \tau_2) \cos k(\tau_1 - \tau_2) \right],
\end{aligned}
$$

and $G_A(k, \tau_1, \tau_2) = G_R(k, \tau_2, \tau_1)$, and where the two point functions depend only on the length of the spatial momentum $k = |\mathbf{k}|$.

We represent the ϕ_C field with a full line and the ϕ_Δ field with a dashed line and so we can write the Feynman rules for the two point functions as

$$\overline{\tau_1 \qquad \tau_2} = G_C(k, \tau_1, \tau_2),$$

$$\overline{\tau_1 \; \text{-} \text{-} \; \tau_2} = -i G_R(k, \tau_1, \tau_2) = -i G_A(k, \tau_2, \tau_1).$$

We have two different vertices. One contains three powers of ϕ_C and one of ϕ_Δ so we draw it with three full lines and one dashed line. The other instead contains one power of ϕ_C and three of ϕ_R, hence a vertex with three dashed lines and one full line. Since we are in a de Sitter background, $\sqrt{-g} = a^4(\tau)$ and the vertices become:

$$-ia^4(\tau)\frac{\lambda}{3!}\phi_C{}^3\phi_R \qquad\qquad -ia^4(\tau)\frac{\lambda}{4!}\phi_C\phi_R{}^3$$

When a two point function is attached to a vertex, the corresponding time has to be integrated over, so we get a $\int d\tau$, while for a closed loop we get an integral over the internal spatial momentum $\int d^3 p/(2\pi)^3$.

Considering the form of G_R we can already exclude the presence of loop with mixed lines, like in figure (5.3). In fact such a loop would close a retarded propagator G_R on the same time $\tau = \tau_1 = \tau_2$ but, due to the embedded $\Theta(\tau_1 - \tau_2)$, it vanishes. So the only possible loop that

we can build with our set of Feynmann's rules is made of a full line. It is given by

$$L(\tau) = \int \frac{d^3 p}{(2\pi)^3} \mathrm{G}_C^{(0)}(p, \tau, \tau) \,, \qquad (5.32)$$

where by the superscript (0) we mean the free correlation functions. Since we will calculate correlation functions at higher orders, the superscript (i) will help us keep track of which order are we considering at each moment. As argued in [76], primitively divergent graphs contain only vertices of the same type. If there were vertices of different type, then at least two internal lines would be retarded propagators, the corresponding momenta would be on shell, the corresponding loop integral would be finite and the graph would not have been primitively divergent. Now the graphs of the in-in effective action with all vertices of the same sign are just the graphs of the in-out theory plus their complex conjugates, so the primitive divergences must be the same. Once the primitive divergences are controlled, it is only a matter of combinatorics to show that the overlapping divergences disappear as well. In fact what we will do in the next chapter is exploring the behaviour of higher order loop corrections to the free correlators and in doing this we will discover how only the vertices with three full lines really contribute to divergences in the infrared limit, which is equivalent to say the late time limit during Inflation.
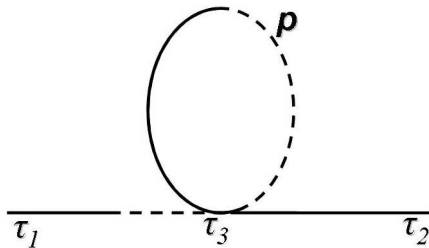
Figure 5.2: The loop is formed by a retarded propagator G_R starting and ending at time τ_3, thus it vanishes.

Chapter 6

Loops and Correlation Functions

We have seen that the non Gaussianity of the curvature perturbation depends on the gravity, but also on the eventual non Gaussianity of the scalar field itself. It has been shown [26, 23, 24] that the loop corrections at the first orders can become very large at late times ($k\tau \ll 1$). It was shown in fact that a self-interacting field develops logarithmic divergences in the late times limit [25]. Moreover these corrections receive powers of N through the integrals over momenta, making so the divergences even worse as one proceeds to higher orders. Thus one would expect unlimited growing corrections as we near the end of Inflation. Yet, all these studies did not address the question of what happens if one tries to resum the divergences. In this chapter, using all the machinery developed in the previous chapters, we address exactly this question: *can the divergences be reabsorbed to produce a non divergent theory?*

6.1 Two-Point Functions

As shown in chapter 3, we are particularly interested to in the 2- and 4-point functions since they are the interesting ones to predict the non Gaussianity.We calculated the free two-point correlation functions in eq. (5.3). In the approximation of late times $(-k\tau_i \ll 1)$ and small internal momenta[1], the free two-point functions $G_C(k,\tau_1,\tau_2)$ and $G_R(k,\tau_1,\tau_2)$ can be expanded in powers of $k\tau_i$ [25]:

$$G_C^{(0)}(k,\tau_1,\tau_2) = \frac{H^2}{2k^3}[1 + O(k^2\tau_i^2)], \qquad (6.1)$$

$$G_R^{(0)}(k,\tau_1,\tau_2) = \theta(\tau_1 - \tau_2)\frac{H^2}{3k^3}[k^3(\tau_1^3 - \tau_2^3) + O(k^5\tau_i^5))]. \qquad (6.2)$$

We have two vertices but we will use only the three full lines and one dashed line. The reason is that the $\langle \phi_C \phi_C \rangle = G_C$ has a momentum depence k^{-3} and thus is divergent in the infrared, while the $\langle \phi_C \phi_\Delta \rangle = G_R$ does not. Moreover, we note that for a vertex with three dashed lines it is not possible to build loops since they vanish identically. We remember that in the previous chapter we explained that divergences could come only from graphs with the same type of vertice, thus in the light of these considerations the vertex with the highest number of possible G_C is the natural choice since we are interested in exploring the late time limit. Let us use these to calculate the corrections produced by graphs containing one or more tadpoles or even more complicated configurations.

6.1.1 First Order Diagrams

The simplest correction to the free propagators $G_C^{(0)}$ and $G_R^{(0)}$ comes from the graphs with a single tadpole. As already argued, it is not possible to have a loop made with dashed lines since $G_{\Delta\Delta}$ vanishes

---

[1]This means that in loops we integrate over momenta which are already outside of the horizon when the considered scale k crosses it. In other words this means that we consider momenta smaller than k.

identically and G_R vanishes when evaluated at the same time. So we include only the full line loop and thus figure 6.1 is the only first order correction to $G_C^{(0)}$: it is clear that due to the simmetry of G_C we must
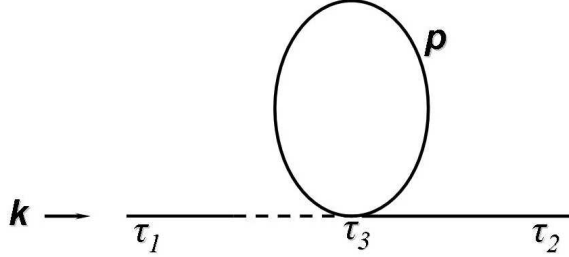

Figure 6.1: One tadpole G_C propagator

consider also the mirror diagram. Using the expressions (6.1) and (6.2), figure 6.1 translates into the following integral,

$$(-i\frac{\lambda}{3!})(-i)\int_{-\frac{1}{k}}^{\tau_1}d\tau_3 a^4(\tau_3)\mathrm{G}_R^{(0)}(k,\tau_1,\tau_3)\int\frac{d^3p}{(2\pi)^3}\mathrm{G}_C^{(0)}(p,\tau_3,\tau_3)\mathrm{G}_C^{(0)}(k,\tau_3,\tau_2)\,,$$

(6.3)

where p is the internal momentum of the tadpole and k the momentum flowing in the diagram. The mirror graph gives

$$(-i\frac{\lambda}{3!})(-i)\int_{-\frac{1}{k}}^{\tau_2}d\tau_3 a^4(\tau_3)\mathrm{G}_R^{(0)}(k,\tau_2,\tau_3)\int\frac{d^3p}{(2\pi)^3}\mathrm{G}_C^{(0)}(p,\tau_3,\tau_3)\mathrm{G}_C^{(0)}(k,\tau_3,\tau_1)\,.$$

(6.4)

We set the inferior limit of integration to $-\frac{1}{k}$ instead of $-\infty$, because we are interested in following perturbations from the moment of horizon exit up to some later time τ. The horizon exit time is given by the condition $-k\tau_h = 1$ and so $\tau_h = -\frac{1}{k}$. Physically this means that we neglect every correlation with what happened before the horizon exit and we start to consider correlations only after the exit of each relevant scale. The tadpole integral over d^3p is divergent but can be in general regularized choosing appropriate infrared and ultraviolet cutoffs, Λ_{IR} and Λ_{UV},

$$\int\frac{d^3p}{(2\pi)^3}\mathrm{G}_C^{(0)}(p,\tau_3,\tau_3)=\frac{H^2}{(2\pi)^2}\ln(\frac{\Lambda_{UV}}{\Lambda_{IR}})\,.$$

(6.5)

75

How can we choose Λ_{IR} and Λ_{UV}? We are interested in super-horizon scales, so we choose Λ_{IR} corresponding to the smallest scale already outside of the horizon at the beginning of Inflation and we choose Λ_{UV} corresponding to the wavelength that leaves the horizon at the final istant of Inflation. In this context though, this choice comes with a natural expression: Λ_{IR} is proportional to $a(t_{in})$ evaluated at the beginning of Inflation, while Λ_{UV} is proportional to the scale factor at the end of Inflation $a(t_{fin}) = a(t_{in})e^N$, therefore the logarithm is proportional to the number of e-folds that Inflation lasts. Before performing the calculation we must also consider the coefficient in front of the graph coming from Wyck's theorem. We have $\phi_\Delta(\phi_C)^3$ from the vertex and the external legs, $\phi_C(\tau_1)$ and $\phi_C(\tau_2)$. So there are three possibilities for contracting $\phi(\tau_2)$ with one of the ϕ_C of the vertex and one for contracting $\phi_C(\tau_1)$ with the vertex's ϕ_Δ, which sum up to 3 in front of the graph. Performing the calculation and considering also the mirror graph, we obtain

$$
\begin{aligned}
\mathrm{G}_C^{(1)} &= 3\frac{\lambda}{3!6k^3}(\frac{H}{2\pi})^2\ln(\frac{\Lambda_{UV}}{\Lambda_{IR}}) \\
&\quad \frac{1}{3}[2 + (k^3\tau_1{}^3 + k^3\tau_2{}^3) + 3(\ln(-k\tau_1) + \ln(-k\tau_2))]\,, \quad (6.6)
\end{aligned}
$$

which at leading order reduces to

$$
\mathrm{G}_C^{(1)}(k, \tau_1, \tau_2) \simeq \frac{H}{2k^3}\frac{\lambda L}{3!H^2}(\ln(-k\tau_1) + \ln(-k\tau_2))\,, \quad (6.7)
$$

where from now on by L we mean eq. (5.32) evaluated between the cutoffs, $L = \left(\frac{H}{2\pi}\right)^2\ln\left(\frac{\Lambda_{UV}}{\Lambda_{IR}}\right)$. Exactly as for the G_C, it is possible to draw a one tadpole G_R as in fig. 6.2. It translates to

$$
\begin{aligned}
-i\mathrm{G}_R^{(1)}(k, \tau_1, \tau_2) &= \int_{\tau_2}^{\tau_1} d\tau_3(-i\frac{\lambda}{3!}a^4(\tau_3))(-i)\mathrm{G}_R^{(0)}(k, \tau_1, \tau_3) \\
&\quad \int \frac{d^3p}{(2\pi)^3}\mathrm{G}_C^{(0)}(p, \tau_3, \tau_3)(-i)\mathrm{G}_R^{(0)}(k, \tau_3, \tau_2) \quad (6.8)
\end{aligned}
$$

In this case there is not a mirror graph due to the oddness of the G_R under exchange of times. The coefficient is again 3 since there are three possibilities to contract $\phi(\tau_2)$ with one of the vertex's ϕ_Cs and one to
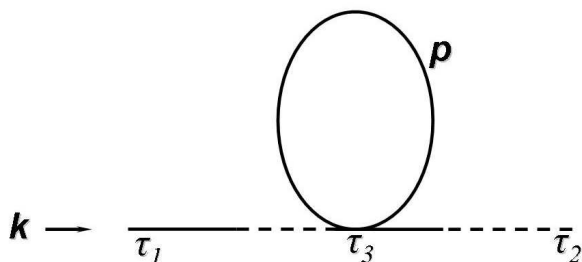
Figure 6.2: One tadpole G_R propagator

contract $\phi_C(\tau_1)$. Then, for a correction to a G_R graph with $\tau_1 > \tau_2$:

$$-i\mathrm{G}_R^{(1)}(k,\tau_1,\tau_2) = 3\theta(\tau_1 - \tau_2)\frac{i\lambda}{3!27}(\frac{H}{2\pi})^2 \ln(\frac{\Lambda_{UV}}{\Lambda_{IR}})[2(\tau_1{}^3 - \tau_2{}^3)$$
$$+3(\tau_1{}^3 + \tau_2{}^3)\ln\left(\frac{\tau_1}{\tau_2}\right)], \tag{6.9}$$

that at leading order reduces to

$$-i\mathrm{G}_R^{(1)}(k,\tau_1,\tau_2) = \theta(\tau_1 - \tau_2)\frac{iH^2}{3}\frac{\lambda L}{3!H^2}(\tau_1{}^3 + \tau_2{}^3)\ln\left(\frac{\tau_1}{\tau_2}\right) \tag{6.10}$$

Note that the first order correction to the retarded propagator is consistently odd under exchange of the times τ_1 and τ_2. Also, we see that in the limit of late times ($k\tau \ll 1$) both propagator have logarithmic divergences. We have so far reproduced in a simple way the results of [26, 27]. In our quest to cure the divergence we now proceed to the second order, hoping to find a hint about what is the right way to reabsorb the infinities.

6.1.2 Second Order Diagrams

Analogously to the one-tadpole graph, a graph with two tadpoles can be easily constructed, basically adding a G_R and closing in a tadpole two of the straight lines of the second vertex, as in figure 6.3.

The amplitude for this diagram is easily calculated:
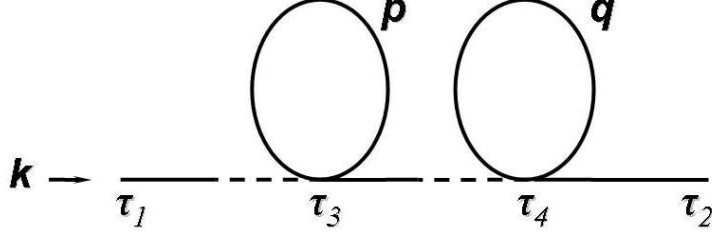
Figure 6.3: Two-tadpole G_C propagator.

$$
\begin{aligned}
G_C^{(2)}(k,\tau_1,\tau_2) &= \int_{-\frac{1}{k}}^{\tau_1} d\tau_3 (-i) G_R^{(0)}(k,\tau_1,\tau_3)(-i\frac{\lambda}{3!}a^4(\tau_3)) \int \frac{d^3p}{(2\pi)^3} G_C^{(0)}(p,\tau_3,\tau_3) \\
&\quad \int_{-\frac{1}{k}}^{\tau_1} d\tau_4 (-i) G_R^{(0)}(k,\tau_3,\tau_4)(-i\frac{\lambda}{3!}a^4(\tau_4)) \\
&\quad \int \frac{d^3q}{(2\pi)^3} G_C^{(0)}(q,\tau_4,\tau_4) G_C^{(0)}(k,\tau_4,\tau_2)\,, \tag{6.11}
\end{aligned}
$$

plus the mirror graph. With the notation of fig. 6.3, there are two vertices so we have two ways to contract $\phi_C(\tau_1)$ with one of the ϕ_Δ, then three possibilities to contract one of the three ϕ_C of the same vertex with the remaining ϕ_Δ and then three more to contract $\phi_C(\tau_2)$ with the one ϕ_C of the second vertex. So the coefficient in front of the amplitude due to Wyck's theorem is $18/2!$. The integral in $d\tau_4$ however is not truly up to τ_1, because the $\theta(\tau_3 - \tau_4)$ embedded in $G_R^{(0)}(k,\tau_3,\tau_4)$ forces $\tau_3 > \tau_4$ and so:

$$
\int_{-\frac{1}{k}}^{\tau_1} d\tau_4 \rightarrow \int_{-\frac{1}{k}}^{\tau_3} d\tau_4 \tag{6.12}
$$

In the end the result is:

$$
\begin{aligned}
G_C^{(2)}(k,\tau_1,\tau_2) &= \frac{18}{2!}\frac{\lambda^2}{3!18k^3}\frac{1}{H^2}[(\frac{H}{2\pi})^2\ln(\frac{\Lambda_{UV}}{\Lambda_{IR}})]^2\frac{1}{6}[4 + 2k^3{\tau_1}^3 + 2k^3{\tau_2}^3 \\
&\quad + \ln(-k\tau_1)(4 - 2k^3{\tau_1}^3) + \ln(-k\tau_2)(4 - 2k^3{\tau_2}^3) \\
&\quad + 3[\ln^2(-k\tau_1) + \ln^2(-k\tau_2)]] \tag{6.13}
\end{aligned}
$$

which at leading order reduces to

$$G_C^{(2)}(k, \tau_1, \tau_2) \simeq \frac{H}{2k^3} \left(\frac{\lambda L}{3!H^2} \right)^2 \frac{1}{2!} (\ln^2(-k\tau_1) + \ln^2(-k\tau_2)) \quad (6.14)$$
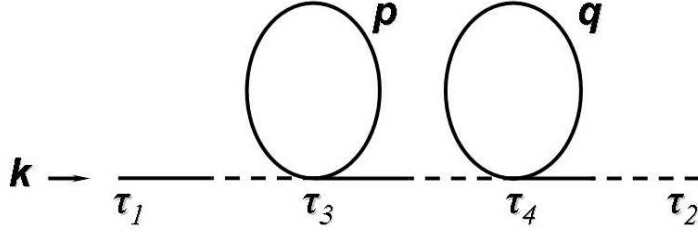

Figure 6.4: Two-tadpole G_R propagator.

The two–tadpole graph for the retarded propagator is shown in figure 6.4. Its amplitude is given by

$$
\begin{aligned}
-iG_R^{(2)}(k, \tau_1, \tau_2) \;=\; & \int_{\tau_2}^{\tau_1} d\tau_3 (-i\frac{\lambda}{3!}a^4(\tau_3))(-i)G_R^{(0)}(k, \tau_1, \tau_3) \qquad (6.15) \\
& \int \frac{d^3p}{(2\pi)^3} G_C^{(0)}(p, \tau_3, \tau_3) \int_{\tau_2}^{\tau_3} d\tau_4 (-i)G_R^{(0)}(k, \tau_3, \tau_4) \\
& (-i\frac{\lambda}{3!}a^4(\tau_4)) \int d^3q\, G_C^{(0)}(q, \tau_4, \tau_4)(-i)G_R^{(0)}(k, \tau_4, \tau_2) \,.
\end{aligned}
$$

where the superior integration limit of the integral in $d\tau_4$ has already been changed to τ_3, due to the $\theta(\tau_3-\tau_4)$ embedded in $G_R^{(0)}(k, \tau_3, \tau_4)$. The combinatorial coefficient is again $18/2!$ and performing the calculation we obtain

$$
\begin{aligned}
-iG_R^{(2)}(k, \tau_1, \tau_2) \;=\; & \frac{18}{2!} \frac{-i\lambda^2}{3!27H^2} \left[(\frac{H}{2\pi})^2 \ln(\frac{\Lambda_{UV}}{\Lambda_{IR}}) \right]^2 \\
& \frac{1}{6} \left\{ 4(\tau_1{}^3 - \tau_2{}^3) - 6(\tau_1{}^3 + \tau_2{}^3) \ln \left(\frac{\tau_1}{\tau_2} \right) \right. \\
& \left. + 3(\tau_1{}^3 - \tau_2{}^3) \ln^2 \left(\frac{\tau_1}{\tau_2} \right) \right\} \qquad (6.16) \\
\simeq\; & \frac{-iH^2}{3} \left(\frac{\lambda L}{3!H^2} \right)^2 \frac{1}{2!} (\tau_1{}^3 - \tau_2{}^3) \ln^2 \left(\frac{\tau_1}{\tau_2} \right) (6.17)
\end{aligned}
$$

79

The diagrams that we have calculated up to now though are not the only ones present at the second order. Indeed, we can draw two more diagrams for each propagator, namely the so-called *sunrise* diagrams, shown in figure 6.5, and the *tower* diagrams, shown in figure 6.6.
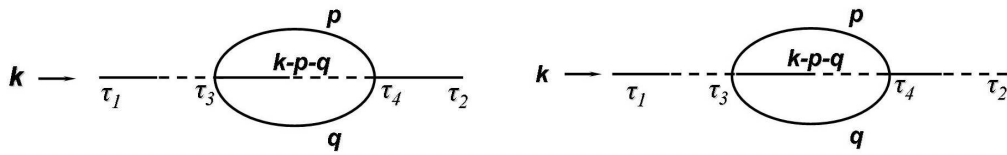

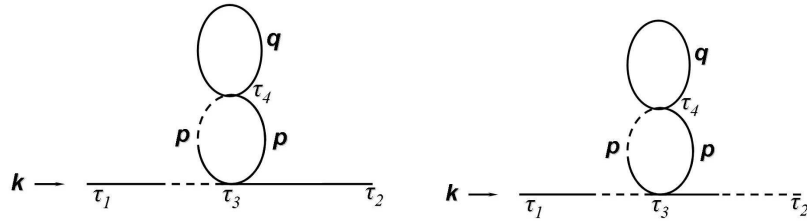Figure 6.5: Second order sunrise diagrams for $G_C(left)$ and $G_R(right)$.

Figure 6.6: Second order tower diagrams for $G_C(left)$ and $G_R(right)$.

Sunrises and Towers Let us start with the *sunrise* diagrams. Despite the graphical difference, these diagrams translate exactly to the two tadpole graphs. We can see in fact that they can be written as:

$$
\begin{aligned}
\mathrm{G}_C^{(2)sun}(k,\tau_1,\tau_2) &= \int_{-\frac{1}{k}}^{\tau_1} d\tau_3 \int \frac{d^3p}{(2\pi)^3} \int \frac{d^3q}{(2\pi)^3} \int_{-\frac{1}{k}}^{\tau_3} d\tau_4 (-i)\mathrm{G}_R^{(0)}(k,\tau_1,\tau_3) \\
&\quad (-i\frac{\lambda}{3!}a^4(\tau_3))\mathrm{G}_C^{(0)}(p,\tau_3,\tau_4)(-i)\mathrm{G}_R^{(0)}(k-p-q,\tau_3,\tau_4) \\
&\quad (-i\frac{\lambda}{3!}a^4(\tau_4))\mathrm{G}_C^{(0)}(q,\tau_3,\tau_4)\mathrm{G}_C^{(0)}(k,\tau_4,\tau_2)\,, \qquad (6.18)
\end{aligned}
$$

$$
\begin{aligned}
-i\mathrm{G}_R^{(2)sun}(k,\tau_1,\tau_2) &= \int_{\tau_2}^{\tau_1} d\tau_3 \int \frac{d^3p}{(2\pi)^3} \int \frac{d^3q}{(2\pi)^3} \int_{\tau_2}^{\tau_3} d\tau_4 (-i\frac{\lambda}{3!}a^4(\tau_3)) \\
&\quad (-i)\mathrm{G}_R^{(0)}(k,\tau_1,\tau_3)\mathrm{G}_C^{(0)}(p,\tau_3,\tau_3)(-i)\mathrm{G}_R^{(0)}(k-p-q,\tau_3,\tau_4) \\
&\quad (-i\frac{\lambda}{3!}a^4(\tau_4))\mathrm{G}_C^{(0)}(q,\tau_4,\tau_4)(-i)\mathrm{G}_R^{(0)}(k,\tau_4,\tau_2)\,. \qquad (6.19)
\end{aligned}
$$

We see by comparison with eq. (6.11) and eq. (6.15) that the only difference is in the $\mathrm{G}_R^{(0)}$ between τ_3 and τ_4. The free retarded propagator in the late time limit does not depend on the momentum flowing through it, so $\mathrm{G}_R^{(0)}(k-p-q,\tau_3,\tau_4) = \mathrm{G}_R^{(0)}(k,\tau_3,\tau_4)$ and we find again the integral (6.15) written for the two tadpole diagrams. We did not mention yet the combinatorial coefficient in front of the intergrals. We have two ways to contract $\phi_C(\tau_1)$ with a ϕ_Δ of the vertices, then three to contract one ϕ_C of the first vertex to the ϕ_Δ of the second and finally six to contract the remaining free ϕ_C in the two vertices. In total we have a 36/2!. We see then that the contributions coming from the tadpole and sunrise diagrams are not exactly equal, but differ for a numerical constant.

In writing the amplitude for the G_C^{tower} at second order we must be more careful. Indeed, we have two loops which are chained one into the other; in the G_R tower diagram from two consecutive retarded propagators $\mathrm{G}_R^{(0)}(k,\tau_1,\tau_3)\mathrm{G}_R^{(0)}(k,\tau_3,\tau_2)$ one obtains $\tau_1 > \tau_3 > \tau_2$ while for the G_C tower diagram one obtains only $\tau_1 > \tau_3$. We note however that the times internal to the loops do not receive constraints from the θ functions relative to τ_1,τ_3,τ_2. The integral over the time $d\tau_4$ must then extend from a loop characteristic time to the upper end which

is given by the θ function embedded in $G_R(p, \tau_3, \tau_4)$. The only time scale available is the one given by the momentum p, thus the integral over $d\tau_4$ is evaluated between $-\frac{1}{p}$ and τ_3. With these considerations the amplitude for the tower G_C diagram is given by

$$
\begin{aligned}
\mathrm{G}_C^{tower(2)}(k, \tau_1, \tau_2) &= \int_{-\frac{1}{k}}^{\tau_1} d\tau_3 \int \frac{d^3 p}{(2\pi)^3} \int \frac{d^3 q}{(2\pi)^3} \int_{-\frac{1}{p}}^{\tau_3} d\tau_4 (-i) \mathrm{G}_R^{(0)}(k, \tau_1, \tau_3) \\
&\quad (-i\frac{\lambda}{3!} a^4(\tau_3)) \mathrm{G}_C^{(0)}(k, \tau_3, \tau_2)(-i) \mathrm{G}_R^{(0)}(p, \tau_3, \tau_4) \\
&\quad (-i\frac{\lambda}{3!} a^4(\tau_4)) \mathrm{G}_C^{(0)}(q, \tau_4, \tau_4) \mathrm{G}_C^{(0)}(p, \tau_4, \tau_3), \quad (6.20)
\end{aligned}
$$

and the amplitude for the retarded propagator is

$$
\begin{aligned}
\mathrm{G}_R^{tower(2)}(k, \tau_1, \tau_2) &= \int_{\tau_2}^{\tau_1} d\tau_3 \int \frac{d^3 p}{(2\pi)^3} \int \frac{d^3 q}{(2\pi)^3} \int_{-\frac{1}{p}}^{\tau_3} d\tau_4 (-i) \mathrm{G}_R^{(0)}(k, \tau_1, \tau_3) \\
&\quad (-i\frac{\lambda}{3!} a^4(\tau_3)) \mathrm{G}_R^{(0)}(k, \tau_3, \tau_2)(-i) \mathrm{G}_R^{(0)}(p, \tau_3, \tau_4) \\
&\quad (-i\frac{\lambda}{3!} a^4(\tau_4)) \mathrm{G}_C^{(0)}(q, \tau_4, \tau_4) \mathrm{G}_C^{(0)}(p, \tau_4, \tau_3), \quad (6.21)
\end{aligned}
$$

Now it is no more indifferent the order with which we perform the integrals, since the momentum p is now in the integration limits of τ_4, so we need to perform first that integral and then the one over p. Performing the calculation:

$$
\begin{aligned}
\mathrm{G}_C^{tow(2)}(k, \tau_1, \tau_2) &= \frac{36}{2!} \left(\frac{\lambda}{3!} \right)^2 \frac{L}{36 k^3} \frac{1}{54 k^3} \left(-2\Lambda_{IR}^3 + 2\Lambda_{UV}^3 - 2k^3 \Lambda_{IR}^3 \tau_1^3 + 2k^3 \Lambda_{UV}^3 \tau_1^3 \right. \\
&\quad -27 k^3 \ln^2[-k] \ln\left[\frac{\Lambda_{UV}}{\Lambda_{IR}} \right] - 3k^3 \ln[-k] \left(-2\Lambda_{IR}^3 \tau_1^3 + 2\Lambda_{UV}^3 \tau_1^3 \right. \\
&\quad +9\ln^2[-\Lambda_{IR}] - 9\ln^2[-\Lambda_{UV}] + \left(-6 + 6k^3 \tau_1^3 \right) \ln\left[\frac{\Lambda_{UV}}{\Lambda_{IR}} \right]) \\
&\quad +6 k^3 \Lambda_{IR}^3 \tau_1^3 \ln[\tau_1] - 6 k^3 \Lambda_{UV}^3 \tau_1^3 \ln[\tau_1] \\
&\quad -9 k^3 \ln^2[-\Lambda_{IR}] \left(1 + k^3 \tau_1^3 + 3 \ln[\tau_1] \right) + 9 k^3 \ln^2[-\Lambda_{UV}] \\
&\quad \left(1 + k^3 \tau_1^3 + 3 \ln[\tau_1] \right) + 3 k^3 \ln\left[\frac{\Lambda_{UV}}{\Lambda_{IR}} \right] \\
&\quad \left. \left(4 + 4k^3 \tau_1^3 + 12 \ln[\tau_1] + 9 \ln^2[\tau_1] \right) . \right. \quad (6.22)
\end{aligned}
$$

Considering also the mirror graph, at leading order we have

$$
\mathrm{G}_C^{tow(2)} \simeq \frac{H^2}{2k^3} \left(\frac{L}{H^2} \right)^2 \frac{1}{2!} [\ln^2(\tau_1) + \ln^2(\tau_2) - 2\ln^2(-\frac{1}{k})] . \quad (6.23)
$$

To obtain a more compact and elegant result we use explicitly the small momenta approximation and, in the integral over τ_4, we integrate from $-\frac{1}{k}$ instead of $-\frac{1}{p}$, obtaining :

$$G_C^{tow(2)} \simeq \frac{H^2}{2k^3} \left(\frac{L}{H^2} \right)^2 \frac{1}{2!} [\ln^2(-k\tau_1) + \ln^2(-k\tau_2)] . \tag{6.24}$$

We note that using this simplification does not alter the physical meaning of our calculation and its validity since what we have been calculating up to now are the super–horizon correlations. Moreover the substitution does not change the divergent behaviour for late times but provides an easier to handle expression.

We can calculate the tower diagram (fig. 6.6) for the retarded propagator and we obtain the following result:

$$
\begin{aligned}
G_R^{tow(2)} \; = \; & \frac{36}{2!} \left(\frac{\lambda L}{3!(2\pi)} \right)^2 \frac{1}{27} \frac{1}{54} \left(\Lambda_{IR}{}^3 \tau_1{}^6 - \Lambda_{UV}{}^3 \tau_1{}^6 - \Lambda_{IR}{}^3 \tau_2{}^6 + \Lambda_{UV}{}^3 \tau_2{}^6 \right. \\
& + 12 \left(\tau_1{}^3 - \tau_2{}^3 \right) \ln \left[\frac{\Lambda_{UV}}{\Lambda_{IR}} \right] \\
& + 6 \left(-\Lambda_{IR}{}^3 + \Lambda_{UV}{}^3 \right) \tau_1{}^3 \tau_2{}^3 \ln \left[\frac{\tau_1}{\tau_2} \right] \\
& - 36 \tau_2{}^3 \ln \left[\frac{\Lambda_{UV}}{\Lambda_{IR}} \right] \ln \left[\frac{\tau_1}{\tau_2} \right] \\
& - 27 \left(\tau_1{}^3 + \tau_2{}^3 \right) \ln \left[\frac{\Lambda_{UV}}{\Lambda_{IR}} \right] \ln^2 \left[\frac{\tau_1}{\tau_2} \right] \\
& + 9 \ln[-\Lambda_{UV}]^2 \left(2\tau_1{}^3 - 2\tau_2{}^3 - 3 \left(\tau_1{}^3 + \tau_2{}^3 \right) \ln \left[\frac{\tau_1}{\tau_2} \right] \right) \\
& + 9 \ln^2[-\Lambda_{IR}] \left(-2\tau_1{}^3 + 2\tau_2{}^3 + 3 \left(\tau_1{}^3 + \tau_2{}^3 \right) \ln \left[\frac{\tau_1}{\tau_2} \right] \right) \\
& + 36 \left(\tau_1{}^3 - \tau_2{}^3 \right) \ln \left[\frac{\Lambda_{UV}}{\Lambda_{IR}} \right] \ln[\tau_2] \\
& \left. - 54 \left(\tau_1{}^3 + \tau_2{}^3 \right) \ln \left[\frac{\Lambda_{UV}}{\Lambda_{IR}} \right] \ln \left[\frac{\tau_1}{\tau_2} \right] \ln[\tau_2] \right. .
\end{aligned}
$$

$$\tag{6.26}$$

At leading order it takes the shorter form

$$-i\mathrm{G}_R^{tow(2)} \simeq \frac{+iH^2}{3} \left(\frac{\lambda L}{3!H^2}\right)^2 \left(\tau_1{}^3 + \tau_2{}^3\right) \ln^2\left[\frac{\tau_1}{\tau_2}\right] . \qquad (6.27)$$

We want to make two observations:

a) In all cases (tadpole graphs, sunrise and tower) we have the same quadratic logarithmic divergence for late times. We can imagine that proceeding to higher orders the powers of the divergent logarithms will grow following the increasing order. For the tadpole graphs this is rather easy to see. Indeed, given a tadpole graph of
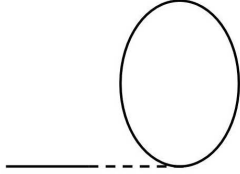
Figure 6.7: Tadpole added at each order

the nth order, which means a graph with n consecutive tadpoles, we can obtain the one with $n + 1$ tadpoles by simply adding a vertex with a tadpole and a $\mathrm{G}_R^{(0)}$ on the left side (see figure 6.7). Dimensionally each free retarded propagator brings a τ^3 while each vertex brings a τ^{-4} and an integral over τ. The tadpole does not contribute to the powers of τ but contributes with a L. So in total we obtain an $L \int \frac{d\tau}{\tau}$, which qualitatively shows why at each order n we expect a divergence $\simeq \ln^n(\tau)$;

b) If we take into consideration only the tadpole graphs, we see that the $\mathrm{G}_C^{(1)}$ and $\mathrm{G}_C^{(2)}$ show the structure of a power series. In particular, if we define the parameter

$$\epsilon = \frac{\lambda L}{3!H^2} \qquad (6.28)$$

we see that they correspond to the first and second order terms of the expansion in powers of ϵ of $\mathrm{G}_C^{(0)} e^{\epsilon \ln(k^2 \tau_1 \tau_2)}$. However the first two corrections to G_R do not show such a simple behaviour. Actually this was expected due to the request of oddness, since at odd orders we must have a term $(\tau_1{}^3 + \tau_2{}^3)$ in front of the logarithm, while at even we need a term of the form $(\tau_1{}^3 - \tau_2{}^3)$, due to the powers of the logarithm being in the two cases, respectively, odd and even. Therefore if we want to have a chance of summing the G_R tadpoles graphs we need to check at least the next odd and even orders, in other words, the third and fourth.

6.1.3   Higher Order Diagrams

The observation at the end of last section prompt us to explore the behaviour of the same type of graphs at higher order. As we proceed to higher orders we find new types of diagrams that we should account for. We restrict our analysis now to the simpler ones, keeping in mind our aim of finding a feasible resummation for those, that could be indicative also of the behaviour of the complete theory. Let us start now with the third and fourth order diagrams for G_R and G_C with only tadpoles. These are the easiest and the calculation is straightforward as it mimicks exactly what we did for the lower orders. The diagrams are shown in figures 6.8 and 6.9 and the results at leading order are:

$$\mathrm{G}_C^{(3)}(k, \tau_1, \tau_2) \;\simeq\; \frac{H}{2k^3} \left(\frac{\lambda L}{3! H^2}\right)^3 \frac{1}{3!} (\ln^3(-k\tau_1) + \ln^3(-k\tau_2)), \quad (6.29)$$

$$\mathrm{G}_C^{(4)}(k, \tau_1, \tau_2) \;\simeq\; \frac{H}{2k^3} \left(\frac{\lambda L}{3! H^2}\right)^4 \frac{1}{4!} (\ln^4(-k\tau_1) + \ln^4(-k\tau_2)), \quad (6.30)$$

$$-i G_R^{(3)}(k, \tau_1, \tau_2) \;\simeq\; \frac{-i H^2}{3} \left(\frac{\lambda L}{3! H^2}\right)^3 \frac{1}{3!} (\tau_1{}^3 + \tau_2{}^3) \ln^3\!\left(\frac{\tau_1}{\tau_2}\right), \quad (6.31)$$

$$-i G_R^{(4)}(k, \tau_1, \tau_2) \;\simeq\; \frac{-i H^2}{3} \left(\frac{\lambda L}{3! H^2}\right)^4 \frac{1}{4!} (\tau_1{}^3 - \tau_2{}^3) \ln^4\!\left(\frac{\tau_1}{\tau_2}\right). \quad (6.32)$$
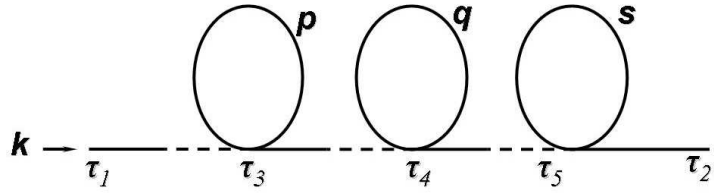
85

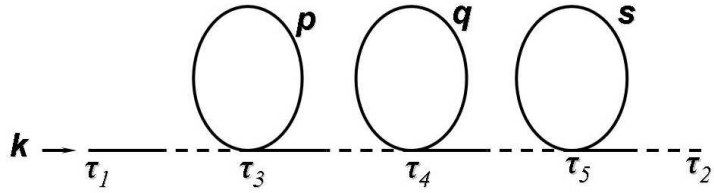Figure 6.8: Three tadpole G_C diagram
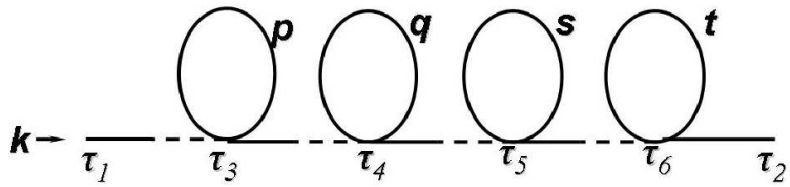

Figure 6.9: Three tadpole G_R diagram

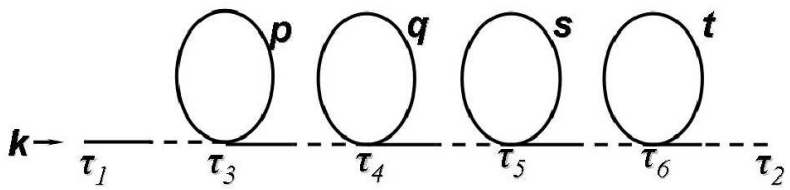Figure 6.10: Four tadpole G_C diagram

Figure 6.11: Three tadpole G_R diagram

86

We see that our guess for G_C is confirmed. In terms of the ϵ defined in eq. (6.28), we define the sum of all the tadpole graphs (at leading order) for G_C as

$$\mathrm{G}_C^{chain}(k, \tau_1, \tau_2) \;=\; \mathrm{G}_C^{(0)} e^{\epsilon \ln(k^2 \tau_1 \tau_2)} \tag{6.33}$$

$$=\; \frac{H^2}{2k^3} e^{\frac{\lambda L}{3! H^2} \ln(k^2 \tau_1 \tau_2)} \,. \tag{6.34}$$

This G_C^{chain} is not anymore divergent for late times! Indeed in that limit it simply goes to 0. This our first important result. We stress that to obtain eq. (6.33) we have discarded all the the sunrise, tower and the more complex diagrams that eventually arise as the order increases. Yet it is a first indication that the resummed theory may be not divergent. Let us focus now on what happens to the G_R. We observe separately the odd and the even order tadpole diagrams. The even terms show a structure of the form:

$$-i\mathrm{G}_R^{(0)} - i\mathrm{G}_R^{(2)} - i\mathrm{G}_R^{(4)} \qquad 1 + \frac{x^2}{2!} + \frac{x^4}{4!} + \ldots \,, \tag{6.35}$$

while odd terms:

$$-i\mathrm{G}_R^{(1)} - i\mathrm{G}_R^{(3)} - i\mathrm{G}_R^{(4)} \qquad -\left(\frac{x}{1!} + \frac{x^3}{3!} + \ldots\right). \tag{6.36}$$

The series expansion (6.35) and (6.36) respectively correspond to those of the hyperbolic cosine and sine. So considering only the tadpole graphs again, we define $\mathrm{G}_R^{chain}(k, \tau_1, \tau_2)$ as:

$$
\begin{aligned}
-i\mathrm{G}_R^{chain}(k, \tau_1, \tau_2) \;&=\; -i\frac{H^2}{3}(\tau_1{}^3 - \tau_2{}^3)\cosh\left[\epsilon \ln\left(\frac{\tau_1}{\tau_2}\right)\right] \\
&\quad +i\frac{H^2}{3}(\tau_1{}^3 + \tau_2{}^3)\sinh\left[\epsilon \ln\left(\frac{\tau_1}{\tau_2}\right)\right] \\
&=\; -i\frac{H^2}{3}(\tau_1{}^3 - \tau_2{}^3)\frac{1}{2}\frac{\tau_1^{2\epsilon} + \tau_2^{2\epsilon}}{(\tau_1\tau_2)^{\epsilon}} \\
&\quad +i\frac{H^2}{3}(\tau_1{}^3 + \tau_2{}^3)\frac{1}{2}\frac{\tau_1^{2\epsilon} - \tau_2^{2\epsilon}}{(\tau_1\tau_2)^{\epsilon}},
\end{aligned}
\tag{6.37}
$$

which can be written in the shorter form

$$-i\mathrm{G}_R^{chain}(k, \tau_1, \tau_2) = -i\frac{H^2}{3}(\tau_1{}^{3-\epsilon}\tau_2{}^{\epsilon} - \tau_1{}^{\epsilon}\tau_2{}^{3-\epsilon}) \tag{6.38}$$
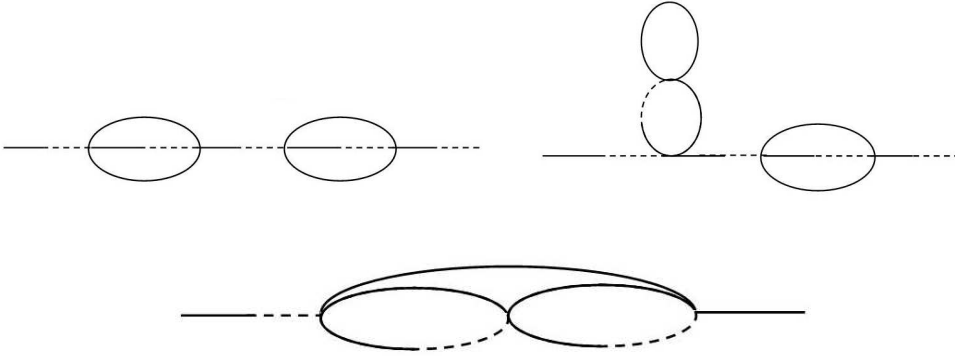
Figure 6.12: Examples of higher order and more complex diagrams.

We note that if $\epsilon < 3$ than also G_R^{chain} does not diverge at late times. Results (6.33) and (6.38) are very important in that they provide a first non perturbative estimate of the behaviour of the theory. Previous attempts have only explored the first [26, 27, 78, 23, 25], sometimes second, order in perturbation theory, stating the presence of the logarithmic divergences but not providing any indication about whether they were curable. Here we have just shown that, at least considering this tadpole class of diagrams, it is possible to obtain a non perturbative finite result for both the propagators.
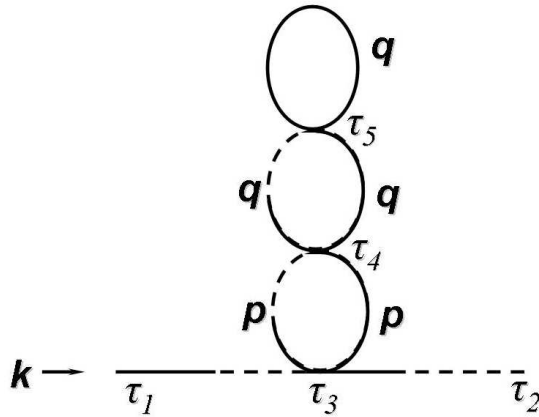
Figure 6.13: Third order G_R tower graph.

A natural problem arises now: we have neglected many diagrams in

our 'resummation', is this justified? In other words, can we somehow show that their contribution is not important in comparison to the tadpoles ones or that, when summed, they are not plagued by malicious divergences? Let us take a look at what happens if we consider the third order tower graph for G_R (fig. 6.13). Its amplitude can be written as:

$$
\begin{aligned}
\mathrm{G}_R^{tower(3)}(k, \tau_1, \tau_2) &= \int_{\tau_2}^{\tau_1} d\tau_3 (-i) \mathrm{G}_R^{(0)}(k, \tau_1, \tau_3)(-i\frac{\lambda}{3!}a^4(\tau_3))\mathrm{G}_R^{(0)}(k, \tau_3, \tau_2) \\
&\int \frac{d^3p}{(2\pi)^3} \int \frac{d^3q}{(2\pi)^3} \int_{-\frac{1}{p}}^{\tau_3} d\tau_4 (-i)\mathrm{G}_R^{(0)}(p, \tau_3, \tau_4) \\
&(-i\frac{\lambda}{3!}a^4(\tau_4))\mathrm{G}_C^{(0)}(q, \tau_4, \tau_3)\int_{-\frac{1}{q}}^{\tau_4}(-i\frac{\lambda}{3!}a^4(\tau_5))\mathrm{G}_R^{(0)}(q, \tau_4, \tau_5) \\
&\mathrm{G}_C^{(0)}(q, \tau_5, \tau_4)\int \frac{d^3t}{(2\pi)^3}\mathrm{G}_C^{(0)}(t, \tau_5, \tau_5)
\end{aligned}
$$

The combinatorial coefficient is $\frac{3^4 2^3}{3!}$ and thus the straightforward calculation gives (at leading order):

$$
\mathrm{G}_R^{tow(3)} = \theta(\tau_1 - \tau_2)\frac{iH^2}{3}\left(\frac{\lambda L}{3!H^2}\right)^3 \frac{2^2}{3!}(\tau_1{}^3 + \tau_2{}^3)\ln^3\left(\frac{\tau_1}{\tau_2}\right) \quad (6.39)
$$

Comparing this result with eq. (6.27) we are tempted to see a trend. If we assume that each higher order has the same dependence of the type

$$
-i\mathrm{G}_R^{tow(n)}(k, \tau_1, \tau_2) = \theta(\tau_1-\tau_2)\frac{iH^2}{3}\epsilon^{2+m}\frac{2^{2m}}{(2+m)!}(\tau_1{}^3+\tau_2{}^3)\ln^{2+m}\left(\frac{\tau_1}{\tau_2}\right),
$$

with m running from 0 to ∞ we may expect to be able to sum the series. In particular we collect a $\theta(\tau_1 - \tau_2)\frac{iH^2}{3}(\tau_1{}^3 + \tau_2{}^3)\ln^2\left(\frac{\tau_1}{\tau_2}\right)$, obtaining the series below

$$
\theta(\tau_1 - \tau_2)\frac{iH^2}{3}(\tau_1{}^3 + \tau_2{}^3)\ln^2\left(\frac{\tau_1}{\tau_2}\right)\left[\frac{\epsilon^2}{2!} + \frac{4\epsilon^3}{3!}\ln\left(\frac{\tau_1}{\tau_2}\right) + \cdots\right],
$$

where the terms in the parenthesis can be summed. The sum gives

$$
\sum_{m=0}^{\infty}\frac{\epsilon^{2+m}}{(2+m)!}\left[4\ln\left(\frac{\tau_1}{\tau_2}\right)\right]^m = -\frac{1 - \left(\frac{\tau_1}{\tau_2}\right)^{4\epsilon} + 4\epsilon\ln\left(\frac{\tau_1}{\tau_2}\right)}{16\ln^2\left(\frac{\tau_1}{\tau_2}\right)}. \quad (6.40)
$$

Multiplying now eq. (6.40) by the expression we collected before, we note that the summed tower graphs are not more divergent than a first order graph anymore. The complete expression is

$$\theta(\tau_1 - \tau_2)\frac{iH^2}{3}(\tau_1{}^3 + \tau_2{}^3)\ln^2\left(\frac{\tau_1}{\tau_2}\right) - \frac{1 - \left(\frac{\tau_1}{\tau_2}\right)^{4\epsilon} + 4\epsilon\ln\left(\frac{\tau_1}{\tau_2}\right)}{16\ln^2\left(\frac{\tau_1}{\tau_2}\right)}.$$

and one sees immediately that it is formed by the sum of three terms. Omitting for clarity the θ functions, we have

$$\frac{-iH^2}{3}(\tau_1{}^3 + \tau_2{}^3) + \frac{iH^2}{3}(\tau_1{}^3 + \tau_2{}^3)\left(\frac{\tau_1}{\tau_2}\right)^{4\epsilon} - \frac{iH^2}{3}(\tau_1{}^3 + \tau_2{}^3)4\epsilon\ln\left(\frac{\tau_1}{\tau_2}\right).$$

For late times the only divergent term is the last one. If we compare it with eq. (6.16), we immediately see that they are equal apart for a factor 4. Thus the resummation of the whole tower graph class is up to a factor equivalent to a tadpole graph. It is first order in the parameter ϵ and has a divergence ln. If we sum the two we obtain

$$-i\mathrm{G}_R^{tad+tower(1)}(k, \tau_1, \tau_2) = \frac{iH^2}{3}(\tau_1{}^3 + \tau_2{}^3)5\epsilon\ln\left(\frac{\tau_1}{\tau_2}\right), \qquad (6.41)$$

where $\mathrm{G}_R^{tad+tower(1)}$ is effectively the $\mathrm{G}_R^{(1)}$ renormalized to include all the tower graphs and the single tadpole graph (which can be viewed as the first order tower). If we define $\epsilon' = 5\epsilon$, one can use this new $\mathrm{G}_R^{tad+tower(1)}$ to build chains as we did before with simple tadpoles and we expect formally the same result,

$$-i\mathrm{G}_R^{chain-tower}(k, \tau_1, \tau_2) = -i\frac{H^2}{3}(\tau_1{}^{3-\epsilon'}\tau_2{}^{\epsilon'} - \tau_1{}^{\epsilon'}\tau_2{}^{3-\epsilon'}). \qquad (6.42)$$

Moreover we see that the odd behaviour of the $-i\mathrm{G}_R^{tow(n)}$ with even n is automatically cured by summing over all the graphs. We do not need to repeat the derivation for the G_C propagator since it differs for a retarded propagator *outside* of the tower, which therefore cannot modify the result that we have just obtained. Analogously we define the resummed propagator G_C over general chains of towers as

$$\mathrm{G}_C^{chain-tower}(k, \tau_1, \tau_2) = \mathrm{G}_C^{(0)}e^{\epsilon'\ln(k^2\tau_1\tau_2)}. \qquad (6.43)$$

One can try to do the same thing for the sunrise diagrams too. However, in this case, it is necessary to sum separately the odd and even terms due to the alternating terms $(\tau_1{}^3 \pm \tau_2{}^3)$. The second order sunrise has already been calculated in eq. 6.18, so we show here that the amplitude of the third order graph (which is the bottom one in figure 6.12) has the same analytical form of the third order tadpole graph. This is an example but the general m–order sunrise with odd m has a similar graph with $m-1$ 'inner'loops. For the third order G_R we write

$$
\begin{aligned}
\mathrm{G}_R^{sun,(3)}(k, \tau_1, \tau_2) \;=\; & \int_{\tau_2}^{\tau_1} d\tau_3 (-i\frac{\lambda}{3!} a^4(\tau_3))(-i)\mathrm{G}_R^{(0)}(k, \tau_1, \tau_3) \qquad (6.44) \\
& \int_{\tau_2}^{\tau_1} d\tau_4 (-i\frac{\lambda}{3!} a^4(\tau_4)) \int \frac{d^3q}{(2\pi)^3}\frac{d^3p}{(2\pi)^3}\frac{d^3t}{(2\pi)^3} \\
& \mathrm{G}_C^{(0)}(p, \tau_3, \tau_5)(-i)\mathrm{G}_R^{(0)}(k-p-q, \tau_3, \tau_4)\mathrm{G}_R^{(0)}(q, \tau_3, \tau_4) \\
& \int_{\tau_2}^{\tau_1} d\tau_5 (-i\frac{\lambda}{3!} a^4(\tau_5))(-i)\mathrm{G}_R^{(0)}(k-p-t, \tau_4, \tau_5) \\
& \mathrm{G}_R^{(0)}(k, \tau_1, \tau_3)\mathrm{G}_R^{(0)}(t, \tau_4, \tau_5)(-i)\mathrm{G}_R^{(0)}(k, \tau_5, \tau_2)\,,
\end{aligned}
$$

but at late times the free retarded propagators do not depend on the momentum flowing through them and the free G_C do not depend on the times, so all the retarded propagators go out of the integrals over p,q and t and we obtain three simple loop integrals as in eq. (5.32),

$$
\begin{aligned}
\mathrm{G}_R^{sun,(3)}(k, \tau_1, \tau_2) \;\equiv\; & \int_{\tau_2}^{\tau_1} d\tau_3 (-i\frac{\lambda}{3!} a^4(\tau_3))(-i)\mathrm{G}_R^{(0)}(k, \tau_1, \tau_3) \qquad (6.45) \\
& \int_{\tau_2}^{\tau_1} d\tau_4 (-i\frac{\lambda}{3!} a^4(\tau_4))(-i)\mathrm{G}_R^{(0)}(k, \tau_3, \tau_4) \\
& \int_{\tau_2}^{\tau_1} d\tau_5 (-i\frac{\lambda}{3!} a^4(\tau_5))(-i)\mathrm{G}_R^{(0)}(k, \tau_4, \tau_5)(-i)\mathrm{G}_R^{(0)}(k, \tau_5, \tau_2) \\
& \int \frac{d^3q}{(2\pi)^3}\frac{d^3p}{(2\pi)^3}\frac{d^3t}{(2\pi)^3}\mathrm{G}_C^{(0)}(p, \tau_3, \tau_5)\mathrm{G}_C^{(0)}(q, \tau_3, \tau_4)\mathrm{G}_C^{(0)}(t, \tau_4, \tau_5)\,,
\end{aligned}
$$

where we put k in the retarded propagators to show the equivalence with the three tadpole case. The only difference is the coefficient due to Wyck's theorem in front of the amplitude. In this case for the second order sunrise is $(3^2 2^3)/2!$ and for the third order $(3^5 2^3)/3!$. Expliciting all the coefficients we obtain two different sums, one for even terms and

one for odd terms. For the even terms we obtain:

$$\simeq \frac{-iH^2}{3}4({\tau_1}^3 - {\tau_2}^3)\ln^2\left(\frac{\tau_1}{\tau_2}\right)\frac{\cosh\left[9\epsilon\ln\left(\frac{\tau_1}{\tau_2}\right)\right] - 1}{81\ln^2\left(\frac{\tau_1}{\tau_2}\right)},$$

and we can see easily that it has no logarithmic divergence, vanishing for late times, while for the odd terms we obtain:

$$\simeq \frac{-iH^2}{3}4({\tau_1}^3 + {\tau_2}^3)\left[\frac{\epsilon}{9}\ln\left(\frac{\tau_1}{\tau_2}\right) - \frac{\epsilon}{81}\sinh\left[9\epsilon\ln\left(\frac{\tau_1}{\tau_2}\right)\right]\right],$$

which instead shows a logarithmic divergence. As opposed to the tower graphs, we cannot sum over chains of sunrise graphs to reabsorb the divergence since we have already done that. Can we cure it somehow? There is a way. Until now we calculated all the graphs using as fundamental bricks the free propagators of (5.32), yet using them we cannot avoid the arising of logarithmic divergences due to the combination of vertex, free retarded propagator and integration over τ. Now however we have at our disposal a more powerful tool: we have summed the tadpole–only chains and we have seen how tower graphs correct them only by a factor in the parameter ϵ. What we can do then is to renormalize the sunrise diagrams by calculating them with the resummed propagators (equations (6.33) and (6.38)) instead of the bare ones. Indeed the second order sunrise becomes non divergent just using the tadpole chain graphs. If we use the new symbols of figure (6.14) for the G_R^{chain}(upper one in the figure) and G_C^{chain}(bottom one), we may
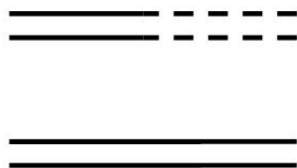

Figure 6.14: Tadpole chain propagators.

formally write the same integral (6.18) substituting the free propagators with the tadpole–chain ones and the corresponding graph is the

92

one in figure 6.15. Then the integrals for the two sunrise second order diagrams are

$$\tilde{G}_C^{(2)sun}(k,\tau_1,\tau_2) = \int_{-\frac{1}{k}}^{\tau_1} d\tau_3 \int \frac{d^3p}{(2\pi)^3} \int \frac{d^3q}{(2\pi)^3} \int_{-\frac{1}{k}}^{\tau_3} d\tau_4 (-i) \mathrm{G}_R^{chain}(k,\tau_1,\tau_3)$$
$$(-i\frac{\lambda}{3!}a^4(\tau_3)) \mathrm{G}_C^{chain}(p,\tau_3,\tau_4)(-i)\mathrm{G}_R^{chain}(k-p-q,\tau_3,\tau_4)$$
$$(-i\frac{\lambda}{3!}a^4(\tau_4)) \mathrm{G}_C^{chain}(q,\tau_3,\tau_4)\mathrm{G}_C^{chain}(k,\tau_4,\tau_2)\,, \qquad (6.46)$$

$$-i\tilde{G}_R^{(2)sun}(k,\tau_1,\tau_2) = \int_{\tau_2}^{\tau_1} d\tau_3 \int \frac{d^3p}{(2\pi)^3} \int \frac{d^3q}{(2\pi)^3} \int_{\tau_2}^{\tau_3} d\tau_4 (-i\frac{\lambda}{3!}a^4(\tau_3))$$
$$(-i)\mathrm{G}_R^{chain}(k,\tau_1,\tau_3)\mathrm{G}_C^{chain}(p,\tau_3,\tau_3)(-i)\mathrm{G}_R^{chain}(k-p-q,\tau_3,\tau_4)$$
$$(-i\frac{\lambda}{3!}a^4(\tau_4)) \mathrm{G}_C^{chain}(q,\tau_4,\tau_4)(-i)\mathrm{G}_R^{chain}(k,\tau_4,\tau_2)\,. \qquad (6.47)$$

Performing the calculations, one see that the resulting $\tilde{G}_R$ and $\tilde{G}_C$ are non divergent for late times. If we consider now a chain of sunrise diagrams built with the resummed diagrams (6.15), the higher order diagrams are less divergent than the one shown above because we will be injecting powers of τ and thus the graphs will depend on powers of τ^ϵ or higher powers, therefore producing an even stronger convergence at late times.

Results (6.33, 6.38, 6.42, 6.43) are extremely important: they show indeed that it is possible to separately resum the tadpoles graphs, the
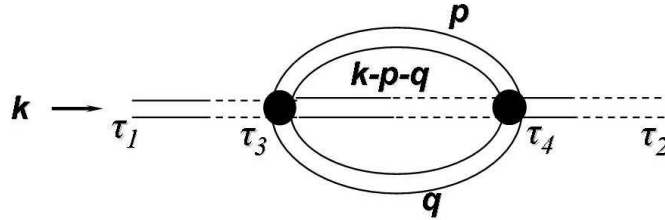

Figure 6.15: Example of sunrise drawn using the resummed tadpole propagators.

tower graphs and even build chains of tower graphs, that we expect to be *non divergent* in the late time limit. We started with logarithmic divergences that kept growing with the increasing orders and found that when considered globally they produce non divergent propagators therefore non divergent two-point correlation functions. It is clear that here we are overlooking many diagrams: actually one could continue to refine the analysis, for example resumming the tadpole graph built with the chain propagator of figure 6.14, and to be able to include all the possible diagrams one should iterate the process infinite times, considering the different type of graphs that arise at the various orders. For example, putting chain of tadpoles 'inside' other chains of tadpoles one builds the so called daisy graphs. Still, our aim was not to renormalize the whole theory but to provide evidence that in the limit of late time during Inflation the divergences arising from higher order loop corrections are naturally reabsorbed by considering more diagrams in the way we have shown. We now have that strong evidence to expect the completely resummed theory to be non divergent. Moreover, the finiteness of the correlation functions at late times allows us to make meaningful predictions about the level of non Gaussianity introduced by the non Gaussian field.

The target in our analysis is calculating the connected part of four–point functions which is not reducible to a product of two–point functions, since, as explained in section 4.2, that is the contribution to the non Gaussianity due only to the intrinsic non linearity of the field. Now we have resummed non divergent propagators that we expect will allow us to obtain a non divergent four–point function.

6.2 Four Point Functions

We want to calculate now the four–point correlation function T arising from our $\lambda\phi^4$ theory. As shown in section 4.2, knowledge of T would allow us to constraint the perturbations non Gaussianity coming from the field itself. Formally it is possible to build 5 different four

point functions, combining ϕ_C and ϕ_Δ. The one we are interested in is $\langle \delta\phi_C \delta\phi_C \delta\phi_C \delta\phi_C \rangle$. In general each of the fields will depend on a moment k_i and on a different time. Still, we are interested evaluating the four–point function at equal times, so more precisely the quantity we want to calculate is:

$$\langle \delta\phi_C(\mathbf{k_1},\tau)\delta\phi_C(\mathbf{k_2},\tau)\delta\phi_C(\mathbf{k_3},\tau)\delta\phi_C(\mathbf{k_4},\tau) \rangle = T(\mathbf{k_1},\mathbf{k_2},\mathbf{k_3},\mathbf{k_4})(2\pi)^3 \delta^3(\mathbf{k_1}+\mathbf{k_2}+\mathbf{k_3}+\mathbf{k_4}).$$
(6.48)

The first thing we can do is to go at tree level and see what happens. The diagram in terms of free propagators at tree level is drawn in figure (6.16). It is easy to build it using three $G_C^{(0)}$ and one $G_R^{(0)}$, but we must
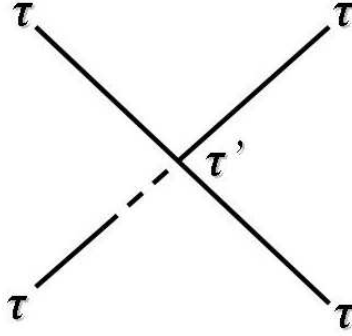
Figure 6.16: Tree level four point function $\langle \delta\phi_C \delta\phi_C \delta\phi_C \delta\phi_C \rangle$.

then sum over the permutations since each of the four momenta can be flowing through the retarded propagator. So the amplitude at tree level is

$$T^{tree}(\mathbf{k_1},\mathbf{k_2},\mathbf{k_3},\mathbf{k_4}) = \sum_{i=1}^{4} \int^{\tau} d\tau' e^{-i(\sum_{l=1}^{4} k_l)\tau'}(-i\frac{\lambda}{3!}a^4(\tau'))$$
(6.49)
$$(-iG_R^{(0)}(k_i,\tau,\tau')) \prod_{j\neq i} G_C^{(0)}(k_j,\tau,\tau') e^{-i[\sum_{i=1}^{4} k_i]\tau'}.$$

The indefinite integral becomes:

$$= \frac{e^{-i(\sum k_i)\tau}\left((-2+i(\sum k_i)\tau+(\sum k_i)^2\tau^2)\,\tau^3 + ie^{i(\sum k_i)\tau}\tau^3\left(6i+(\sum k_i)^3\tau^3\right)\right)}{6\tau^3}$$
$$Ei(-i(\sum k_i)\tau),$$
(6.50)

95

where $Ei(z)$ is:

$$Ei[x] = -\int_{-x}^{\infty} \frac{e^{-s}}{s} ds \,. \tag{6.51}$$

And so in the limit of late times, neglecting terms of order $k\tau$:

$$T^{tree}(\mathbf{k}_1, \mathbf{k}_2, \mathbf{k}_3, \mathbf{k}_4, \tau) = -\frac{\lambda H^4}{3!24 \prod k_i^3} \sum k_i^3 \left[-\gamma - \frac{i\pi}{2} - \ln\left[-(\sum k_i)\tau \right] \right] \,. \tag{6.52}$$

Equation (6.52) reproduces in a simple way the result obtained by Bernardeau *et al.* in [28]. In their analysis they provide also a next to leading term, which is actually a form factor of the momenta configuration. In our analysis we have systematically dropped them for easiness of calculation since, in calculating loop terms, they tend to quickly multiply, soon becoming of difficult handling. It is important still that we have obtained the same leading behaviour for the tree level 4–point function. We stress that for late times T shows again a logarithmic divergence.

We want now to see whether also this divergence is reabsorbed by summing over many diagrams. We have shown that the tadpole, tower and sunrise classes can be made finite by considering a sufficient number of graphs. We also showed how adding more diagrams cannot produce divergences but just reinforce the convergence for late times. So among our set of 'resummed' propagators we choose the tadpole chain propagators (6.33, 6.38). Our hope is to find that considering only the tadpole graphs is enough to reabsorb the divergence. It would be indeed a powerful result. So we draw again the four–point function but this time we use the 'double-line' propagators as in fig. 6.17. The amplitude is

$$
\begin{aligned}
T^{chain}(\mathbf{k}_1, \mathbf{k}_2, \mathbf{k}_3, \mathbf{k}_4) &= \sum_{i=1}^{4} \int^{\tau} d\tau' e^{-i(\sum_{l=1}^{4} k_l)\tau'}\left(-i\frac{\lambda}{3!}a^4(\tau')\right) \\
&\quad (-i\mathrm{G}_R^{chain}(k_i, \tau, \tau')) \prod_{j\neq i} \mathrm{G}_C^{chain}(k_j, \tau, \tau') e^{-i[\sum_{i=1}^{4} k_i]\tau'} \\
&= -\frac{\lambda}{3!}\frac{H^4}{24}\frac{1}{\prod_{i=1}^{4} k_i^3} \sum_{i=1}^{4} k_i^3
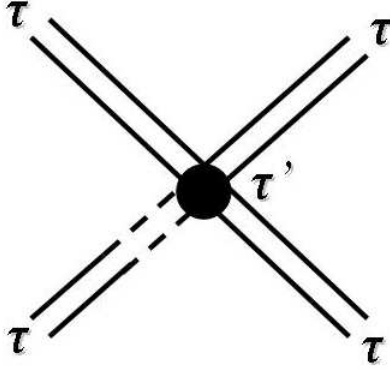\end{aligned} \tag{6.53}
$$

Figure 6.17: 4–point function calculated using G_C^{chain} and G_R^{chain}.

$$\prod_{j\neq i} k_j{}^{2\epsilon}\tau^{6\epsilon}\left[-E_{4-4\epsilon}(ik_t\tau) + E_{1-2\epsilon}(ik_t\tau)\right]\,, \quad (6.54)$$

where the function $E_n(z)$ is defined as

$$E_n(z) = \int_1^{\infty} \frac{e^{-zt}}{t^n}dt\,, \quad (6.55)$$

and thus in the limit $-k\tau \ll 1$ the amplitude becomes:

$$
\begin{aligned}
T^{chain}(\mathbf{k}_1, \mathbf{k}_2, \mathbf{k}_3, \mathbf{k}_4) &= -\frac{\lambda}{3!}\frac{H^4}{24}\frac{1}{\prod_{i=1}^4 k_i{}^3}\sum_{i=1}^4 k_i{}^3\prod_{j\neq i}k_j{}^{2\epsilon} \qquad (6.56)\\
&\quad \tau^{6\epsilon}(ik_t\tau)^{-4\epsilon}\left[(ik_t\tau)^{2\epsilon}\Gamma(2\epsilon, ik_t\tau) + ik^3\tau^3\Gamma(4\epsilon-3, ik_t\tau)\right]
\end{aligned}
$$

Performing the limit for $k\tau \to 0$ we find that $T^{chain}(\mathbf{k}_1, \mathbf{k}_2, \mathbf{k}_3, \mathbf{k}_4)$ vanishes. Figure 6.18 is the plot of the amplitude's absolute value $|T|$ near $k\tau = 0$ for $\epsilon = 0.1$, while figure 6.19 shows the behaviour of $|T|$ as a function of both ϵ and $k\tau$. Once again we see that the simple inclusion of more graphs is enough to reabsorb the divergence of the 4–point functions and even more it makes it vanishingly small at late times.

This was the result we have been pursuing in this work. We have shown that in the case of a minimally coupled massless scalar field with a ϕ^4 self–interaction the contribution to the non Gaussianity of ζ coming from the intrinsic non linearity of the field is vanishingly small at large times. Thus, the non gaussian contributions to ζ come only from the

97

effects of gravity.

It must be stressed that (6.56) is valid for *any minimally coupled massless scalar field* not only for the inflaton. So the resut applies to any scalar field present during Inflation.

It must be specified that in our calculations we made an assumption ($H = constant$) which is contradictory with identifying ϕ with the inflaton. In effect, if we say that ϕ is the inflaton with a ϕ^4 potential then $H^2 \simeq V \simeq \phi^4$ and so we would need a constant field all over the space to obtain a constant H, but this contrasts with the equation of motion, which gives $\dot{\phi} \neq 0$. If instead we say that ϕ is not the inflaton, we have no problems in having a costant H, but we have to account for the change in ζ due to the presence of multiple fields. However our results are meaningful under the suitable hypothesis of, respectively, a slowly changing H or a neglectable $\zeta_{inflaton}$ for the inflaton field.
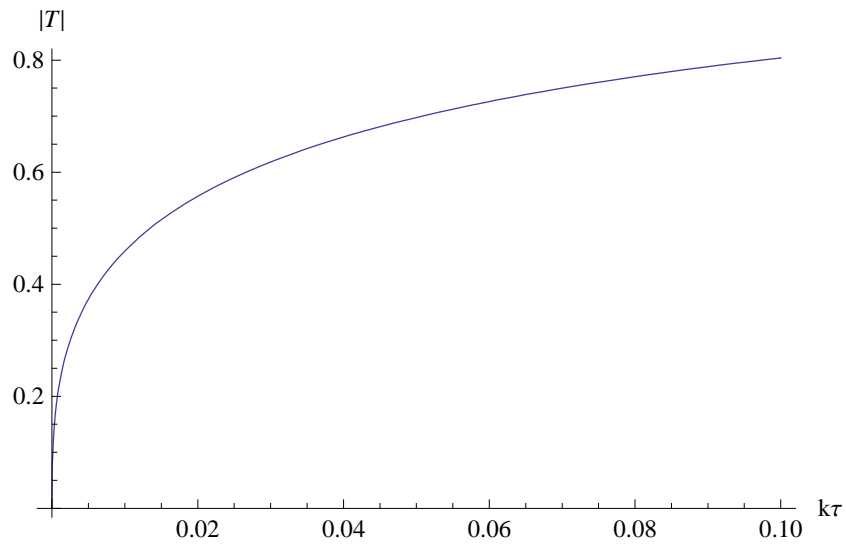
Figure 6.18: Plot of $|T|$ for a square configuration ($k_1 = k_2 = k_3 = k_4$) with $\epsilon = 0.1$, showing the steep decrease of the amplitude absolute value for small $k\tau$.
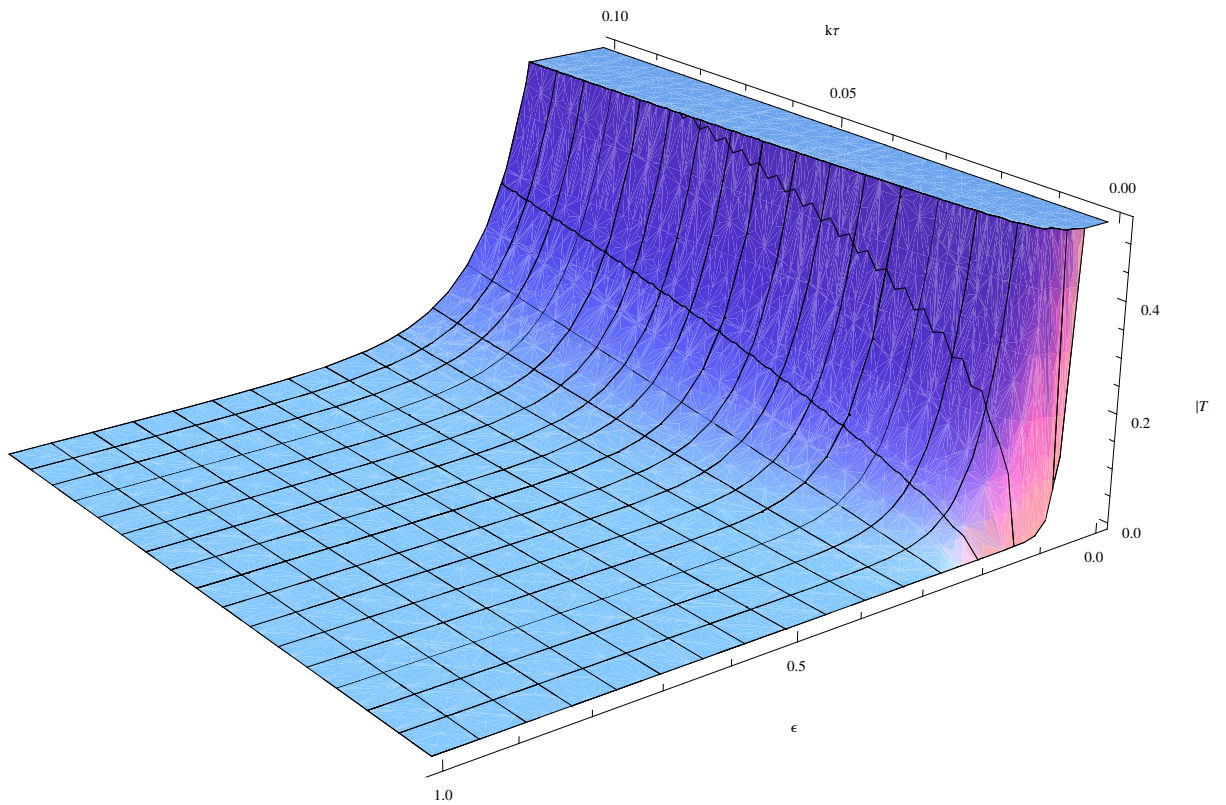

99

Figure 6.19: 3D Plot of $|T|$ for a square configuration ($k_1 = k_2 = k_3 = k_4$) for values of $k\tau$ and ϵ: $0 < k\tau < 0.1$ and $\epsilon < 1$. It is evident the fast decrease of the amplitude for small $k\tau$.

6.3 Diagrams Selection and $O(N)$ symmetry

Up to now we have shown that it is possible to resum the tadpole and tower diagrams obtaining non divergent propagators, we have also tried to resum the sunrise diagrams but we have obtained is an extremely large propagator that can be made non divergent recalculating it with the tadpole–chain propagator. Then we have used those *resummed* propagators to calculate the 4-point correlation function at tree level finding it to be non divergent in the late time limit. However what happens to the whole lot of the diagrams that we have not taken into account? When we have first summed over tadpole chains of arbitrarily length, we found finite propagators but at the same time we renounced to the benefits of a perturbative approach and put ourselves in the uncomfortable position of having to account for *all* the diagrams, of every order and topology. Our choice proved to be interesting even if tricky. However there is a way to deal in a single swipe with all the diagrams we have left out. We need however to change slightly the terms of our problem and invoke a $O(N)$ symmetry over N fields[2]. Following [95], we consider a theory of N real scalar fields, ϕ^a, with $O(N)$–symmetric quartic interactions. The Lagrangian density for the theory is

$$\mathcal{L} = \frac{1}{2}\partial_\mu \phi^{\partial^\mu}\phi^a - \frac{\lambda}{8N}(\phi^a\phi^a)^2 \, , \qquad (6.57)$$

where the sum over repeated indices is implied. This model can be analyzed in two ways: one is ordinary perturbation theory in λ for fixed N, the other is perturbation theory in $1/N$ for fixed λ. It has been shown that in the second expansion, at least to leading order in $1/N$, it is possible to obtain formulas for many quantities of physical interest. These formulas typically display richer structures than the corresponding leading–order expressions in ordinary perturbation theory. This is because the leading $1/N$ approximation preserves much more of the

---

[2]Here N has nothing to do with the δN formalism and the doubling of notation is sadly due to literature conventions.

nonlinear structure of the exact theory that does ordinary lowest–order perturbation theory. We are interested in this theory since it provides a natural way to show how certaing Feynman diagrams become suppressed in the large–N limit.

We note as first thing that each interaction vertex has field indices distributed as in figure 6.20. Each vertex brings a factor $1/N$ due to the
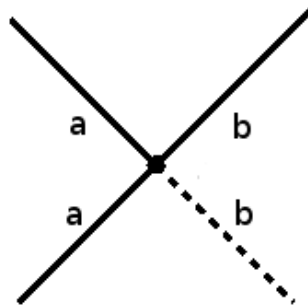

Figure 6.20: Vertex showing the fields' indices.

potential normalization. A diagram with r vertices then has a suppression factor of $1/N^r$. However when considering loop diagrams there is the possibility of summing over free field indices. As meaningful examples we propose the first order tadpole diagram (fig. 6.21), the second order tower diagram (fig. 6.22) and the second order sunrise diagram (fig. 6.23).

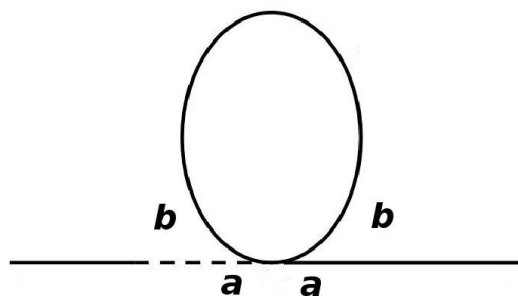In the tadpole one the propagated field is labeled by a and so the

Figure 6.21: Tadpole graph showing fields' indices.

two b legs of the vertex are closed together. This leaves the choice of

the field flowing in the tadpole free and therefore the sum produces a factor N. The tadpole diagram then has a suppression factor of order $1/N \times N = 1$. Thus tadpole diagrams are not suppressed, since at each vertex corresponds a loop and so the factors cancel. In the tower graph
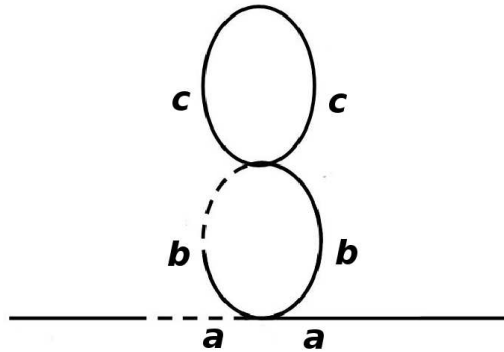

Figure 6.22: Tower graph showing fields' indices.

of fig. 6.22 the propagated field is again labeled by a. In the figure we see that despite the presence of two vertices $(1/N^2)$ there are also two loops where the flowing fields can be freely chosen and that gives a N^2. So also this diagram is not suppressed. Higher order tower graphs are not suppressed either since for each additional vertex there is an additional loop, as in the tadpole case. The sunrise diagram is the first
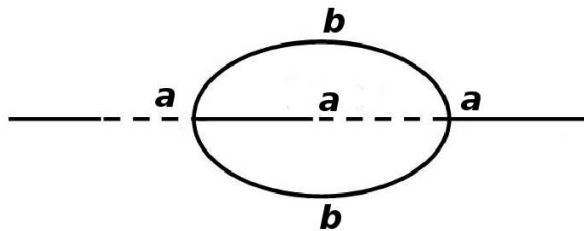

Figure 6.23: Sunrise graph showing fields' indices.

diagram we find to have a different behaviour. In fact the two vertices give a $1/N^2$ factor but here we do not have two free indices to sum over and cancel the factor. In fact we have only the field labeled by b as a

102

free choice and so we get just a N factor. Thus the sunrise diagram is suppressed by $1/N$. In the large–N limit the sunrise diagrams, which -we remind- were the divergent ones also after resumming them, are naturally less important than the tadpole and tower graphs, since the nth order tadpole or tower graph has always a factor 1 in front, while the corresponding sunrise a $1/N^{\frac{n}{2}}$ for even n and $1/N^{n-1}$ for odd n. However, starting from the third order and going up one can start to draw diagrams which do not belong to any of classes we analyzed, so a natural question arises: *are those other diagrams suppressed in this $O(N)$ theory or do they still represent an unsolved issue?*

Let us suppose to have a general diagram Υ of order l. This means that it has l vertices and thus a factor $1/N^l$. We have seen that the leading diagrams have at all orders a global factor 1. So for our diagram Υ to be dangerous we need to find a way for it to produce l loops where the internal summation over fields is free, or in other words l free field indices. To have a free index though we need the loop to be indipendent of the propagated field (which we usually denoted as a in the previous pictures). This can be done in two ways:

1. closing two legs of each vertex on themselves, so that all the vertices themselves give a factor 1. However a diagram of this kind is by definition a tadpole graph and so it has already been accounted for;

2. closing two legs of a vertex on a second one which is completely indipendent of the propagated field and that will not reconnect to it. However this produces invariably tower graphs, which again have been already accounted for.

Every other graph is suppressed at least by a factor $1/N$.

We see now that our choice to focus on only particular classes of diagrams has been daring but somehow rewarding: we found a reasonable reason to neglect the contributions of all classes of diagrams expect the tadpole and tower ones. It is clear that this result is valid only in the

large–N limit while until now we have always considered just one field at a time. However the $O(N)$ symmetry that we invoked allows us to apply the same argument to our case.

Chapter 7

Conclusions

We have presented the tools needed to calculate correlation functions of arbitrary order during a de Sitter stage in the case of a scalar field with a potential $V[\phi] = \frac{\lambda}{4!}\phi^4$. We have showed how the divergences at late times are generated when using the free two–point functions and how they persist at higher orders. We have then chosen different classes of diagrams and shown how considering the resummation of each class it is possible to reabsorb the divergences. In particular we have found that for late times the tadpole and tower resummed two–point functions are vanishingly small. These resummed two–point functions have then been used to calculate the connected four–point function $\langle \delta\phi_C \delta\phi_C \delta\phi_C \delta\phi_C \rangle$ and it was shown to be vanishingly small in the late time limit. A justification for neglecting different classes of diagrams has been given under the assumption of a large number N of scalar field obeying a $O(N)$ symmetry. Our main result is thus that a scalar field with a quartic potential does not contribute to the non Gaussianity of the curvature pertubation ζ, since both the two– and four–point correlation functions vanish at the end of the de Sitter stage.

We stress that our work was performed with a particular potential, however a generalization to a ϕ^n potential would be natural and interesting. As a final remark, we point out that we calculated the propagators at lower orders and then built up to loop corrections. It would be

interesting at this point to investigate whether a stochastic approach to the calculation of field correlation functions does account -and in what measure- for loop corrections and whether it can provide a complete solution.

Acknowledgments

My first acknowledgments go to my tutor in Switzerland, Dr. Antonio Riotto, whose patient yet strong guidance and explanations helped me through the solitary work for this thesis, done in the retirement of my little house in Petit-Lancy on the outskirts of Geneva. I would like to thank also my tutor in Pisa, Dr. Dario Grasso, for his quiet and incisive remarks.

On a personal level, I *must* thank my mother for the complete trust she always gave me and for the undemanding support she granted to me. She is my first artificer in more than one sense since her strength, endurance and wisdom have been the strongest and most inspiring example. I dedicate this work to her and to my father's memory.

I want to acknowledge the importance of two friends, Prof. Andrea Bizzeti, in my upbringing and education, thus symbolically in the completion of this thesis, and Prof. Diego Manzoni, especially for our continuing and funny bantering about everything, from religion to Middle Earth.

Then come my friends, buddies and loved ones: the ones that have always been there, even when they were far far away, and the ones that I found in this Swiss adventure. Each of you, guys, knows how much you helped me in getting this done and -in particular- in making me a better person, more than and differently from any of the 'old ones'. To you all go my most profound thanks and respect (!).

Bibliography

[1] Hoyle, F., Burbidge, G., and Narlikar, J. V. *A quasi-steady state cosmological model with creation of matter*, The Astrophysical Journal, 410, 437-457, 1993.

[2] A.H. Guth, *The Inflationary Universe: A Possible Solution To The Horizon And Flatness Problems*, Phys. Rev. D 23, 347 (1981).

[3] S.W. Hawking, *The Development Of Irregularities In A Single Bubble Inflationary Universe*, Phys. Lett. B 115, 295 (1982).

[4] A.H. Guth and S.Y. Pi, *Fluctuations In The New Inflationary Universe*, Phys. Rev. Lett. 49, 1110 (1982).

[5] A.D. Linde, *A New Inflationary Universe Scenario: A Possible Solution Of The Horizon, Flatness, Homogeneity, Isotropy And Primordial Monopole Problems*, Phys. Lett. B 108 (1982) 389.

[6] A. Albrecht, P.J. Steinhardt, M. S. Turner and F. Wilczek, *Reheating An Inflationary Universe*, Phys. Rev. Lett. 48 (1982) 1437.

[7] G.F. Smoot, *COBE observations and results*, AIP Conf. Proc. 476 (1999) 1, [astro-ph/9902027].

[8] C.L. Bennett *et al.*, *4-Year COBE DMR Cosmic Microwave Background Observations: Maps and Basic Results*, Astrophys. J. 464, L1 (1996), [astro-ph/9601067].

[9] V.F. Mukhanov and G.V. Chibisov, *Quantum Fluctuation And Nonsingular Universe. (In Russian)*, JETP Lett. 33, 532 (1981) [Pisma Zh. Eksp. Teor. Fiz. 33, 549 (1981)].

[10] C.L. Bennett *et al.* [WMAP Collaboration], *First Year Wilkinson Microwave Anisotropy Probe (WMAP) Observations: Preliminary*

Maps and Basic Results, Astrophys. J. Suppl. 148, 1 (2003), [astro-ph/0302207].

[11] H. V. Peiris, et al., *First year Wilkinson Microwave Anisotropy Probe (WMAP) observations: Implications for Inflation*, Astrophys. J. Suppl. 148 (2003) 213, [astro-ph/0302225].

[12] W. H. Kinney, E. W. Kolb, A. Melchiorri and A. Riotto, *WMAP-ping inflationary physics*, Phys. Rev. D 69, 103516 (2004), [hep-ph/0305130]

[13] G. Dvali, A. Gruzinov and M. Zaldarriaga, *A new mechanism for generating density perturbations from Inflation*, Phys. Rev. D 69 (2004) 023505, [astro-ph/0303591].

[14] L.A. Kofman, *Probing String Theory with Modulated Cosmological Fluctuations*, [astro-ph/0303614].

[15] S. Matarrese and A. Riotto, *Large-scale curvature perturbations with spatial and time variations of the inflaton decay rate*, JCAP 0308, 007 (2003), [astro-ph/0306416].

[16] R. Allahverdi, *Scenarios of modulated perturbations*, Phys.Rev. D70 (2004) 043507, [astro-ph/0403351].

[17] N. Arkani-Hamed, H. C. Cheng, M. A. Luty and S. Mukohyama, *Ghost condensation and a consistent infrared modification of gravity*, JHEP 0405 (2004) 074, [hep-th/0312099].

[18] E. Silverstein and D. Tong, *Scalar speed limits and cosmology: Acceleration from D-cceleration*, Phys.Rev. D70 (2004) 103505, [hep-th/0310221].

[19] L. Pilo, A. Riotto and A. Zaffaroni, *On the amount of gravitational waves from Inflation*, Phys.Rev.Lett. 92 (2004) 201303 , [astro-ph/0401302].

[20] N. Bartolo, E. Komatsu, S. Matarrese and A. Riotto, *Non-Gaussianity from Inflation: Theory and Observations*, Phys.Rept. 402 (2004) 103-266, [astro-ph/0406398v2].

[21] D.H. Lyth and A. Riotto, *Particle physics models of Inflation and the cosmological density perturbation*, Phys. Rept. 314, 1 (1999), [hep-ph/9807278].

[22]   `www.rssd.esa.int/PLANCK/`

[23] S. Weinberg, *Quantum Contributions to Cosmological Correlations*, Phys.Rev. D72 (2005) 043514, [hep-th/0506236].

[24] S. Weinberg, *Quantum Contribution to Cosmological Correlations II: Can these corrections become large?*, Phys.Rev. D74 (2006) 023508, [hep-th/0605244].

[25] M. van der Meulen and J. Smit, *Classical approximation to quantum cosmological correlations*, ITFA-2007-28, Jul 2007, [hep-th/0707.0842].

[26] M.S. Sloth,*On the One Loop Corrections to Inflation and the CMB Anisotropies*,Nucl.Phys. B748 (2006) 149-169, [astro-ph/0604488].

[27] M.S. Sloth, *On the One Loop Corrections to Inflation II:The Consistency Relation*, Nucl. Phys. B 775 (2007) 78, [hep-th/0612138v3].

[28] F. Bernardeau and J.P. Uzan, *High order correlation functions for self interacting scalar field in de Sitter space*, Phys.Rev. D69 (2004) 063520, [astro-ph/0311422].

[29] A. Vilenkin, *Quantum Fluctuations in the New Inflationary Universe*, Nuclear Physics B226 (1983) 527-546.

[30] D. Seery, J.E. Lidsey and M.S. Sloth, *The inflationary trispectrum*, JCAP 0701 (2007) 027, [astro-ph/0610210].

[31] E.Kolb, *The Early Universe*, 1993, Perseus Books Group, ISBN-13: 978-0201626742.

[32] G. Hinshaw *et al.* [WMAP Collaboration], *Three-year Wilkinson Microwave Anisotropy Probe (WMAP) observations: Temperature analysis*, Astrophys. J. Suppl. 170 (2007) 288, [astro-ph/0603451].

[33] D.N. Spergel *et al.* [WMAP Collaboration],*Wilkinson Microwave Anisotropy Probe (WMAP) three year results: Implications*

for cosmology, Astrophys. J. Suppl. 170 (2007) 377, [astro-ph/0603449].

[34] A. Riotto, *Inflation and the Theory of Cosmological Perturbations*, DFPD-TH/02/22, [hep-ph/0210162v1].

[35] A. Riotto, *Theories of Baryogenesis*, lectures delivered at the *ICTP Summer School in High-Energy Physics and Cosmology*,Miramare, Trieste, Italy, 29 Jun - 17 Jul 1998, [hep-ph/9807454].

[36] A. Riotto and M. Trodden, *Recent progress in baryogenesis*, Ann. Rev. Nucl. Part. Sci. 49, 35 (1999), [hep-ph/9901362].

[37] J.C. Mather *et al.*, *Measurement of the Cosmic Microwave Background spectrum by the COBE FIRAS instrument*, Astrophys. J. 420, 439 (1994).

[38] P.J.E. Peebles, D.N. Schramm, E. Turner, and R. Kron, *Nature* 352, 769 (1991).

[39] A.D. Linde, *Particle Physiscs and Inflationary Cosmology*, 1990, Contemporary Concepts in Physics, volume 5, Harwood Academic, Switzerland.

[40] A.R. Liddle and D.H. Lyth, *The Cold dark matter density perturbation*, Phys. Rept. 231, 1 (1993), [astro-ph/9303019].

[41] V.F. Mukhanov, H.A. Feldman and R.H. Brandenberger, *Theory of cosmological perturbations. Part 1. Classical perturbations. Part 2. Quantum theory of perturbations. Part 3. Extensions*, Phys. Rept. 215, 203 (1992).

[42] S. Dodelson, *Modern Cosmology*, 2003, Academic Press, ISBN 978-0-12-219141-1.

[43] J.E. Lidsey, A.R. Liddle, E.W. Kolb, E.J. Copeland, T. Barreiro and M. Abney, *Reconstructing the inflaton potential: An overview*, Rev. Mod. Phys. 69, 373 (1997), [astro-ph/9508078].

[44] A. R. Liddle, P. Parsons and J. D. Barrow, *Formalizing the slow roll approximation in Inflation*, Phys. Rev. D 50, 7222 (1994), [astro-ph/9408015].

[45] S. Dodelson, W.H. Kinney and E.W. Kolb, *Cosmic microwave background measurements can discriminate among Inflation models*, Phys. Rev. D 56, 3207 (1997), [astro-ph/9702166]

[46] V. Barger, H.S. Lee and D. Marfatia, *WMAP and Inflation*, Phys. Lett. B 565, 33 (2003), [hep-ph/0302150].

[47] S. M. Leach and A. R. Liddle, *Constraining slow–roll Inflation with WMAP and 2dF*, Phys.Rev. D68 (2003) 123508, [astro-ph/0306305].

[48] P.J.E. Peebles, *The Large–Scale Structure of the Universe*, 1980, Princeton University Press, Princeton, 978-0691082400.

[49] P. Coles and. F. Lucchin, *Cosmology, The origin and Evolution of Cosmic Structure*, 1995, John Wiley & Sons, Chichester, 978-0471489092.

[50] D. Lyth, K.A. Malik, M. Sasaki, *A general proof of the conservation of the curvature perturbation*, JCAP 0505 (2005) 004, [astro-ph/0411220].

[51] D. Lyth, D. Wands, *Conserved cosmological perturbations*, Phys.Rev. D68 (2003) 103515, [astro-ph/0306498].

[52] A.A. Starobinsky, *Cosmic Background Anisotropy Induced by Isotropic Flat-Spectrum Gravitational-Wave Perturbations*, Sov. Astron. Lett. 11, 133 (1985).

[53] D.S. Salopek, *Characteristics of Cosmic Time*, Phys.Rev. D52 (1995) 5563-5575, [astro-ph/9506146].

[54] T. Takahiro and E.D. Stewart, *The spectrum of cosmological perturbations produced by a multi-component inflaton to second order in the slow-roll approximation*, Phys.Lett. B381 (1996) 413-419, [astro-ph/9604103]

[55] D. Wands, K. A. Malik, D. H. Lyth and A. R. Liddle,*A new approach to the evolution of cosmological perturbations on large scales*, Phys.Rev. D62 (2000) 043527, [astro-ph/0003278].

[56] D.H. Lyth, A.Riotto,*Particle Physics Models of Inflation and the Cosmological Density Perturbation*, Phys.Rept. 314 (1999) 1-146, [hep-ph/9807278].

[57] V.F. Mukhanov, *Quantum Theory of Gauge Invariant Cosmological Perturbations* Sov. Phys. JETP 67, 1297 (1988) [Zh. Eksp. Teor. Fiz. 94N7, 1 (1988)].

[58] D. Seery, *One-loop corrections to the curvature perturbation from Inflation*, [astro-ph/0707.3378].

[59] D. Seery, *One-loop corrections to a scalar field during Inflation*, [astro-ph/0707.3377].

[60] X.Chen, M.Huang, S.Kachru, G.Shiu, *Observational Signatures and Non-Gaussianities of General Single Field Inflation*, JCAP 0701 (2007) 002, [hep-th/0605045v3].

[61] D.Seery, J.E.Lidsey, *Primordial non-gaussianities in single field Inflation*, JCAP 0506 (2005) 003, [astro-ph/0503692].

[62] P. Creminelli, L. Senatore, M. Zaldarriaga and M. Tegmark, *Limits on f_{NL} parameters from WMAP 3yr data*, JCAP 0703 (2007) 005, [astro-ph/0610600].

[63] C.T. Byrnes, M. Sasaki and D. Wands, *The primordial trispectrum*, Phys.Rev. D74 (2006) 123519, [astro-ph/0611075v2].

[64] C.T. Byrnes, K. Koyama, M. Sasaki and D. Wands, *Diagrammatic approach to non-Gaussianity from Inflation*, (2007), [hep-th/07054096v2].

[65] L.E.Allen, S. Gupta and D. Wands, *Non-Gaussian perturbations from multi-field Inflation*, JCAP 0601 (2006) 006, [astro-ph/0509719].

[66] J. M. Maldacena,*Non-Gaussian features of primordial fluctuations in single field inflationary models*, JHEP 0305 (2003) 013, [astro-ph/0210603].

[67] D. Seery, J.E. Lidsey, *Primordial non-gaussianities from multiple-field Inflation*, JCAP 0509 (2005) 011, [astro-ph/0506056].

[68] D. Lyth, Y. Rodriguez, *The inflationary prediction for primordial non-gaussianity*, Phys.Rev.Lett. 95 (2005) 121302, [astro-ph/0504045].

[69] L. Alabidi and D. Lyth, *Inflation models and observation*, JCAP 0605 (2006) 016, [astro-ph/0510441v2].

[70] M.Sasaki, K. Valiviita and D. Wands, *Non-Gaussianity of the primordial perturbation in the curvaton model*, Phys.Rev. D74 (2006) 103003, [astro-ph/0607627].

[71] N. Bartolo, S. Matarrese and A. Riotto, *Non-Gaussianity of Large-Scale Cosmic Microwave Background Anisotropies beyond Perturbation Theory*, JCAP 0508 (2005) 010, [astro-ph/0506410].

[72] N. Bartolo, S. Matarrese and A. Riotto, *Gauge-Invariant Temperature Anisotropies and Primordial Non-Gaussianity*, Phys.Rev.Lett. 93 (2004) 231301 [astro-ph/0407505].

[73] J.S. Schwinger, *Brownian motion of a quantum oscillator*, J. Math. Phys. 2, 407(1961).

[74] L.V. Keldysh,*Diagram technique for nonequilibrium processes*, Zh. Eksp. Teor. Fiz. 47, 1515 (1964)[Sov. Phys. JETP 20, 1018 (1965)].

[75] V. Koreman, Ann. Phys. (N.Y.) 39, 72 (1966).

[76] E. Calzetta and B.L.Hu, *Closed-time-path functional formalism in curved spacetime: Application to cosmological back-reaction problems*, Phys. Rev. D 35, (1987).

[77] G. Aarts and J. Smit, *Classical approximation for time-dependent quantum field theory: Diagrammatic analysis for hot scalar fields*, Nucl. Phys. B511 (1998) 451–478, [hep-ph/9707342].

[78] D. Boyanovsky, H.J. de Vega and N.G. Sanchez, *Quantum corrections to slow roll Inflation and new scaling of superhorizon fluctuations*, Nucl. Phys. B 747 (2006) 25, [astro-ph/0503669].

[79] E.O. Kahya and R.P. Woodard, *Quantum Gravity Corrections to the One Loop Scalar Self-Mass during Inflation*, UFIFT-QG-07-04, [gr-qc/0709.0536v2].

[80] S.Hawking and G.F.R. Ellis, *Large scale structure of the spacetime*, 1973, Cambridge University Press, 978-0521099066.

[81] N.D.Birrel and P.C.W. Davies, *Quantum fields in curved space*, Cambridge University Press (1982).

[82] A. Vilenkin, *Phase Transitions In De Sitter Space*, Nucl. Phys. B 226 (1983) 504.

[83] M. Sasaki and E.D. Stewart, *A General analytic formula for the spectral index of the density perturbations produced during Inflation*, Prog.Theor.Phys. 95 (1996) 71-78, [astro-ph/9507001].

[84] J. Martin and D.J. Schwarz, *The influence of cosmological transitions on the evolution of density perturbations* Phys. Rev. D 57, 3302 (1998), [gr-qc/9704049].

[85] E.D.Stewart and D.H.Lyth, *A more accurate analytic calculation of the spectrum of cosmological perturbations produced during Inflation*, Phys.Lett. B302 (1993) 171-175, [gr-qc/9302019v1].

[86] K.A.Malik, D.Wands, *Evolution of second-order cosmological perturbations*, Class.Quant.Grav. 21 (2004) L65-L72, [astro-ph/0307055v3]

[87] W. Friedmann, plenary talk given at *COSMO02*, Chicago, Illinois, USA, September 18-21, 2002.

[88] J.R. Bond et *al.*, *The Cosmic Microwave Background Inflation, Then Now*, AIP Conf.Proc. 646 (2003) 15-33, [astro-ph/0210007].

[89] T.Okamoto, W. Hu, *The Angular Trispectra of CMB Temperature and Polarization*, Phys. Rev. D 66, 063008 (2002), [astro-ph/0206155].

[90] E. Calzetta and B.L. Hu, *Nonequilibrium Quantum Fields: Closed Time Path Effective Action, Wigner Function and Boltzmann Equation*, Phys. Rev. D 37, 2878 (1988).

[91] Z.b. Su, L.y. Chen, X.t. Yu and K.c. Chou, *Influence Functional, Closed Time Path Green's Function And Quasidistribution Functional*, AS-ITP-87-017.

[92] N. Arkani-Hamed, P. Creminelli, S. Mukohyama and M. Zaldar-riaga, *Ghost Inflation*, JCAP 0404 (2004) 001, [hep-th/0312100].

[93] `map.gsfc.nasa.gov/`

[94] G. Dvali, A. Gruzinov and M. Zaldarriaga, *Cosmological perturbations from inhomogeneous reheating, freezeout, and mass domination*, Phys. Rev. D 69, 083505 (2004), [astro-ph/0305548].

[95] S. R. Coleman, R. Jackiw and H. D. Politzer, *Spontaneous Symmetry Breaking In The O(N) Model For Large N**, Phys. Rev. D 10 (1974) 2491.